SURFACTANT AND CHROMATE SORPTION TO CLINOPTILOLITE ZEOLITE: MECHANISMS AND SURFACE CONFIGURATION

by

Enid J. Sullivan

Submitted in partial fulfillment of the requirements for

the degree of Doctor of Philosophy in Hydrology

Department of Earth and Environmental Science

New Mexico Institute of Mining and Technology

Socorro, New Mexico

April 1997

ABSTRACT

In this dissertation, mechanisms of sorption of cationic surfactants to clinoptilolite, and the subsequent sorption of chromate to surfactant-modified clinoptilolite are proposed. Innovative instrumental and traditional wet chemistry methods were used to measure and interpret the sorption processes.

Tapping-mode atomic force microscopy was used to obtain molecular-scale images of both the unmodified clinoptilolite surface, and clinoptilolite modified with hexadecyltrimethylammonium bromide (HDTMA) surfactant to loading levels below its external cation exchange capacity (ECEC). Clinoptilolite showed a distinct repeating pattern on the surface comparable to its unit cell size, and HDTMA was found to produce clusters of surfactant which became more organized and linear in shape with increased loading. Thermogravimetric analysis was used to measure the stability of the HDTMA-clinoptilolite interaction at different loading levels of HDTMA. Differences in thermal stability indicated different binding energies for HDTMA sorbed above and below the ECEC.

Microcalorimetry was used to measure the heat of sorption of HDTMA and tetraethylammonium bromide (TEA) to clinoptilolite. A simple sorption model was used to determine equilibrium constants for the sorption reactions and to estimate values for the Gibbs free energy and entropy of sorption. The presence of the long hydrophobic tail

group on HDTMA strongly promoted stability of HDTMA sorption at all loading levels. A significant kinetic effect was noted in the sorption isotherms.

Fourier-transform Raman spectroscopy was used to probe the structure of sorbed surfactant and chromate. Batch studies measured the ion balance for HDTMA, the bromide counterion, and subsequent chromate sorption. The methods indicated that HDTMA micelles sorbed above the ECEC have a similar structure to solution micelles and retain anion exchange sites. HDTMA sorbed below the ECEC exhibited more disorder and had no anion exchange sites. Sorption of chromate may occur by two mechanisms based on shifted and split spectral peaks. Anion exchange appears to predominate, while Lewis acid-type interactions may account for minor sorption.

Surfactant and chromate counterion sorption are more complex than indicated solely by batch studies. Surfactant structure, concentration, and sorption kinetics play an important role in the sorption mechanisms observed. This information is essential for the successful development and application of surfactant-modified mineral systems.

Acknowledgment

This dissertation was supported by a number of funding sources, most notably the U.S. Department of Energy, a student research grant from The Clay Minerals Society, the Oak Ridge Institute for Science and Education research travel program, and the Waste-Management Education and Research Consortium (WERC). Rob Bowman supervised this research and provided encouragement and insight throughout the project.

Doug Hunter of the Advanced Analytical Center for Environmental Sciences at the Savannah River Ecology Laboratory (SREL) provided use of and training for several instruments as well as review of this work. Others at SREL who provided assistance included Brian Teppen, John Seaman, and Paul Bertsch. Kathy Nagy of Sandia National Laboratories reviewed the TMAFM images.

Bill Carey of Los Alamos National Laboratory gave considerable assistance to the thermodynamic analysis. He also provided the XRD analysis of clinoptilolite. Eric Brosha and Fernando Garzon of LANL provided use of the calorimeter and plenty of advice. Emily Keene and Jeanne Verploegh of New Mexico Tech performed a number of invaluable laboratory analyses. Jill Buckley of the Petroleum Recovery Research Center at NM Tech provided use of the surface tensiometer. Alan Dutton of the Texas Bureau of Economic Geology generously supported the final stages of work. Bill and Bobbie Partain provided housing in Los Alamos, good food, and the hot tub after long days at the lab.

Ioana Anghel, Emily Keene, Susan Sompayrac and the "Delaware clan" were unfailingly supportive. To all these people, and to others unmentioned, I give my thanks.

This dissertation is dedicated to Mom and Dad, Gary, my family, and the cats.

TABLE OF CONTENTS

Page

Page

Page

LIST OF FIGURES

Figure Page

Figure Page

Figure Page

LIST OF TABLES

CHAPTER 1

INTRODUCTION

STATEMENT OF THE PROBLEM

Effective remediation of ground-water contamination became a concern to the public over 30 years ago, when industrial chemicals began to be discovered in public drinking water supplies. Since then, a number of methods for removing these chemicals from subsurface water supplies have been developed, using existing and innovative technologies to reduce consumer risk. The cost of treatment, however, remains high, and some contaminants have properties which make them exceptionally difficult to remove, particularly at low concentrations. Low-cost methods that can reduce the time required for remediation and reduce the risk to receptor populations are therefore in demand.

Sorbent materials are frequently used in remediation systems. Activated carbon is specific only for organic compounds, and exchange resins only sorb cations and anions. Currently these sorbents are relatively expensive, particularly for long-term and large-scale use, and the presence of certain compounds or particulates in the treatment stream can interfere with sorptive properties. Sites with a variety of contaminants in ground water may require more than one sorbent to remove all of the contaminants of concern. This points out a need for materials which are inexpensive, can be produced in bulk, and have a heterogeneous sorptive capability.

Organoclays were first investigated in the 1950s and 1960s as part of a group of ion-exchanged clays (Slabaugh, 1954; Cowan and White, 1957; Slabaugh and Kupka,

1958; Barrer et al. 1967). These cationic surfactant-modified clays were an extension of research that focused on inorganic cation exchange properties of clays and were generally ignored because no clear use for the materials had yet emerged. Organoclays recently have found application as excellent sorbents for organic compounds in contaminated waters (Zhang et al., 1993; Smith and Galan, 1995; Xu and Boyd, 1995). The modified clays had the advantage of retaining some of their cation exchange properties, thus expanding the sorption versatility. Anion exchange, however, was not noted or investigated in these recent studies.

Recently, zeolites were proposed as an alternative to clay for substrate modification (Bowman et al., 1995; Haggerty and Bowman 1994). Modified clinoptilolite was first developed as a sorbent for organic compounds such as benzene, toluene, and xylene (Neel and Bowman 1991). The material was also capable of sorbing chlorinated organic compounds, and was noted to retain its cation exchange capability. Of great interest, however, was the discovery of anion sorption to the modified clinoptilolite (Haggerty and Bowman 1994). This material thus holds promise for remediation of ground water containing multiple contaminants.

PROJECT SCOPE

This dissertation is part of a larger project to develop surfactant-modified zeolite (SMZ) into a demonstrably useful material for field use in sorbing multiple types of chemicals from contaminated ground water. The overall project focuses on applied laboratory, pilot-scale, and field-scale demonstrations of the sorption properties of SMZ.

The need to design and engineer field applications also produced the need for background research into the surfactant sorption theory and anion sorption mechanism of the SMZ system, in order to appropriately define experimental and application procedures and to properly interpret the results.

Previous theories for anion sorption to SMZ included surface precipitation (Haggerty and Bowman 1994) and anion exchange (Cadena et al. 1992). These theories depend strongly on the configuration and chemical interactions of the surfactant with the clinoptilolite surface, and the subsequent interactions between the sorbing oxyanion and the surfactant-modified surface. The conformation of the surfactant on the surface is also important during preparation of SMZ, can have an effect on the stability of the SMZ during long-term use, and ultimately, affects the cost of the prepared material and the effectiveness of the remediation process. So, an understanding of the fundamental chemistry of the system has a direct effect on cost and viability of SMZ.

This study applied various methods of examining surface chemistry to expand the information available on the structure of hexadecyltrimethylammonium bromide (HDTMA) sorbed to clinoptilolite and how this structure affects or produces anion sorption. Previously, batch studies were the most commonly used method to study the sorption mechanism. However, those studies necessitated an inferred rather than direct observation of the surfactant on the surface. There also were gaps in knowledge because of a lack of complete clinoptilolite characterization and a lack of a complete ion balance in the system. This study was intended to accomplish two goals: (1) Rigorously determine the fundamental properties of the clinoptilolite, including surface area, internal

and external exchange capacities, and mineralogy, and (2) Apply a variety of innovative methods of surface characterization to directly observe, if possible, and understand the sorption mechanisms of surfactant and oxyanions to clinoptilolite.

RESEARCH TOPICS

Each chapter in this document discusses a particular topic related to the mechanisms of surfactant and anion sorption, and the stability of SMZ. Chapter 1 (this chapter) introduces the rationale for the research, and background information about the zeolite and surfactant used in the study. Appendix I includes experimental methods and results of these background studies which describe both zeolite properties and surfactant behavior. This includes surface area measurements, internal and external cation exchange capacity measurements, X-ray diffraction to determine the clinoptilolite mineralogy, and verification of the critical micelle concentration (CMC) of the HDTMA used in this study.

Chapter 2 contains the text and illustrations of a paper published in the journal Clays and Clay minerals (Sullivan et al. 1997b). Tapping-mode atomic force microscopy was used to image and measure the conformation of HDTMA on the clinoptilolite surface at various loading levels. The relative strength of the surfactant binding at various loading levels was measured with thermogravimetric analysis (TGA).

Chapter 3 is the text of a paper submitted to the Journal of Colloid and Interface Science (Sullivan et al. 1997a), detailing calorimetric and batch studies of the sorption of HDTMA and tetraethylammonium bromide (TEA) surfactants to clinoptilolite. The

microcalorimetry added thermodynamic detail to the known sorption isotherm information and also helped define the stability of the HDTMA on the clinoptilolite surface. Sorption of HDTMA from monomer and micelle solutions was measured in both the batch and calorimetric studies to determine if the initial form of the HDTMA affected the stability of the SMZ and the final form of the surfactant on the clinoptilolite surface. TEA was utilized as an analog for the headgroup of the HDTMA, to help measure the thermodynamic effects and sorption stabilization due only to the HDTMA tail group. Appendix II contains the thermodynamic and isotherm data used in that paper.

Chapter 4 is the text of a paper submitted to Environmental Science and Technology (Sullivan et al. 1997c). This paper describes the characterization of the SMZ using Fourier-transform Raman spectroscopy. FT-Raman can give important structural information about sorbed molecules in hydrated systems. A series of SMZ samples modified to different levels was characterized, along with chromate adsorbed to the SMZ. A batch study illustrating the anion balance in SMZ systems modified to less than and greater than the ECEC is also presented. Appendix III contains details of that data.

Chapter 5 concludes the dissertation and presents suggestions for future research.

BACKGROUND

Clinoptilolite

The clinoptilolite used in these studies is from the St. Cloud Mine in Winston, New Mexico. Clinoptilolite is the most common commercially-available zeolite and is relatively inexpensive. The mineral is a hydrated aluminum tectosilicate which is

isomorphic with heulandite, with the approximate formula (Ca, Na_2, $K_2)_3[Al_6Si_{30}O_{72}]$•24 H_2O. It has a complex, fixed structure including three sets of channels within the unit cell. One eight- and one ten-ring channel run parallel to each other along the b-axis while the third eight-ring channel intersects the others at a vertical right angle. The presence of these channels produces planes of weakness in the crystal and thus a pronounced cleavage parallel to the b-axis. The absence of shrink-swell properties, and the highly porous nature of the fixed channel system has led to the mineral's use in flow-through water treatment systems.

The clinoptilolite surface has a negative charge produced by the substitution of aluminum for silicon in the chemical formula. This charge is balanced by the presence of counterions. Calcium is the predominant counterion in the St. Cloud material, followed by potassium and sodium with minor magnesium (White et al.1996). As received, the material used in these studies consisted of about 74 % clinoptilolite, 5 % smectite clay, 10 % quartz and cristobalite, 10 % feldspar, and 1 % mica, based on internal standard X-ray diffraction analysis (Appendix I).

The surface properties of clinoptilolite are similar in many ways to those of clay minerals. Zeolites have a very high specific surface area compared to other fixed-structure silicate minerals, but less than that of clays. The sample used in these studies exhibited a variable surface area depending upon the degree of dehydration (Appendix I). Clinoptilolite, like other zeolites, can be used as a molecular sieve, allowing small ions or molecules to enter the channels while others are excluded. Cation exchange occurs both on the surface outside the pores (external surface) for most cations, while smaller cations

may also exchange at sites within the pores (internal surface). The internal cation exchange capacity (ICEC) of the material was about 650 to 900 meq/kg while the external CEC (ECEC) was measured to be about 90 meq/kg (Appendix I). Clinoptilolite does not form plate-like structures in water like clays, but can fractionate into small crystals along the pronounced b-axis cleavage plane. The presence of large exchanging surfactant molecules may enhance this breakage, similar to clay expansion by surfactants.

Cationic Surfactants

The surfactant used most frequently in these studies is hexadecyltrimethyl-ammonium bromide (HDTMA). SMZ treated with HDTMA produced the strongest sorption of oxyanions in previous studies (Haggerty and Bowman, 1994) as well as strong sorption of organic compounds (Bowman et al. 1995). HDTMA is composed of a 16-carbon hydrophobic tail group attached to a 3-methyl hydrophilic ammonium headgroup with a fixed +1 charge. HDTMA molecules in solution undergo self-assembly at a critical concentration to form micelles as the dominant solution form. This minimizes the contact of the hydrophobic group with water and stabilizes the system. This concentration is known as the critical micelle concentration (CMC) and occurs for HDTMA at 0.9 mmol/L at 25°C (Appendix I; Israelachvili, 1991). Below this concentration, the surfactant exists in solution as monomers which have limited interaction with each other.

Monomer conformation in solution may consist of tail groups contracted or curled so as to minimize contact of the hydrophobic moiety with water (Chen et al. 1992).

Micelle shape depends upon temperature, concentration, and the structure of the surfactant molecule. Spheres, tubes, and flat bilayers may be found. HDTMA micelles have been described as spherical at lower concentrations, and as flat bilayers in solution at high concentrations (Israelachvili, 1991). At concentrations well above the CMC or at low temperatures, HDTMA exists as liquid crystals.

Surfactant sorption is related to concentration, temperature, and the interactions which occur at the surface, such as electrostatic or hydrophobic interactions. Chen et al. (1992) described a number of different surfactant conformations on surfaces, including mono- and bilayers as well as admicelles (sorbed micelles) and hemimicelles (sorbed partial micelles). Here, the presence of a bilayer or admicelles is significant, because they incorporate the adsorption of surfactant counterions which may subsequently exchange with other anions in solution. A combination of electrostatic (ion exchange) and van der Waals forces is responsible for this configuration. Alternately, adsorption of counterions at low sorbed surfactant concentrations may imply a surface precipitation mechanism. The type of surfactant-surface interaction controls the surfactant conformation and thus, the mechanism of anion exchange.

Surface Force Interactions

A number of interactions can occur among the clinoptilolite surface, HDTMA, and oxyanions. The most significant in this system are Coulombic, van der Waals, and hydrophobic force interactions (Israelachvili, 1991). Coulombic interactions are relatively long-range, strong interactions between opposite charges. These forces are

responsible for ion exchange at the clinoptilolite surface and potentially for counterion (anion) exchange at the bilayer-water interface. Van der Waals interactions comprise a number of effects including dispersion forces from induced dipoles, are relatively long-range in influence, and are not dependent upon the existence of permanent charges. These forces induce attractions between the tail groups of surfactant molecules, between tail groups and the clinoptilolite surface, or between the surfactant-counterion pair and the surface. Finally, the hydrophobic "force" or effect may be considered as a contributor to the stability of micelles, surfactant bilayers, and admicelles. The hydrophobic effect arises from the favorable energy contribution when large non-polar molecules are removed from the disrupted water structure. This energy can be divided into two parts: energy from the collapse of the water cavity upon removal of the non-polar molecule; and the energy from water restructuring after the removal (Costas et al. 1994; Kronberg et al. 1995). Thus, micelles are stable at certain temperatures and surfactant concentrations because the hydrophobic tail groups are removed from interaction with the water structure. Admicelle or bilayer stability is also a result of this effect, as is the flocculation of SMZ particles when monolayer quantities of surfactant are adsorbed. The particles are hydrophobic in nature and, thus, adhere to each other.

OVERVIEW OF METHODS

Previous studies used batch sorption studies to quantify and describe the sorption of inorganic oxyanions to SMZ (Haggerty and Bowman 1994; Bowman et al. 1995). Because of uncertainties in the fundamental properties of the clinoptilolite, and because

of batch study variability, however, information about the surface conformation of HDTMA and anion sorption mechanisms was still lacking. Other means of probing the SMZ surface can give additional information which then can be interpreted with the batch data to give a better picture of the anion sorption process. Because anion sorption depends greatly on the conformation of the HDTMA, the primary topic of these studies is HDTMA conformation on the surface. New methods used included tapping-mode atomic force microscopy (TMAFM) and FT-Raman spectroscopy. Established methods included thermogravimetric analysis (TGA) and microcalorimetry. Detailed information about sample preparation for each method is contained in chapters 2 through 4, however, a brief description of the various analytical methods and the information derived from each method is given below.

Tapping-mode Atomic Force Microscopy

Atomic force microscopy has been used extensively to characterize nano-scale surface topography for nonconducting materials. The sample is usually a dry powder or surface film mounted with adhesive on a smooth metal disk. A molecularly-sharp probe traverses a reproducible x-y pattern on the surface (Figure 1.1). Vertical (z-dimension) movements of the probe as it moves over surface topography are recorded and the resultant x-y-z map of the surface is then displayed on a computer screen. The scale of observation is on the order of nanometers; the surface can be scanned dry or under fluid in a fluid cell. Repulsive forces between the probe tip and the surface can produce molecular-scale images with relative ease. Tapping mode is a recent development (K. Kjoller,

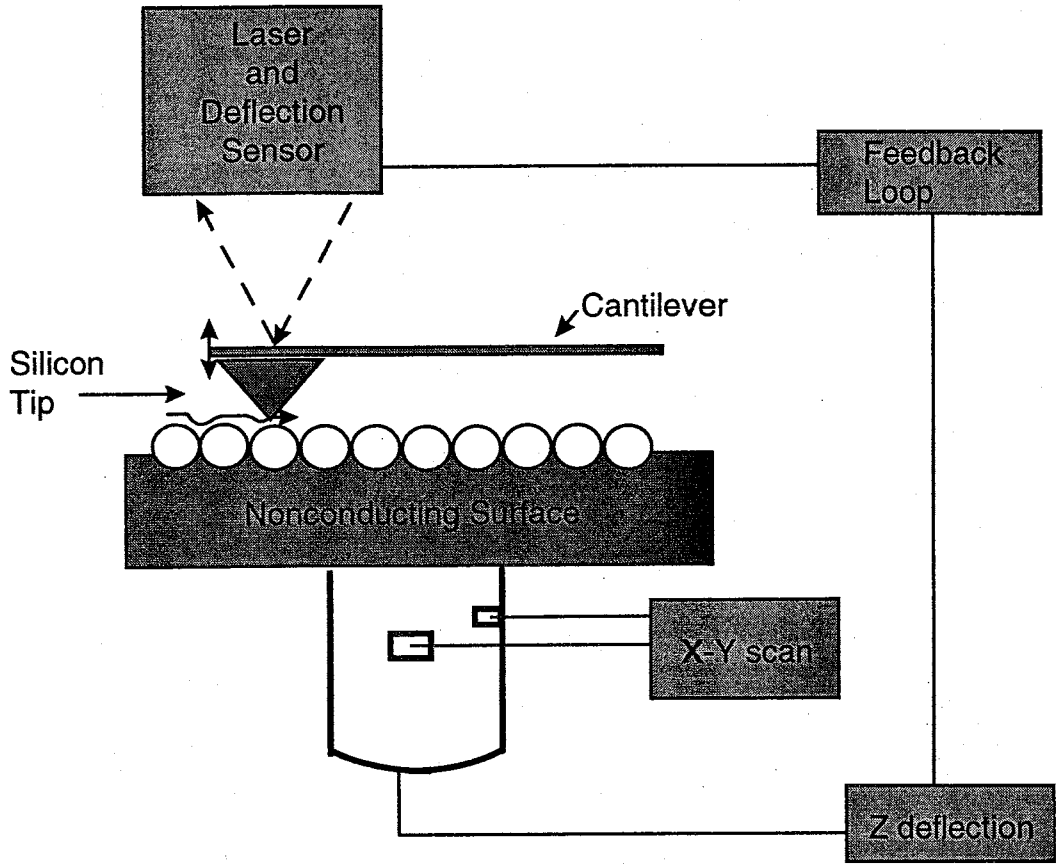

Figure 1.1. Conceptual Illustration of an Atomic Force Microscope

Digital Instruments, Inc., personal communication, 1994) in which the probe is vibrated by an electrical voltage during the imaging process. The advantage to tapping mode is that it is much gentler on soft surfaces, minimizing abrasion and probe damage, making the method ideal for observation of the "soft" SMZ surface. Unmodified clinoptilolite was found to have a distinctive surface topography under the AFM (Weisenhorn et al. 1991; Scandella et al. 1993; Komiyama and Yashima 1994). The HDTMA dimensions including length and thickness (z-dimension) as well as the clustering of tail groups on the surface at low coverages were measured by comparison of the SMZ at various loading levels with the known clinoptilolite topography (Sullivan et al. 1997b).

High-Resolution Thermogravimetric Analysis

Thermogravimetric analysis is a well established method which provides information about the strength of the bond between sorbed materials and a surface. Zeolites are frequently studied with TGA to determine the relative binding energies of water in different environments on the internal and external crystal surfaces. Clinoptilolite samples treated with various quantities of HDTMA were weighed, placed on a nonreactive platinum weighing dish, and sequentially heated from room temperature to 800°C under helium (Figure 1.2). The weight losses of the samples were recorded and graphed both directly and as the derivative with respect to temperature, versus temperature. Changes in slope and differences in derivative peak heights and widths were compared. The data showed stronger bonding of surfactant at low loading levels and weaker bonding at higher loading levels, distinguishing between mono- and bilayers on the surface.

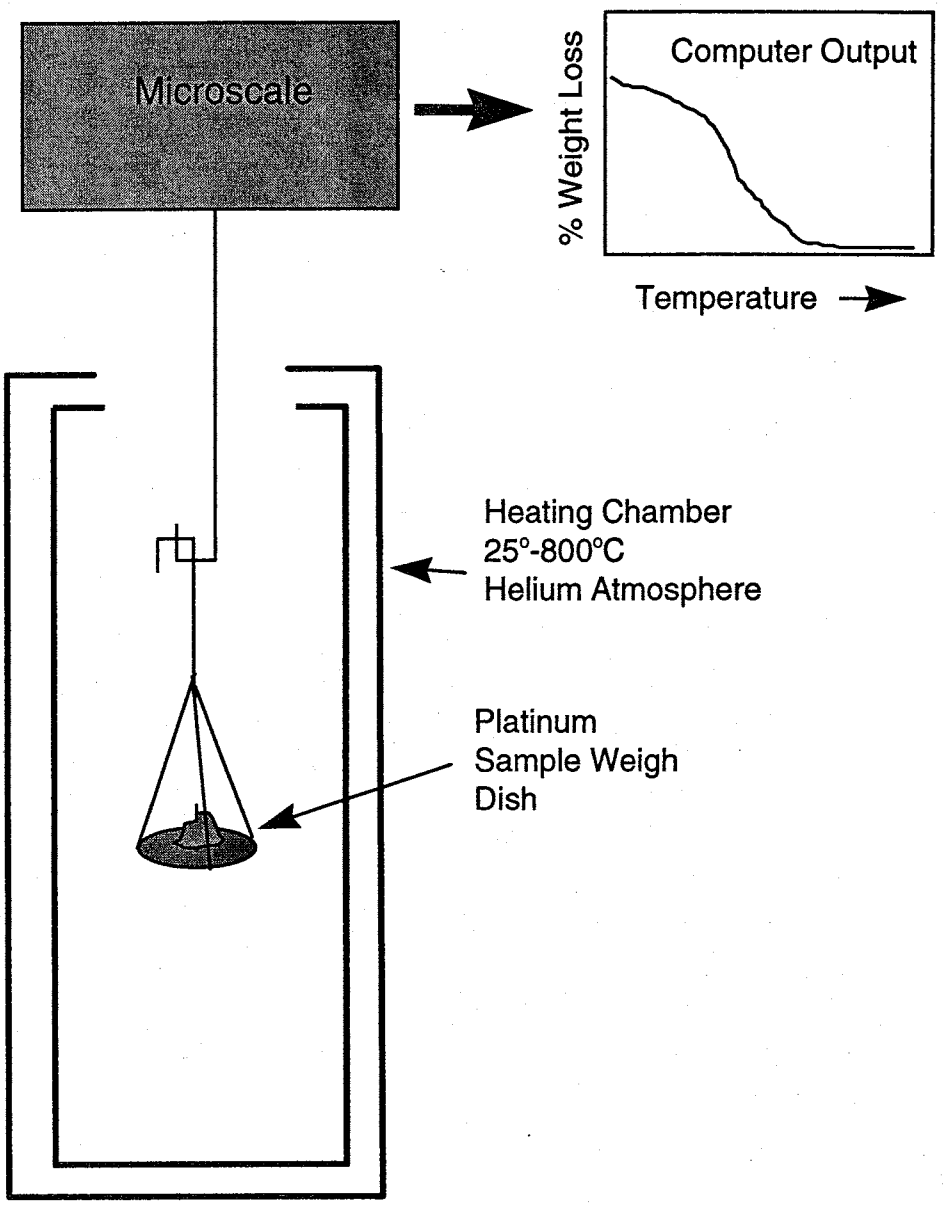

Figure 1.2. Schematic of HR-TGA instrument.

The change in binding energy took place at coverages above 100% of the ECEC.

Microcalorimetry

Calorimetric methods can provide more detail about the thermodynamics and stability of a sorption process than can batch methods. The stability of the final sorbed product may predict the likelihood of HDTMA washoff and the effectiveness of the SMZ as a result of preparation conditions. A microcalorimeter was utilized with HDTMA solutions formulated above and below the CMC to determine if there was a difference in HDTMA binding due to HDTMA conformation in solution. Another surfactant, tetraethylammonium bromide (TEA), was used as an approximation of the interaction of the HDTMA headgroup with the clinoptilolite surface, to isolate the effects of the headgroup. The surfactant solutions were placed in a calorimeter vessel which was equipped with a stirring paddle, heating and cooling probes, and a temperature sensor (Figure 1.3). The calorimeter was held in a large water bath which was maintained at 25°C to reduce equilibration time. The raw clinoptilolite was placed in a glass ampoule which was mounted within the calorimeter. The apparatus was allowed to equilibrate at 25°C and then the zeolite was added by remotely breaking the ampoule within the calorimeter. The amount of heating or cooling necessary to return the calorimeter to the equilibrium temperature was measured and output to a computer screen. Heat was presented in counts which are related to voltage. Counts were plotted versus time and the total heat input or output was determined by integrating under the plotted curve across a baseline. An exothermic molar enthalpy was recorded for HDTMA and a near zero to small endothermic molar enthalpy was noted for TEA.

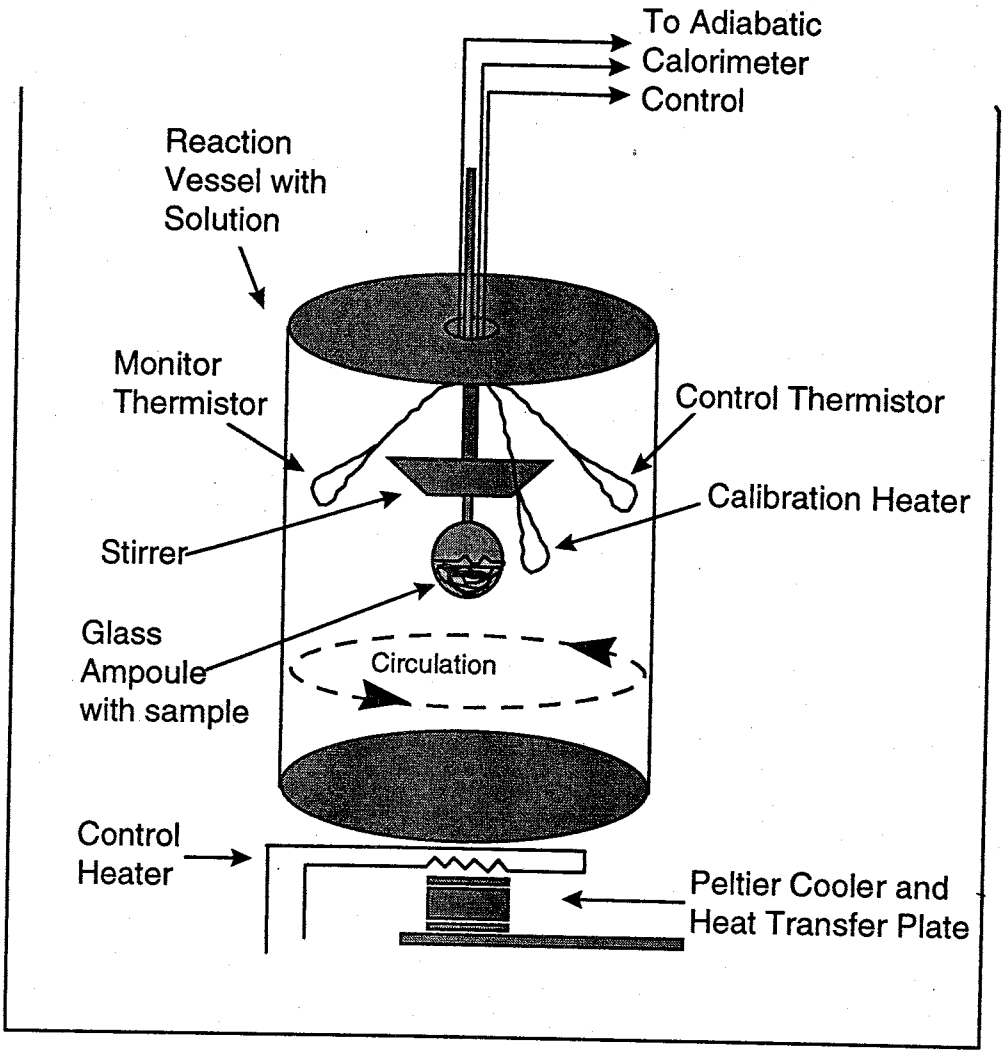

Figure 1.3. Schematic of Calorimeter with Sensors and Sample Mount

Fourier-transform Raman Spectroscopy

Raman spectroscopy is a well tested method of surface analysis which was recently updated with Fourier-transform data interpretation and greatly improved excitation sources and detectors. The Raman effect is the basis for this spectroscopy which is closely related to infrared spectroscopic methods. The Raman spectrum arises from changes in molecular polarizability during visible, infrared, or ultraviolet-induced molecular vibrations. Hendra et al. (1991) described the Raman effect as follows:

Application of an electric field gradient of magnitude E (V/m) can induce a dipole of magnitude P (V/m)

$$P = \alpha E \tag{1}$$

where α is the polarizability. If the field is supplied by electromagnetic radiation of frequency ν_0 (Hz) then:

$$P = \alpha E_0 \cos(2\pi \nu_0 t) \tag{2}$$

where t is time. The irradiated polarizable molecule vibrates at frequency ν_{vib} so that its distortion q from the equilibrium position is given by:

$$q = q_0 \cos(2\pi \nu_{vib} t) \tag{3}$$

where q_0 is the maximum distortion and ν_{vib} is the vibrational frequency (Hz). The polarizability of the periodically distorting molecule becomes:

$$\alpha = \alpha_0 + \left(\frac{\delta\alpha}{\delta q}\right)_0 q \tag{4}$$

where α_0 is the polarizability of the molecule in the equilibrium position, and $(\delta\alpha/\delta a)_0$ is the rate of change of that polarizability with distortion around the equilibrium structure. The variation in polarizability as the molecule vibrates is described by:

$$\alpha = \alpha_0 + \left(\frac{\delta\alpha}{\delta q}\right)_0 q_0 \cos(2\pi\nu_{vib} t) \tag{5}$$

If we substitute equation (5) into equation (2), and use some manipulation, we get an equation in the form of:

$$P = \alpha_0 E_0 \cos(2\pi\nu_0 t) + \frac{1}{2}\left(\frac{\delta\alpha}{\delta q}\right)_0 q_0 \left\{\cos(2\pi[\nu_0 + \nu_{vib}]t) + \cos(2\pi[\nu_0 + \nu_{vib}]t)\right\} \tag{6}$$

In effect, the induced dipole vibrating with frequency ν_{vib} and irradiated at frequency ν_0 will vary as ν_0 and also $(\nu_0 + \nu_{vib})$ and $(\nu_0 - \nu_{vib})$. The polarization process is endothermic, and so the spontaneous relaxation process produces releases of energy which correspond to the incident frequency, ν_0, and scattering frequencies $(\nu_0 + \nu_{vib})$ and $(\nu_0 - \nu_{vib})$. The very weak "scatter" is an inelastic process and is known as Raman scatter. Changes in the chemical environment which affect the polarizability of a bond will thus shift or remove a band in a Raman spectrum.

The result is a method which can be used on samples *in-situ* and can provide remarkably detailed information about surface binding effects on different compounds including both HDTMA and chromate. SMZ treated to low and high levels with HDTMA, which included both monolayers and bilayers or admicelles, and SMZ containing sorbed chromate were both examined. Each sample was placed in a non-fluorescing Nicolet nuclear magnetic resonance (NMR) glass tube and mounted in the

instrument where a near-infrared visible light laser was used to excite the sample (Figure 1.4). The emission spectrum contains multiple lines corresponding to particular molecular vibrations and rotations. These molecular changes are dependent upon the bonding environment on the surface and can be assigned to movement of a particular structural unit on the molecule of interest. Here, assignments were based on literature values and comparisons between spectra. Spectra from samples containing monolayers or bilayers (possibly admicelles) were compared, particularly spectral regions corresponding to chain vibrations such as the CH_2 symmetric and anti-symmetric stretches as well as headgroup vibrations. Sorbed and solution chromate vibrations were also compared.

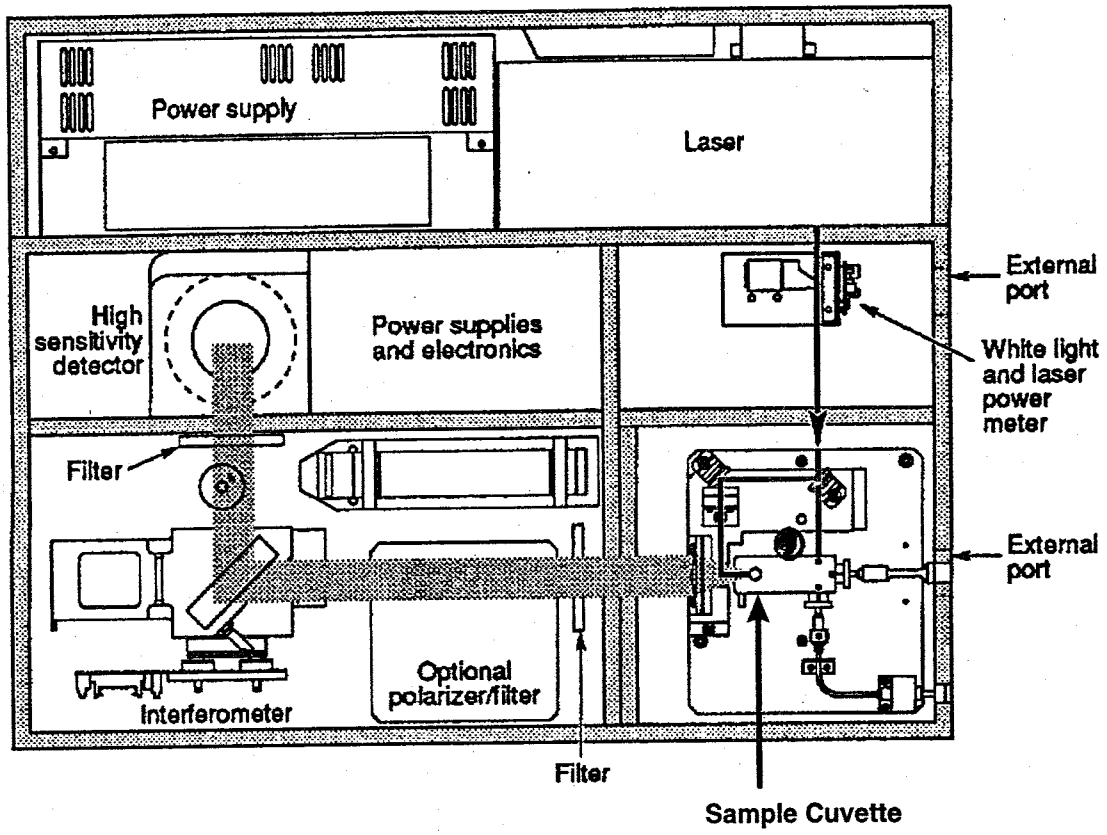

Figure 1.4. Schematic FT-Raman Instrument showing Laser and Sample Cuvette.

REFERENCES

Barrer, R.M., Papadopoulos, R., and Rees, L.V.C., Exchange of sodium in clinoptilolite by organic cations. *J. Inorg. Nucl. Chem.* **29,** 2047 (1967).

Bowman, R.S., Haggerty, G.M., Huddleston, R.G., Neel, D., and Flynn, M.M. Sorption of nonpolar organic compounds, inorganic cations, and inorganic oxyanions by surfactant-modified zeolites. In: Surfactant-Enhanced Subsurface Remediation. ACS Symposium Series 594, Sabatini, D.A., Knox, R.C., and Harwell, J.H., Eds. Washington, DC: American Chemical Society, 54-64, (1995).

Cadena et al., In: New Mexico Waste-Management Education and Research Consortium, Technical Completion Report (WERC-91-41), 22 pp. (1992).

Chen, Y.L., Chen, S., Frank, C., Israelachvili, J., Molecular mechanisms and kinetics during the self-assembly of surfactant layers. *J. Coll. Int. Sci.* **153**, 1, 244 (1992).

Costas, M., Kronberg, B., and Silveston, R., General thermodynamic analysis of the dissolution of non-polar molecules into water. *Chem. Soc. Faraday Trans.* **90**, 11, 1513 (1994).

Cowan, C.T., and White, D., The mechanism of exchange reactions occurring between sodium montmorillonite and various *n*-primary aliphatic amine salts. *Trans. Faraday Soc.* **54,** 691 (1957).

Haggerty, G.M., and Bowman, R.S., Sorption of chromate and other inorganic anions by organo-zeolite. *Environ. Sci. and Technol.* **28**, 3, 452, (1994).

Hendra, P., Jones, C., and Warnes, G., Fourier Transform Raman Spectroscopy, Instrumentation and Applications. Ellis Horwood, New York, 259 pp. (1991).

Israelachvili J N. Intermolecular and Surface Forces. 2nd Ed. San Diego, CA: Academic Press, Inc., 450 pp. (1991).

Komiyama, M., and Yashima, T., Atomic force microscopy images of natural zeolite surfaces observed under ambient conditions. *Jpn. J. Appl. Phys.* **33**, 1,6B, 3761, (1994).

Kronberg, B., Costas, M., and Silveston, R., Thermodynamics of the hydrophobic effect in surfactant solutions-micellization and adsorption. *Pure & Appl. Chem.* **67**, 6, 897 (1995).

Neel, D., and Bowman, R.S. Sorption of organics to surface-altered zeolites. Proc. 36th Annual New Mexico Water Conference; November 7-8, 1990, 57-61. (1991).

Scandella, L., Kruse N., Prins, R., Imaging of zeolite surface structures by atomic force microscopy. *Surf. Sci. Letters* **281**, 331, (1993).

Slabaugh, W.H., and Kupka, F., Organic cation exchange properties of calcium montmorillonite. *J. Phys. Chem.* **62**, 599 (1958).

Slabaugh, W.H., Cation exchange properties of bentonite. *J. Phys. Chem.* **58**, 162 (1954).

Smith, J.A., and Galan, A., Sorption of nonionic organic contaminants to single and dual organic cation bentonites from water. *Environ. Sci. Technol.* **29**, 3, 685 (1995).

Sullivan, E.J.; Carey, J.W.; Bowman, R.S. Thermodynamics of Cationic Surfactant Sorption onto Clinoptilolite. Submitted to *J. Coll. Int. Sci.*, January, 1997, (1997a).

Sullivan, E.J., Hunter, D.B., and Bowman, R.S. Topological and thermal properties of surfactant-modified clinoptilolite studied by Tapping-Mode™ atomic force microscopy and high-resolution thermogravimetric analysis. *Clays and Clay Minerals* **45,** in press (1997b).

Sullivan, E.J., Hunter, D.B., and Bowman, R.S. Fourier-transform raman spectroscopy of sorbed HDTMA and the mechanism of chromate sorption to surfactant-modified clinoptilolite. Submitted to *Environ. Sci. Technol.* March, 1997, (1997c).

Weisenhorn, A.L., MacDougall, J.E., Gould, A.C., Cox, S.D., Wise, W.S., Massie, J., Maivald, P., Elings, V.B., Stucky, G.D., Hansma, P.K. Imaging and manipulating molecules on a zeolite surface with an atomic force microscope. *Science* **24**, 1330, (1991).

White, J.L., Chavez, W.X., and Barker, J.M. Economic geology of the St. Cloud Mining Company (Cuchillo Negro) clinoptilolite deposit, Sierra County, New Mexico. In: New Mexico Bureau of Mines and Minerals Resources, Bulletin 154, Geology of Industrial Minerals 31st Forum, Socorro, New Mexico, 113 (1996).

Xu, S., and Boyd S.A. Cationic surfactant adsorption by swelling and nonswelling layer silicates. *Langmuir* **11**, 2508 (1995).

Zhang, Z.Z., Sparks, D.L., and Scrivner, N.C., Sorption and desorption of quaternary amine cations on clays. *Environ. Sci. Technol.* **27**, 1625 (1993).

CHAPTER 2

TOPOLOGICAL AND THERMAL PROPERTIES OF SURFACTANT-MODIFIED CLINOPTILOLITE STUDIED BY TAPPING-MODE™ ATOMIC FORCE MICROSCOPY AND HIGH-RESOLUTION THERMOGRAVIMETRIC ANALYSIS

(Published by Clays and Clay Minerals, V. 45, No. 1, January/February, 1997)

ABSTRACT

Unmodified and surfactant-modified clinoptilolite-rich tuff (referred to here as clinoptilolite) and muscovite mica were examined with tapping-mode atomic force microscopy (TMAFM) and high-resolution thermogravimetric analysis (HR-TGA) in order to elucidate patterns of hexadecyltrimethylammonium bromide (HDTMA) sorption on the treated surface and to understand the mechanisms of this sorption. TMAFM images were obtained to a scale of 50 nm by 50 nm. The images of unmodified clinoptilolite showed a framework pattern on the a-c plane, comparable to previously reported images. Images of modified clinoptilolite at 12.5 % and 25 % of external cation-exchange capacity (ECEC) coverage by HDTMA showed evidence of the HDTMA molecules arranged as elongated, topographically raised features on the a-c plane. At 50 % HDTMA coverage, the images contained what appeared to be agglomerations of surfactant tail groups. The z-direction thickness of the raised features on the 12.5 % coverage sample corresponded to the thickness of the carbon chain of the surfactant tail-group (0.4 nm), whereas the z-thickness on the 25 % coverage sample was between 0.4 and 0.8 nm, indicating crossing or doubling of tail groups. Repulsive forces between the

modified clinoptilolite and the silicon TMAFM probe increased with increasing HDTMA coverage. HR-TGA showed a 100° C increase in HDTMA pyrolysis temperatures at coverages of less than 50 %, probably due to an increased stabilization of the HDTMA due to direct tail interactions with the clinoptilolite surface at lower coverages versus smaller stabilization due to surfactant tail-tail interactions at higher coverages. Our results indicate that buildup of HDTMA admicelles or some form of a bilayer begins before full monolayer coverage is complete.

INTRODUCTION

Surfactant-modified clay minerals, particularly smectite, are undergoing extensive study because of their potential use as environmental sorbents. Zeolite minerals have surface chemistries similar to clays, but display superior hydraulic properties. Surfactant-modified clinoptilolite-rich tuff (referred to here as clinoptilolite) was shown in batch sorption studies to be an effective sorbent of both nonpolar organic compounds and inorganic anions from water (Bowman et al. 1995; Haggerty and Bowman 1994; Neel and Bowman 1992; Gao et al. 1991). While the mechanism of organic sorption appears to be partitioning, the mechanism of inorganic anion sorption is not clear. To understand both mechanisms, we utilized tapping-mode atomic force microscopy (TMAFM) and high-resolution thermal gravimetric analysis (HR-TGA) to characterize hexadecyltrimethylammonium bromide (HDTMA) sorption on clinoptilolite. The atomic force microscopy gave direct information about the placement of the surfactant on the

clinoptilolite surface whereas HR-TGA indicated intermolecular interactions between surfactant and clinoptilolite and between neighboring surfactant molecules.

Cationic surfactants, such as HDTMA, exchange with native cations, such as Na^+, K^+, or Ca^{2+}, on the clinoptilolite surface producing an organic carbon-enriched surface (Haggerty and Bowman 1994). Large surfactants are excluded from the interior channels of the clinoptilolite and, thus, exchange only with cations on the exterior of the crystal. The HDTMA molecule consists of a 16-carbon chain tail group attached to a 3-methyl quaternary amine head group with a permanent 1+ charge. It is water soluble and exists as monomers in solution below the critical micelle concentration (CMC) or as micelles above the CMC of 9×10^{-4} M at 25°C (Israelachvili 1991). Summation of the van der Waals packing radii for a 3-methyl ammonium head group yields a diameter of 0.694 nm. A fully-extended HDTMA chain length of 3.5 nm can be calculated by adding the effective van der Waals radii for the appropriate number of $-CH_2$ and $-CH_3$ groups (Israelachvili 1991). A typical carbon chain diameter of 0.4 nm can also be calculated from the packing radii (Israelachvili 1991). The HDTMA molecule is large compared with the clinoptilolite cage structure and surface topography and is, thus, a good candidate for observation by TMAFM. The mean aggregation number of the micelles, based on head group area, was calculated to be about 95 monomers per micelle, assuming a spherical micelle (Israelachvili 1991). Although this value can vary with temperature and concentration, it is well within published ranges (Reiss-Husson and Luzzati 1964, Malliaris et al. 1986).

Sorption of ionic surfactants onto a charged solid surface can proceed by at least two pathways, depending upon surfactant concentration in solution. Below the CMC, surfactant monomers are sorbed, eventually developing a monolayer or a bilayer configuration depending upon the amount of surfactant available (Figures 2.1a-2.1c). Monomers sorb individually by coulombic interactions to available exchange sites and also by hydrophobic tail group interactions. Chen et al. (1992) presented a model of sorption of HDTMA to muscovite above the CMC. Micelles rapidly sorb to the surface and rearrange as space and charge permit (Figures 2.1d-2.1f). A loosely packed bilayer is formed, growing to form a more densely packed bilayer. As the surface coverage increases, rearrangement slows. The hydrophilic micelles are less attracted to the increasingly hydrophobic surface, the release of the charge-balancing ions, such as Na^+ surface ions and Br^- counterions, is slowed through the bilayer, and slower growth toward the equilibrium bilayer arrangement occurs. Rearrangement and micelle sorption continue, based on electroneutrality, up to equilibrium.

Manne and Gaub (1995) presented an alternative to this final arrangement on the mineral surface. They used non-contact mode AFM to observe tetradecyltrimethylammonium on mica surfaces. Instead of rearrangement of the sorbed micelles to a bilayer, they noted the formation of linear features which were interpreted as elongated, tubular-type micelles. The features were mostly parallel, with some random scattering.

Atomic force microscopy (AFM) produces molecular-scale images of non-conducting substrates and has been used successfully to characterize zeolites at scales

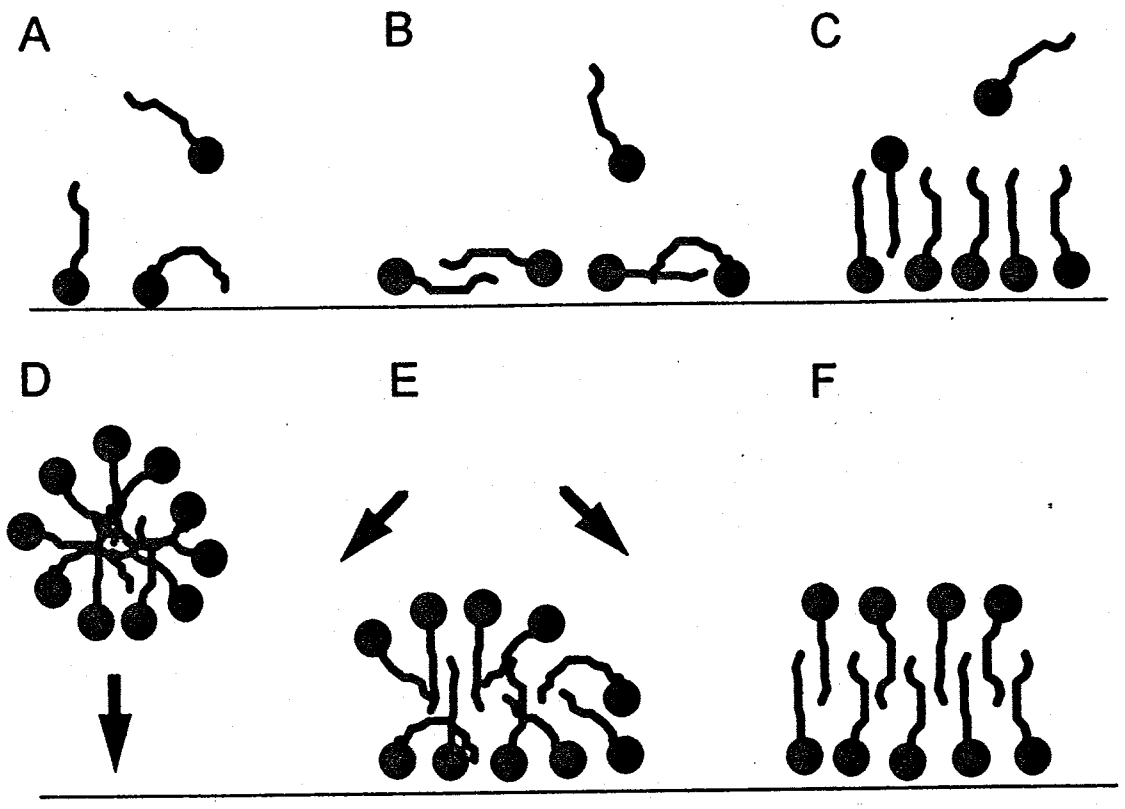

Figure 2.1. Concept of monomer, bilayer, and admicelle sorption on mineral surfaces. A and B show potential monomer conformations after sorption. C shows beginning development of a bilayer from monomer sorption. D through F show admicelle sorption, rearrangement and bilayer development when the solution is above the critical micelle concentration (adapted from Chen et al.1992.)

from 10 μm to 5 nm. Large crystals (>50 μm) of clinoptilolite are uncommon, and thus, studies of the mineral structure and surface are difficult at best (Smyth et al. 1990). To date, the reported AFM studies of zeolites describe macrocrystalline zeolites that were artificially cleaved; the present study, however, is concerned with microcrystalline clinoptilolite. Previous images produced with contact-mode AFM showed a repeating pattern comparable to unit-cell dimensions. Komiyama and Yashima (1994) imaged heulandite (isostructural with clinoptilolite) in air. Their images showed corrugations as they approached atomic resolution, but the structure did not match with crystallographic data. Scandella et al. (1993) found a similar framework structure on the a-c plane of heulandite with contact-mode AFM. They also noted that the surface unit-cell measurements were 26 % larger than the bulk unit-cell measurements made by X-ray diffraction. Weisenhorn et al. (1991) used contact-mode AFM with a fluid cell to image an artificially cleaved clinoptilolite surface that had been exposed to tert-butanol or tert-butyl ammonium ion. They observed a framework pattern comparable to repeating clinoptilolite unit cells. Clusters of tert-butanol molecules were observed on the clinoptilolite surface, but no clustering of the tert-butyl ammonium was detected.

We imaged at the near-molecular scale to view the distribution, conformation, and x, y, and z dimensions of the HDTMA molecules on the clinoptilolite surface. Most studies cited above used contact mode AFM, in which the tip is in continuous contact with the surface. This method has the disadvantage of applying lateral forces that can disturb fragile sample surfaces. Contact-mode AFM on dry samples often results in high repulsive forces between the probe and surface, which can damage the surface and limit

resolution (Zhong et al. 1993; Maurice, 1995). In TMAFM an applied voltage oscillates the probe so that it taps the surface many times for each data point. This produces extremely high resolution by reducing net repulsive and lateral forces to the range of 0.1 to 1 nanonewton (nN), preserving the probe and minimizing surface distortion (Zhong et al. 1993; Maurice 1995). Oscillation voltages can be varied to overcome repulsive forces from mineralogical changes, surfactant coatings, or other surface-probe interactions. The present study shows that TMAFM can be used to image sequential sorption of HDTMA onto a microcrystalline clinoptilolite surface. Molecular-scale images (to 50 nm) were obtained in air for clinoptilolite and surfactant-modified clinoptilolite, as well as for surfactant-modified muscovite as a comparison. We observed the surface structure of the unmodified clinoptilolite and the conformation of HDTMA on clinoptilolite and muscovite. We also measured the dimensions of HDTMA molecules on clinoptilolite and muscovite surfaces. An empirical estimate of modified clinoptilolite surface properties derived from TMAFM set point values is presented.

We compared the quantities of HDTMA sorbed via batch studies with the results of the HR-TGA analysis. HR-TGA is improved over previous thermal methods by the computerized correlation of temperature changes with measured weight loss. As discrete weight losses occur, the temperature is held constant until the loss is completed. TGA is widely used in the analysis of zeolites (Bish 1988, Ming and Mumpton 1989). HR-TGA pyrolysis temperatures should be higher for samples with more strongly bound HDTMA, such as that bound with both coulombic and van der Waals forces at sub-monolayer coverages (Figure 2.1a). If some of the HDTMA is bound only with hydrophobic forces,

such as in a bilayer (Figure 2.1f), the pyrolysis temperatures should be considerably lower. Here we present HR-TGA data showing the temperatures of water desorption and the pyrolysis and subsequent desorption of HDTMA. Desorption derivative peaks were correlated with breakdown of HDTMA in the outer and inner parts of the surface bilayer or admicelles.

MATERIALS AND METHODS

Materials

The zeolite investigated is a clinoptilolite-rich tuff from the St. Cloud mine in Winston, New Mexico. It consists of about 74 % clinoptilolite, 5 % smectite clay, 10 % quartz and cristobalite, 10 % feldspar, and 1 % illite, based on internal standard X-ray diffraction analysis (J. W. Carey, Los Alamos National Laboratory, personal communication, 1995; Chipera and Bish 1995). We measured an external cation-exchange capacity (ECEC) of 70 to 90 meq/kg for the St. Cloud clinoptilolite using the method of Ming and Dixon (1987). We also measured an external surface area of 15.7 m^2/g on a sample dried for 24 hours at 200°C. The analysis was performed with an ASAP 2000 surface area analyzer (Micromeritics, Inc., Norcross, GA) using the BET nitrogen adsorption method (Brunauer et al. 1938). The surfactant used for clinoptilolite surface modification was HDTMA bromide of greater than 99 % purity (Sigma Chemicals). Muscovite mica (Ted Pella, Inc., Redding, California) was freshly cleaved, treated with HDTMA, and imaged for comparison with the modified clinoptilolite. All aqueous solutions were made with 18.2 $Mohm \cdot cm^{-1}$ (ASTM Type I) water.

Surfactant modification

The clinoptilolite was saturated with sodium to ensure a uniform substrate by shaking 40 g of clinoptilolite for three 15-min rinses with 120 ml of 1 *N*, pH 5 sodium acetate buffer in a 500-ml polypropylene centrifuge bottle. The samples were centrifuged at 14500 x g, the supernatant discarded, and the entire sequence repeated two more times. This was followed by three rinses with Type I water and three rinses with 95 % ethanol, then air drying.

The sodium-saturated clinoptilolite was modified with surfactant to 0 %, 12.5 %, 25 %, 50 %, 100 %, and 200 % of its ECEC, where 100 % was assumed equal to 70 meq/kg clinoptilolite. Surfactant modification consisted of shaking 5 g of clinoptilolite with 20 ml of the selected HDTMA solution (0 to 70 mM) for 12 hr at 25°C in a 50-ml polypropylene Oak Ridge centrifuge tube. This amount of time was shown to be sufficient for complete reaction of HDTMA on clinoptilolite (Sullivan et al.1994). All solutions were well above the HDTMA CMC of 9×10^{-4} M. The HDTMA-modified clinoptilolite was centrifuged at 14500 x g and excess HDTMA solution decanted. The clinoptilolite was placed on a polypropylene filter in a Buchner funnel, rinsed with 3 to 5 ml of Type I water, and air-dried prior to analysis by TMAFM and HR-TGA. Appropriate blanks without clinoptilolite or HDTMA were also prepared.

The muscovite was cleaved to expose a fresh surface, immersed in a 5×10^{-4} M aqueous HDTMA solution for 10 minutes, removed, and allowed to air dry before TMAFM.

Tapping-mode atomic force microscopy

Sample mounts for the TMAFM were prepared by peeling a thin layer of dried clinoptilolite from the filter and attaching the peel to a magnetic sample disc with double-sided adhesive. This method ensured that no adhesive was imaged or could damage the TMAFM probe. Modified muscovite sheets were mounted with adhesive and trimmed to fit the mounting disc.

A Nanoscope III Scanning Probe Microscope station operating a Multi-Mode Atomic Force Microscope (Digital Instruments, Santa Barbara, California) was used in TappingMode™ for all scans. The microscope was equipped with a 12-μm nominal maximum scan-range scanner and 125-nm diameter silicon Nanoprobes. Scan rate and set-point voltages were adjusted for each sample as appropriate. Scan rates ranged from about 0.8 to 2 Hz. Relative humidity at the time of scanning was about 50 percent. Imaging was performed at the lowest possible tip pressure (set point), which was adjusted by retracting the tip until the surface was disengaged, then gradually readvancing the tip until the surface was contacted with minimum pressure. Scanned areas ranged from 8 μm by 8 μm square to 50 nm by 50 nm square. Each sample was scanned in a series from larger to smaller scan size while maintaining the beginning x-y coordinates, with areas of interest selected from the previous scan. This way, locations on specific crystal faces and specific features of interest could be correlated among different images. This method reduced the likelihood of mistaking noise or resonant frequencies for actual surface

features. Most images were scanned at a resolution of 512 data points per scan line. Some images were scanned at 256 points per line.

Post-image processing was kept to a minimum. Low-pass filtering was applied to most sample images and did not affect the features of the images. Some images were flattened to resolve the z-scale, and some were very slightly contrast-enhanced to improve clarity. The flattening and contrast enhancement also did not affect the features of the images except to bring forward darkened areas at the edges of the scanned region. This was necessary due to the low microscopic topography encountered in some samples. The shading of the z-scale was adjusted as appropriate for each image depending upon topography. Surface topography was measured with the image processing software provided with the Nanoscope system. Horizontal and relative vertical measurements were made from point to point on the screen using the mouse and cursor. At least 20 relative vertical scale measurements were chosen from the x,y,z data files for each image of modified clinoptilolite or modified muscovite to measure the thickness of the HDTMA imaged on the surface. Relative z-values given here are the average values.

High-resolution thermogravimetric analysis

HR-TGA was performed on a Hi-Res™ TGA 2950 (TA Instruments, New Castle, DE). About 10 mg of dried, modified or unmodified clinoptilolite was placed on a platinum micro-balance pan. The oven was purged with He gas, and the clinoptilolite weight loss was measured from 30°C to 900°C. Optimum resolution was obtained with a resolution setting of 4 and a sensitivity setting of 4. These two parameters permit

adjustment of the equipment's patented feed-back algorithm. The resolution setting adjusts the temperature ramp in response to a weight change, whereas the sensitivity setting adjusts when a weight changed is detected. Both these parameters are relative to the preset temperature ramp rate. These parameters are empirical and optimal settings are arrived at by repeated trials. We used weight loss vs. temperature curves and the resulting derivative curves in our analysis. The derivative of the weight loss curve was calculated at 2.5°C min^{-1} smoothing.

RESULTS AND DISCUSSION

Low-resolution TMAFM images

Unmodified clinoptilolite samples at the 1.25-μm scale (Figure 2.2) exhibited well-defined, monoclinic crystals with excellent crystal faces, and well-defined crystal edges in the a-c plane. Small crystal fragments which had adhered to the flat crystal faces and edges were observed. Step heights of 65.7, 35.7, and 17.5 nm were measured, which closely correspond to multiples of the 17.9-nm b-spacing of a unit cell. Figure 2.2 also clearly shows crystals with a β angle of 116°. These images are comparable to microprobe or electron microscopy images in quality and scale.

As surface coverage of HDTMA increased, smaller, more agglomerated crystals and more poorly-defined crystal edges were noted in the 1-μm (approximate) scale samples (Figure 2.3). The apparent sharpness of the images decreased with increasing surfactant coverage. In addition, increased topography was noted, and fewer flat crystal surfaces were available for imaging. Some samples showed a buildup of striated

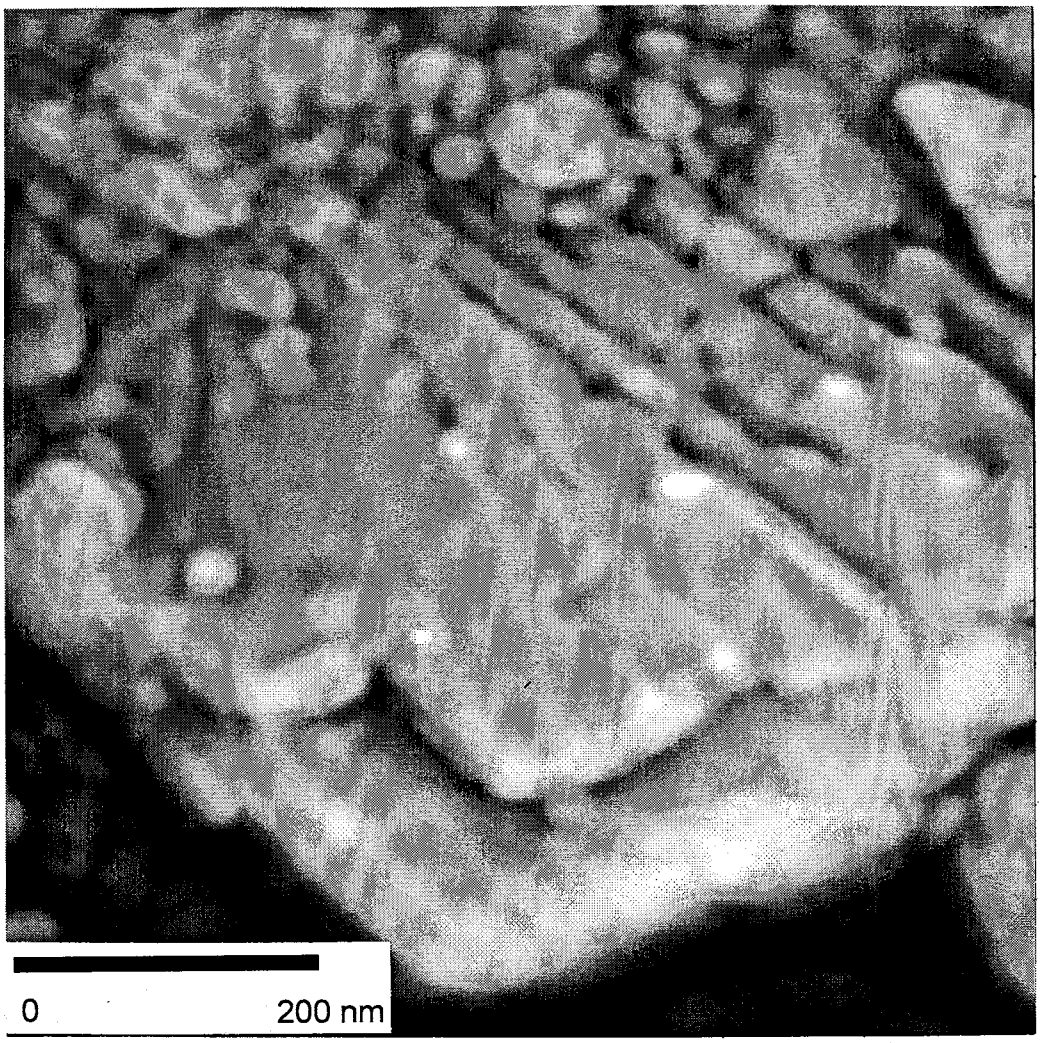

Figure 2.2. Unmodified St. Cloud clinoptilolite. Image covers 1.25-μm by 1.25-μm.

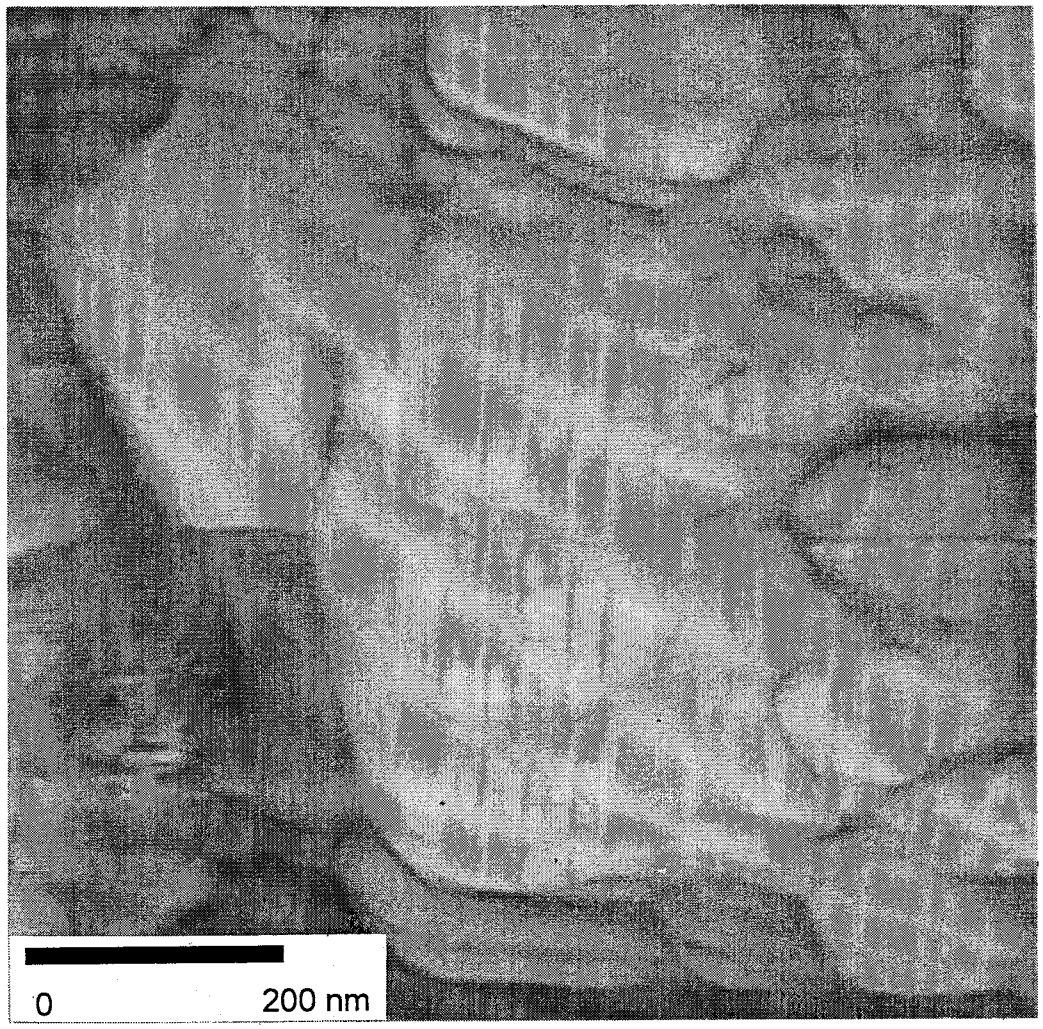

Figure 2.3. Clinoptilolite modified to 25 % of ECEC with HDTMA. Image covers1-μm by 1-μm.

surfactant material at and above 50 % coverage (Figure 2.4). These features are likely clusters of HDTMA molecules lying on the surface. It is unlikely that the features are the result of dragging of HDTMA material by the TMAFM probe because of the low pressure exerted by the probe on the surface and because the striations appear to follow the orientation of the crystal surface, not the left-to-right probe scan direction. These linear features lie along different directions for different crystals, indicating that they may be controlled by the underlying structure of the crystal. The surfaces appear to be completely covered with these features. When they are distinct, they are similar to linear features reported by Manne and Gaub (1995) on mica, which were spaced 5.3 nm apart. The ridge-like features here are about 5- to 9-nm wide and are separated by about 5- to 9-nm wide spaces. At 100 % treatment, the crystals are more rounded and less distinct (Figure 2.5). Flat surfaces and cleavage planes are less visible, although small crystals can still be seen. In the 200 % coverage image (Figure 2.6), there appears to be excess buildup of HDTMA at the edges of crystal cleavage planes or steps. Additional exchange sites may be available in these locations due to the exposure of parts of the interior channel structure.

High-resolution TMAFM images

A distinct, reproducible, grid-like pattern was noted on the unmodified sample (Figure 2.7) and also on the 12.5 % and 25 % modified samples at the 50 nm by 50 nm scale (Figures 2.8 and 2.9). No pattern was distinguishable at higher treatment levels (Figure 2.10). The grid spacing varied in scale slightly between images, most likely due

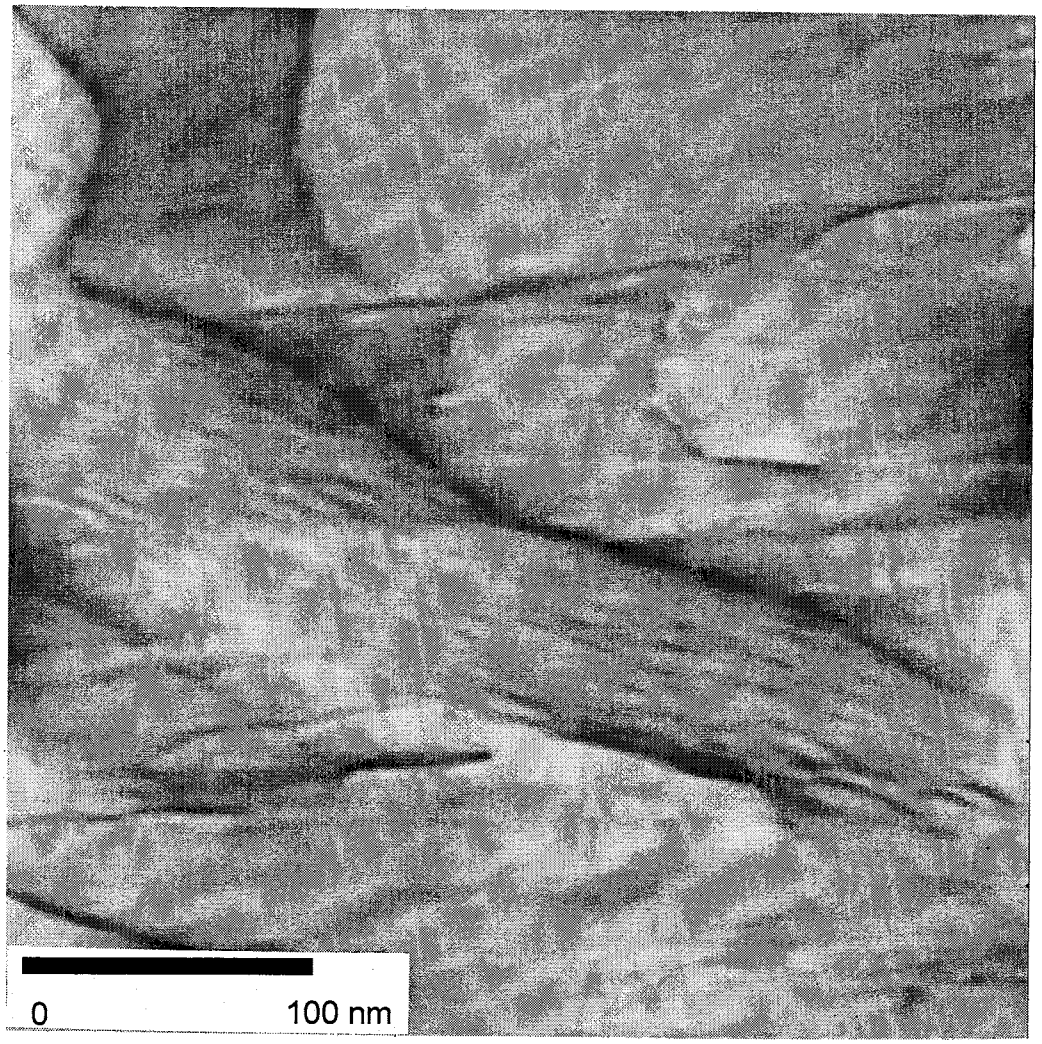

Figure 2.4. Clinoptilolite modified to 50 % of ECEC with HDTMA. Image covers 1-μm by 1-μm.

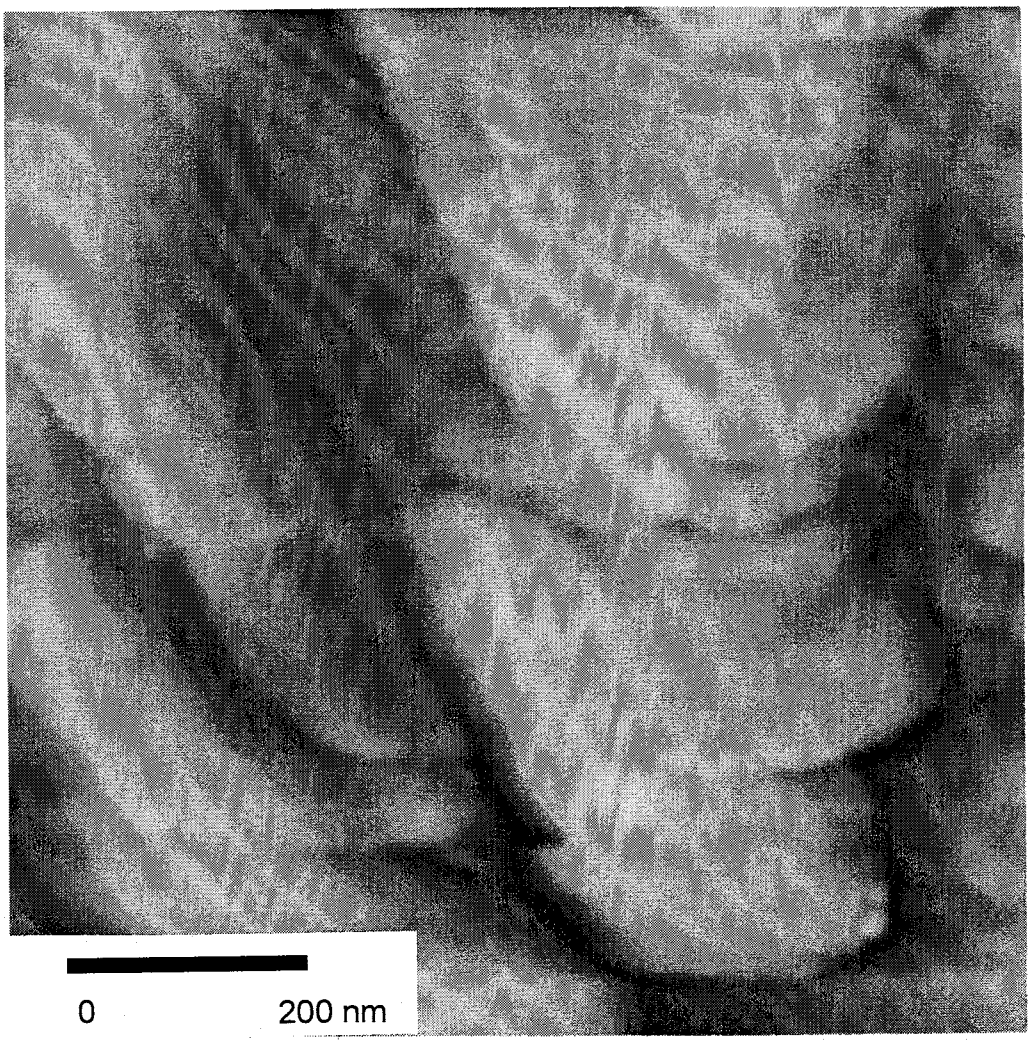

Figure 2.5. Clinoptilolite modified to 100 % of ECEC with HDTMA. Image covers 1-μm by 1-μm.

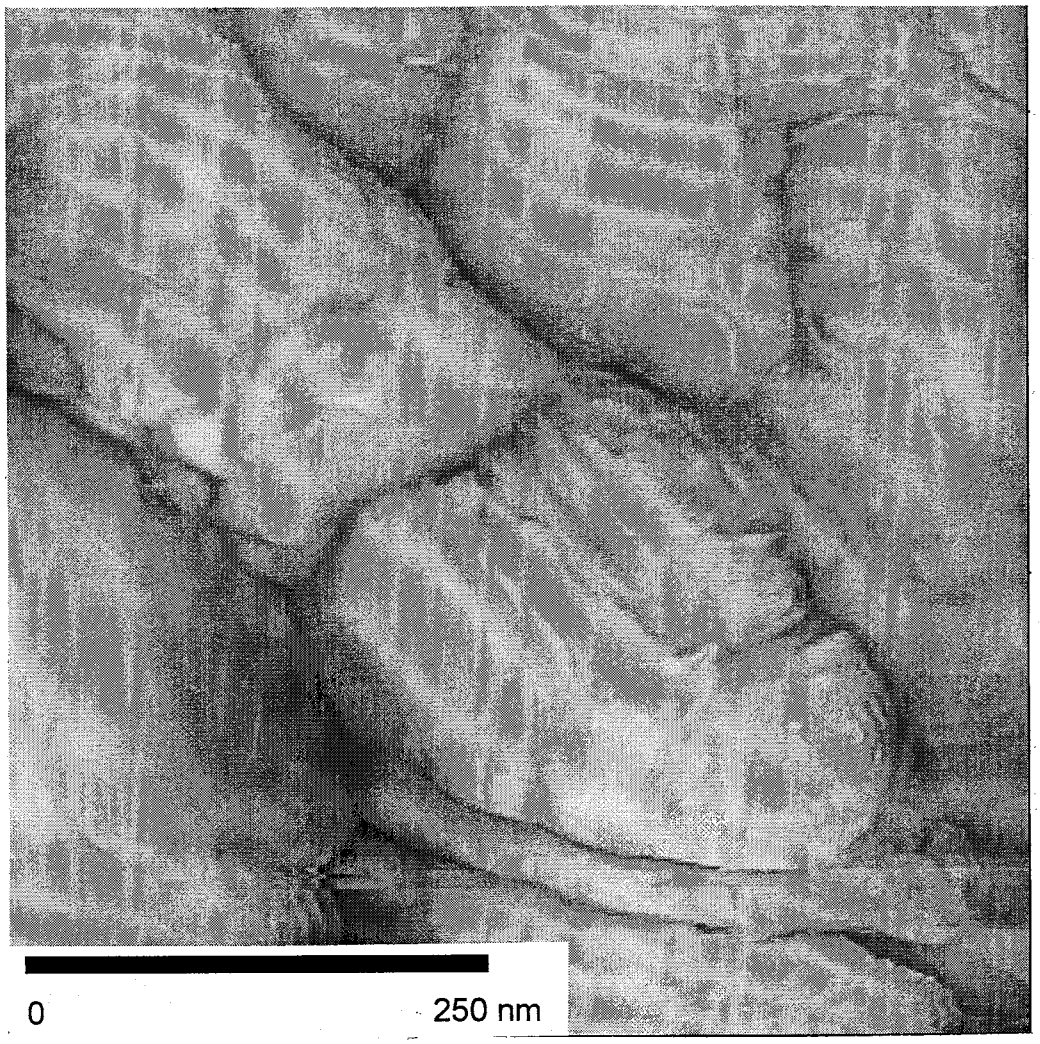

Figure 2.6. Clinoptilolite modified to 200 % of ECEC with HDTMA. Image covers 1-μm by 1-μm.

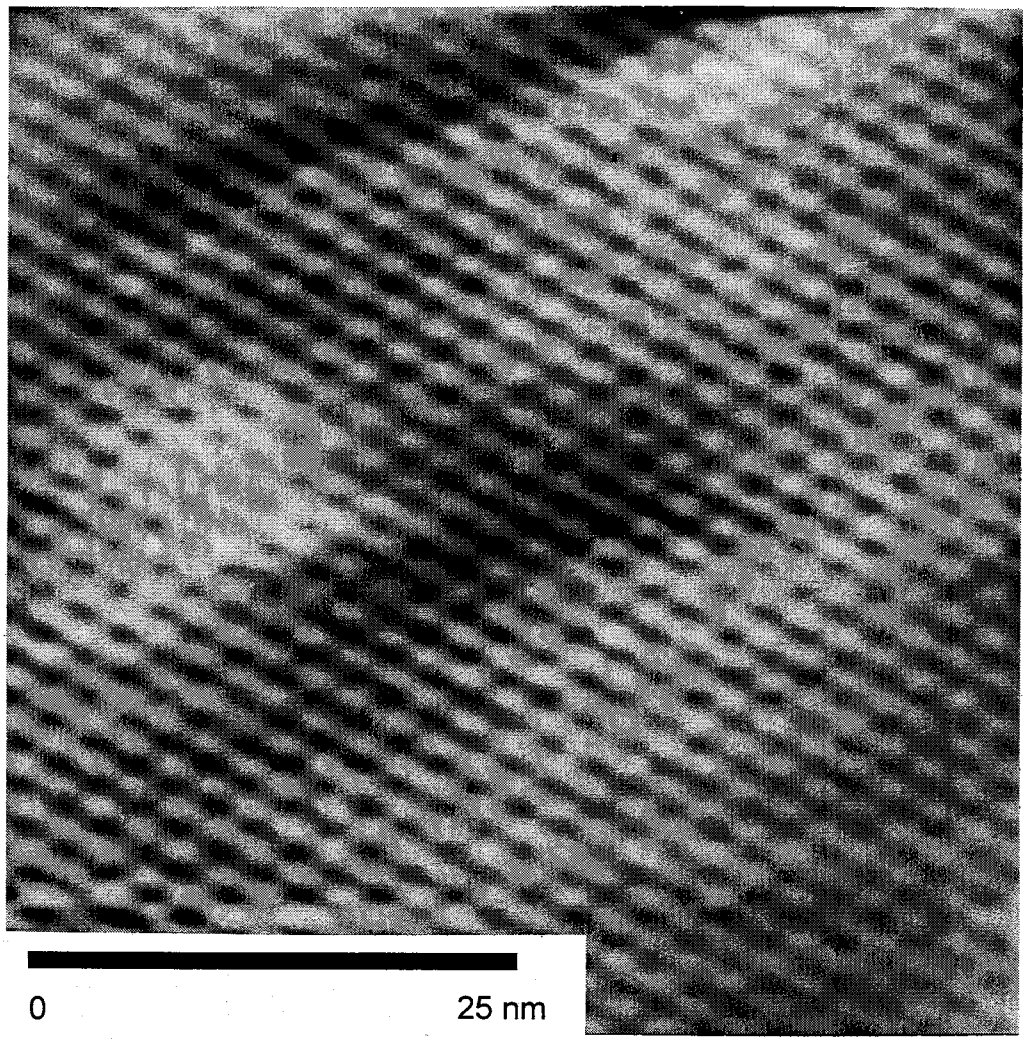

Figure 2.7. Unmodified clinoptilolite sample. Image covers 50-nm by 50-nm.

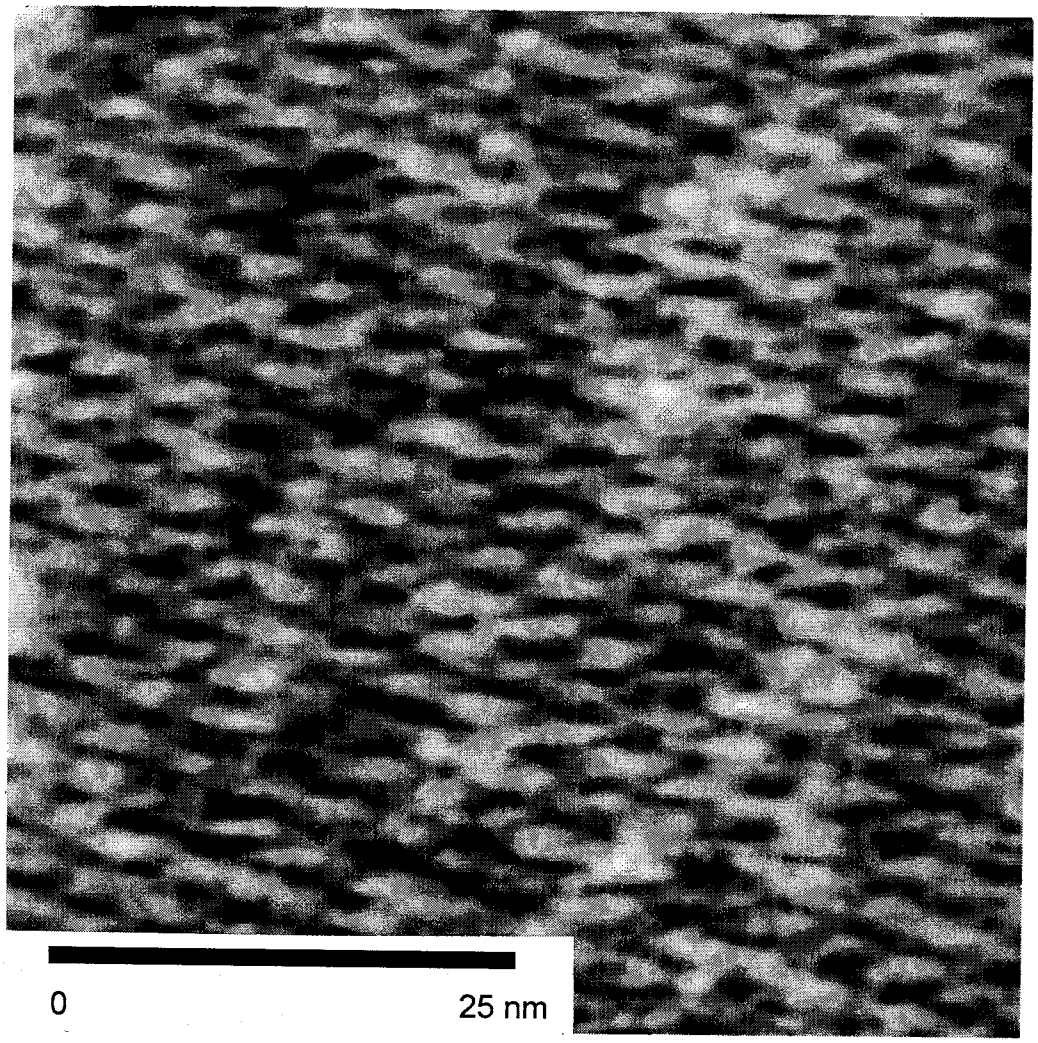

Figure 2.8. Clinoptilolite modified to 12.5 % of ECEC with HDTMA. Image covers 50-nm by 50-nm.

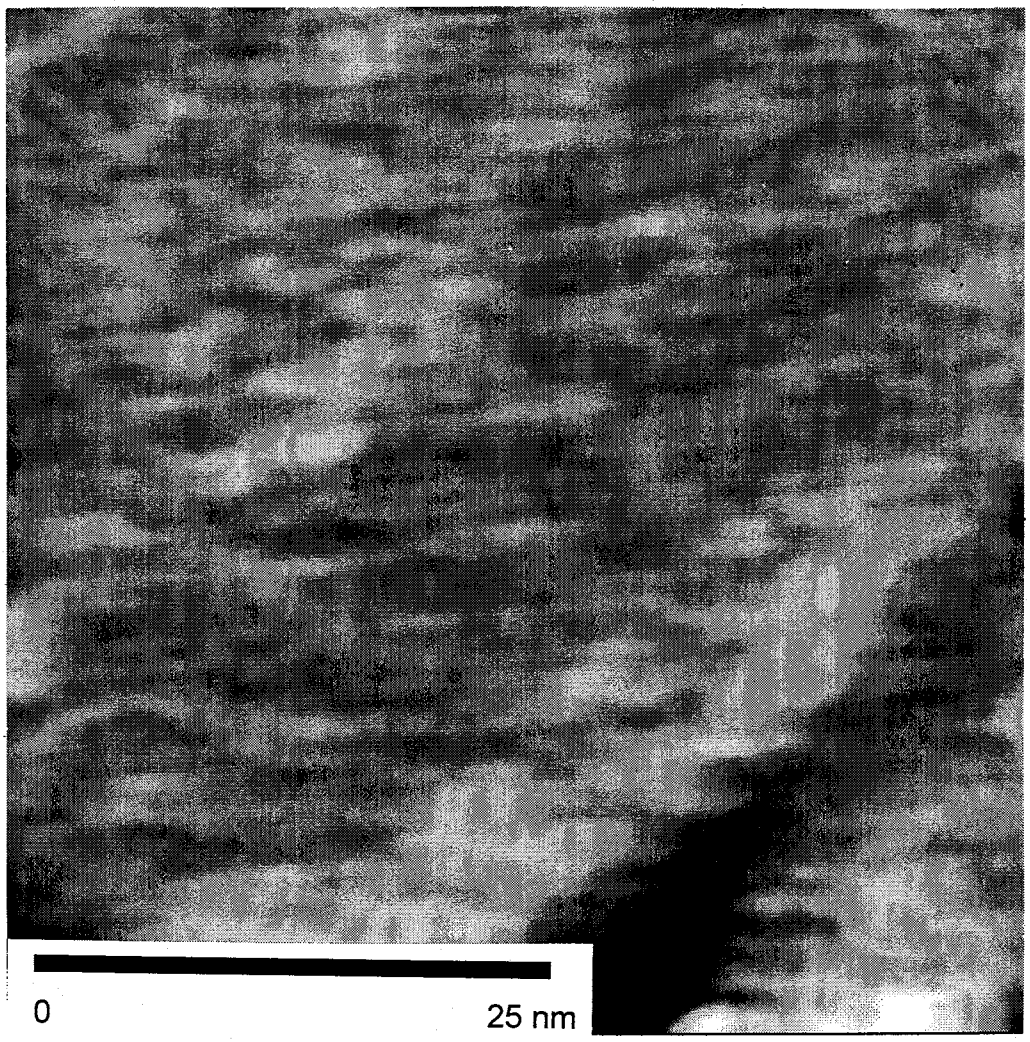

Figure 2.9. Clinoptilolite modified to 25 % of ECEC with HDTMA. Image covers 50-nm by 50-nm.

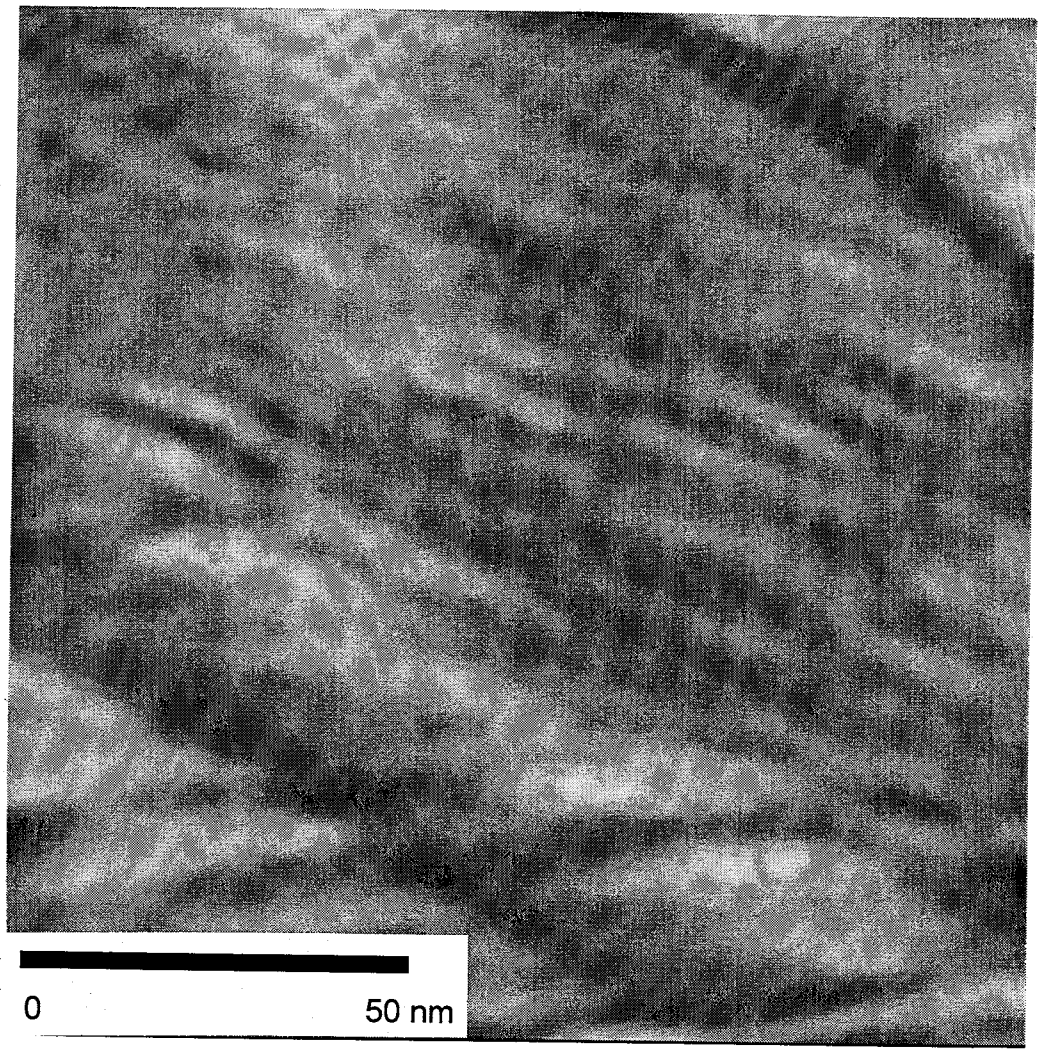

Figure 2.10. Clinoptilolite modified to 50 % of ECEC with HDTMA (close-up of figure 2.4, center section). Image covers 125-nm by 125-nm.

to the angle of the crystal and tip interaction. The grid pattern can be compared to previously published clinoptilolite images of the a-c plane from contact-mode microscopy under fluid (Scandella et al. 1993; Weisenhorn et al. 1991). Those images, however, were of large (1.9 x 1.2 mm) crystals that had been artificially cleaved while these are of uncleaved, air-dried crystals. Topographic features at this scale are controlled by the shape of the repulsive electron clouds (Stipp et al. 1994) and are to some extent a convolution of the shape of the tip and the surface topography, although this is minimized by tapping mode (MacDougall et al. 1991; Zhong et al. 1993). The high points correspond to electron-dense sites, such as the hydroxyl groups, that form at cleavage sites on the a-c plane, and also correspond to some framework oxygen locations. The pattern is interpreted to be an expression of these hydroxyl groups or oxygens which extend slightly above the a-c plane.

HDTMA appears on the surface of the clinoptilolite as elongated zones or linear features that obscure the surface grid pattern (Figures 2.8, 2.9 and 2.10). The size of these features on the 12.5 % treatment sample is about 20 nm in length, 2 nm across, and 0.4 nm high in relation to the adjacent clinoptilolite surface, based on a number of measurements made from the x, y, and z data file. These features are several times longer, but about the same z-dimension, as the most elongated possible dimension of an HDTMA molecule (3.5 nm long by 0.4 nm diameter), and wider than the average HDTMA micelle diameter of approximately 4.3 nm (Israelachvili 1991). These features are probably horizontally oriented clusters of surfactant molecules. A single micelle with an aggregation number of 95, when rearranged to a monolayer, could cover about 83 nm^2

on the surface with closely packed HDTMA molecules (Israelachvili 1991), about double the observed feature size. The z-dimension of the features is an indication that the HDTMA tail groups are lying close to the surface. In these images, HDTMA appears sorbed in elongated clusters, rather than regularly distributed across the surface or in rounded areas, which might be expected from symmetrical micelle spreading. This may be an indication of the distribution of cation exchange sites on the surface, rearrangements of the surfactant due to agitation during the equilibration process, or other effects, such as attractive forces between HDTMA tail groups. On the 25 % treatment sample (Figure 2.9), the linear features are thicker (about 0.8 nm) and are almost fully covering the grid pattern on the surface. At 50 % treatment (Figure 2.10), no grid pattern was apparent and the surface appears coated with linear agglomerations of HDTMA. No reference surface was visible to measure the z-dimension of the HDTMA at 50 % treatment or greater.

Figure 2.11 is an image of unmodified muscovite and Figure 2.12 is an image of muscovite which was exposed to an aqueous HDTMA solution. The purpose of these images was to compare HDTMA sorbed on a well-understood, frequently imaged surface versus the lesser-studied and more variable natural clinoptilolite surface. The HDTMA on the surface of the muscovite appears as two types of features (Figure 2.12). Small, round features as well as regions of dendritic features are visible. The round features have an average diameter of about 6 nm. These are likely small clusters of HDTMA monomers. The height of the round features is between 0.2 to 0.4 nm, similar to the expected z-dimension of an HDTMA molecule at the surface. The dendritic features

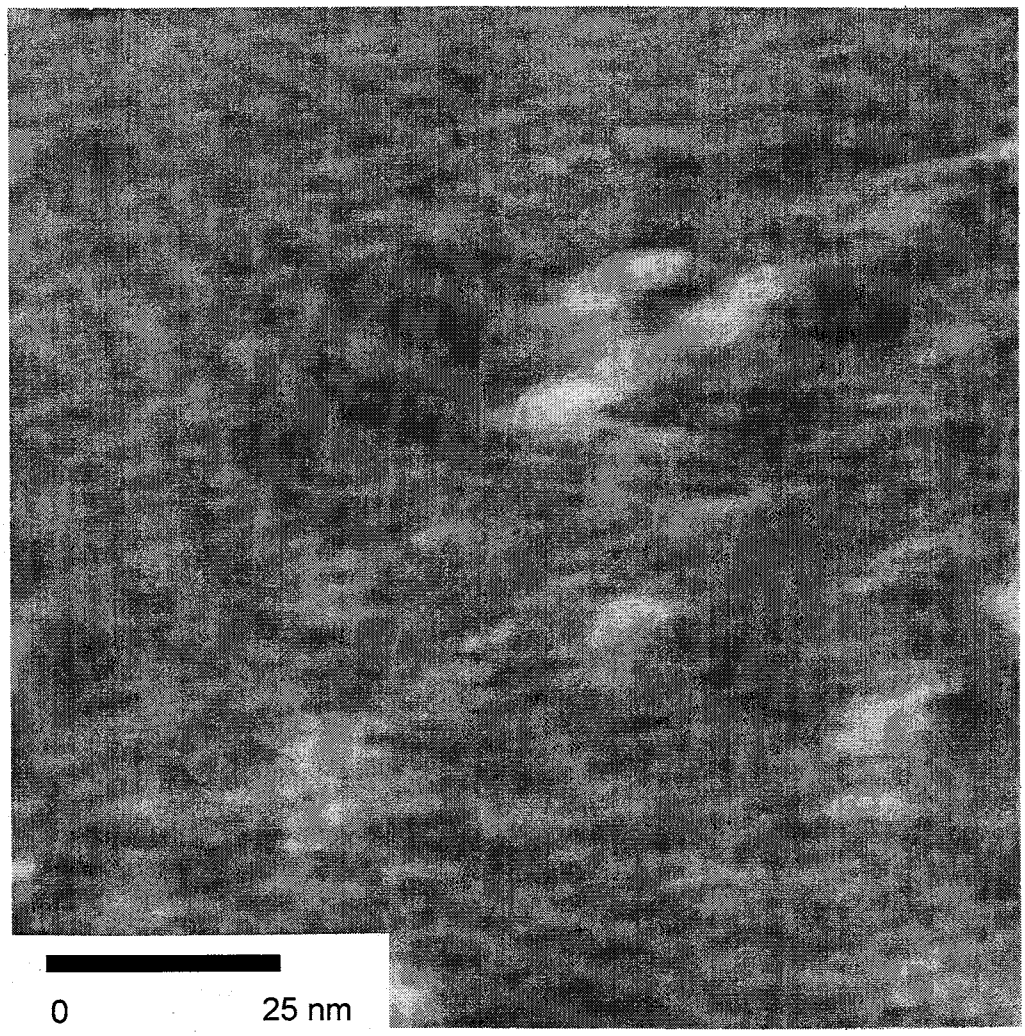

Figure 2.11. Unmodified muscovite mica sample. Image covers 100-nm by 100-nm.

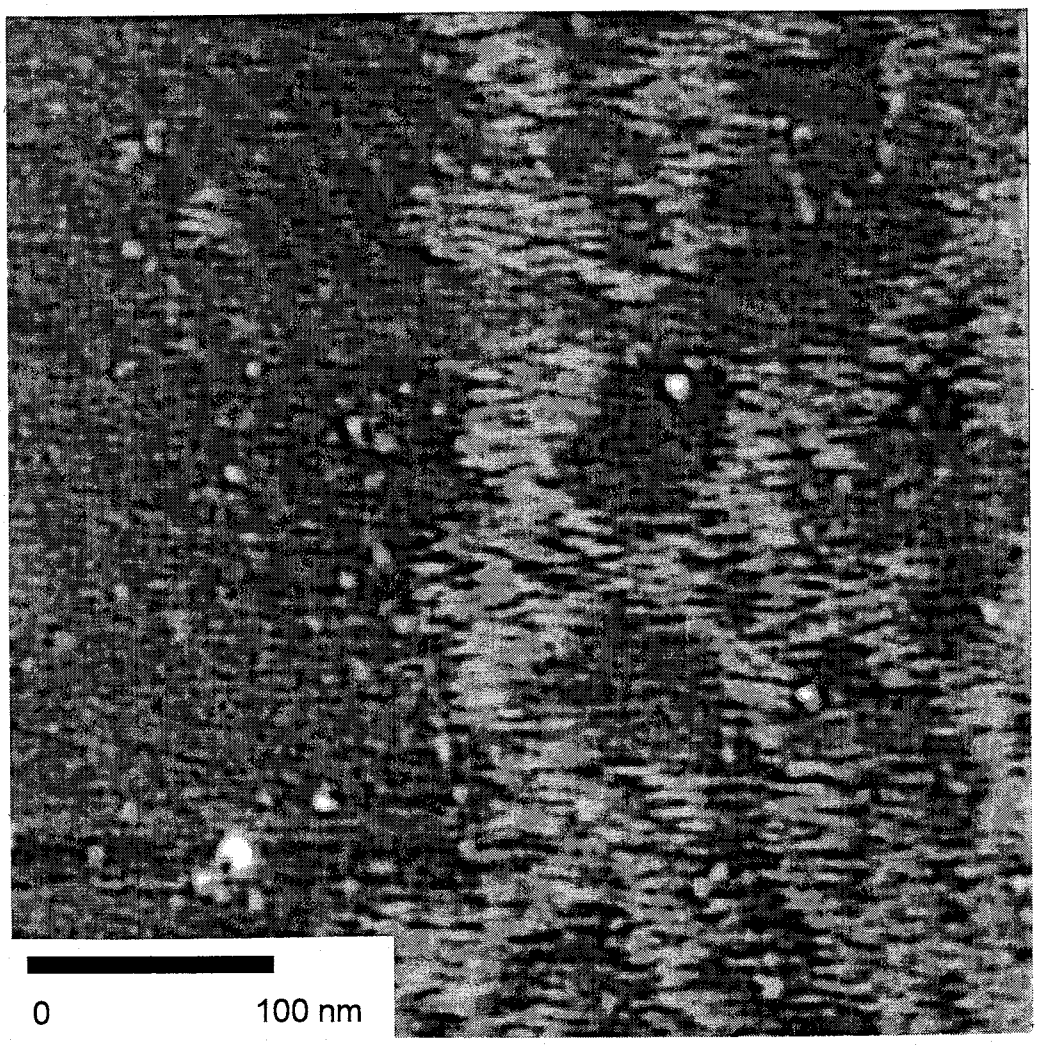

Figure 2.12. Muscovite mica exposed to an aqueous HDTMA solution. Image covers 100-nm by 100-nm.

average 3.4 nm in width and 0.2 to 0.4 nm in height. These features are similar in dimension and form to those seen on the clinoptilolite modified to 12.5 % and 25 % of the ECEC. The z-dimensions compare favorably to the HDTMA molecule thickness calculated above.

Although the TMAFM images are from air-dry clinoptilolite samples, they give some indication of the topology of the surfactant-modified surface and the extent and conformation of HDTMA coverage on a small scale. Sorption of HDTMA on clinoptilolite is in clusters if the solution concentration is greater than the CMC. At lower loading (12.5 %), the z-dimension of the HDTMA clusters is no greater than one HDTMA molecule diameter, indicating that rearrangement to a monolayer has occurred, and that the tail groups lie close to the clinoptilolite surface (Figure 2.1b). This is predicted by the model presented by Chen et al. (1992). At higher loading (25 %), the z-dimension increases, indicating localized "stacking" or crossing of tail groups, and possibly buildup of a loose bilayer or admicelles. The images at all surfactant loadings show close association between the surfactant tails and the surface. At a surface loading rate of 70 meq/kg of HDTMA (100 % of ECEC), the surfactant molecules would cover no less than 15.9 m^2/g, based solely on the head group van der Waals radius and ignoring any space taken up by the tail groups (Israelachvili 1991). This molecular area is about the same as the available external surface area of 15.7 m^2/g. At lower loading rates, the tail groups would probably take up space on the surface and overlap. Buildup of admicelles or some form of a bilayer is likely on these samples due to the spatial limitations of the surface. Another possibility is the buildup of cylindrical surfactant

aggregates (Manne and Gaub 1995), which may account for the linear features in Figures 2.4, 2.8, 2.9 and 2.10.

Zhang et al. (1993) theorized that the stability of the HDTMA sorption to montmorillonite was due not only to cation-exchange effects but also was a function of the length of the tail group and the subsequent van der Waals forces between the tail and the surface. Entropic or hydrophobic forces also tend to exclude large hydrocarbon chains from the bulk water structure (Israelachvili 1991). HDTMA-modified clinoptilolite has been shown to be very stable even in the presence of high ionic strength solutions or organic solvents (Bowman et al. 1995). The above observations show that HDTMA sorption to clinoptilolite is a function of cation exchange, van der Waals forces, and hydrophobic forces acting together.

HR-TGA results (see below) show that a significant amount of water was still adsorbed to the external clinoptilolite surface during these room-temperature TMAFM measurements. The gravimetric water content of the unmodified and surfactant-modified zeolites changed from about 11 % before to 7 % after drying at 200°C, based on the HR-TGA data below. The water lost below 200°C can be assumed to be external surface water (D. L. Bish, Los Alamos National Laboratories, personal communication, 1995). Assuming a van der Waals radius for water of 0.0616 nm, the water content can be translated to more than nine layers of water on the external surface of the clinoptilolite. Studies of organic vapor sorption onto mineral surfaces have indicated that surface water at thicknesses greater than four layers tends to behave more as bulk water than as structurally "fixed" water (Ong and Lion 1991; Petersen et al. 1995). The presence of

this bulk water on the surface of the air-dry clinoptilolite implies that surfactant behavior in these studies may be similar to that for water-saturated systems.

TMAFM probe-surface interactions

Changes in the set point voltage, or tapping force, of the TMAFM probe may indicate surface changes. This is true if the probe used and the drive and root-mean-squared (RMS) amplitudes remain the same throughout and between images (K. Kjoller, Digital Instruments Corp., Santa Barbara, California, personal communication, 1995). The set point is an averaged value for an entire scan or set of scans and is most relevant to the total surface area scanned, rather than specific areas or features measured.

Surfactant buildup on the clinoptilolite surface produced increased repulsion of the silicon TMAFM probe. An increased set point was needed to provide enough voltage to allow the tip to contact the surface and overcome this repulsion. The mean set point voltage for five different series of images is plotted as the mean and standard deviation vs. the HDTMA surface treatment level in Figure 2.13. A single probe was used sequentially on a minimum of 10 similarly modified samples for each series. Probes were changed between samples modified at different loading levels but the RMS amplitude was consistently set at zero and not changed throughout the series. The set point voltage under these conditions was noted to increase from the 0 % treatment level through the 25 %, 50 %, and 100 % treatments (Figure 2.13), which was interpreted as an increase in average surface hydrophobicity. A decrease in the mean was noted for the 200 % samples, probably due to a decrease in average surface hydrophobicity because of charge

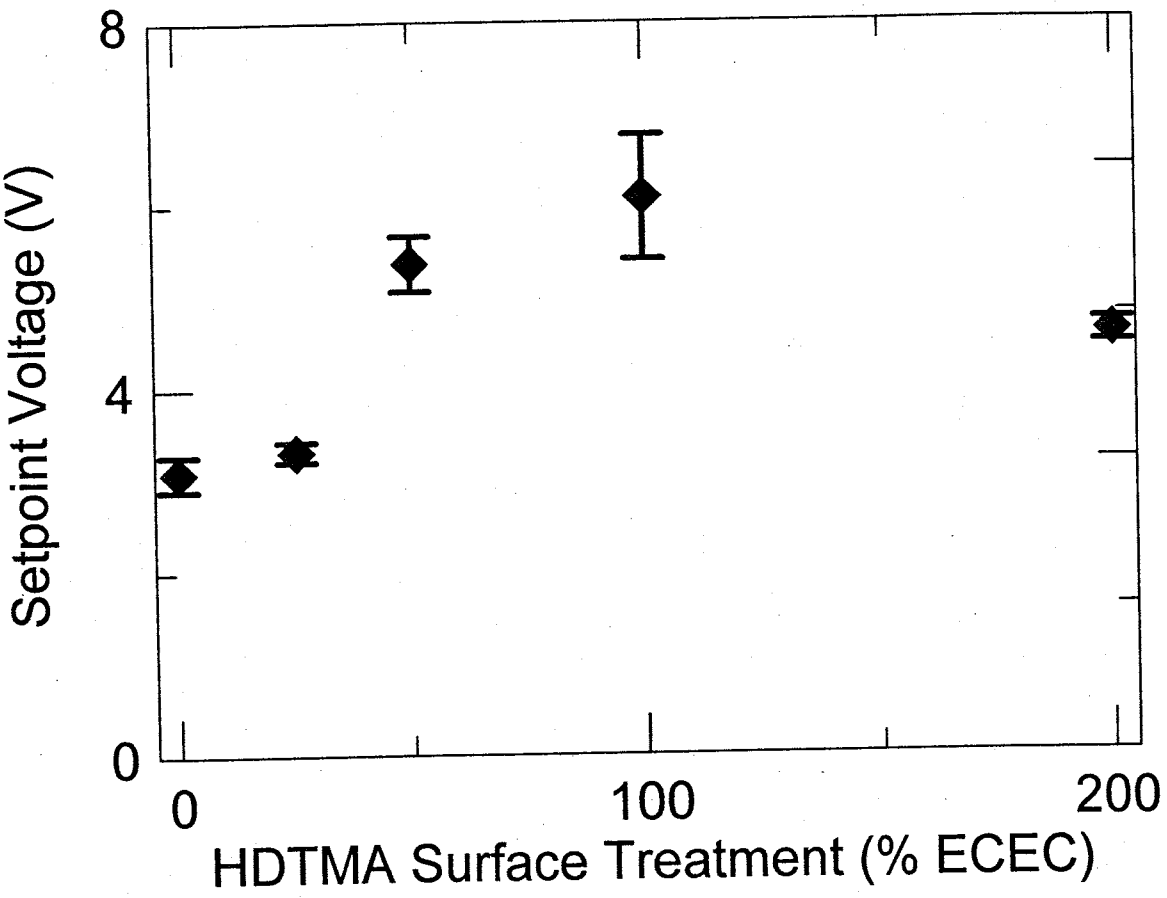

Figure 2.13. Mean set point voltage for five different series of images, plotted as the mean and standard deviation versus the HDTMA surface treatment level.

reversal on the surface with buildup of the surfactant and a change in surfactant orientation to expose hydrophilic head groups. Other explanations of the observed trend include increasing "softness" of the surface due to HDTMA buildup on the probe, or the presence of increasing amounts of water on the surface. A consistent downturn, however, for all samples at the 200 % treatment level contraindicates the effect of "softness", because it is unlikely that these effects would have occurred at 200 % and not on the 100 % treatment samples, which appear very similar in the micrographs. HR-TGA results below indicate that water content is about the same for all samples, regardless of treatment level, and therefore attractive forces due to sorbed surface water should be approximately constant among all samples.

High-resolution thermogravimetric analysis

The results of the HR-TGA are shown as weight loss curves in Figure 2.14 and the accompanying derivative curves in Figure 2.15. The figures show weight losses for clinoptilolite, HDTMA, and a series of HDTMA-modified clinoptilolite samples, from 25 % to 200 % of ECEC. Almost all of the weight of HDTMA bromide is lost upon heating to 232°C and is seen clearly as a large, sharp peak in the derivative curve (Figure 2.15). A small amount of weight loss, about 11 %, occurs for the unmodified clinoptilolite from 30° to 400°C. This is due to water desorption (Bish 1988). In the weight loss curves (Figure 2.14) for the modified clinoptilolite, we observed a sequential loss of mass due to both water desorption and HDTMA pyrolysis and desorption. The 25 % and 50 % modifications showed similar behavior to each other, however, replication of these

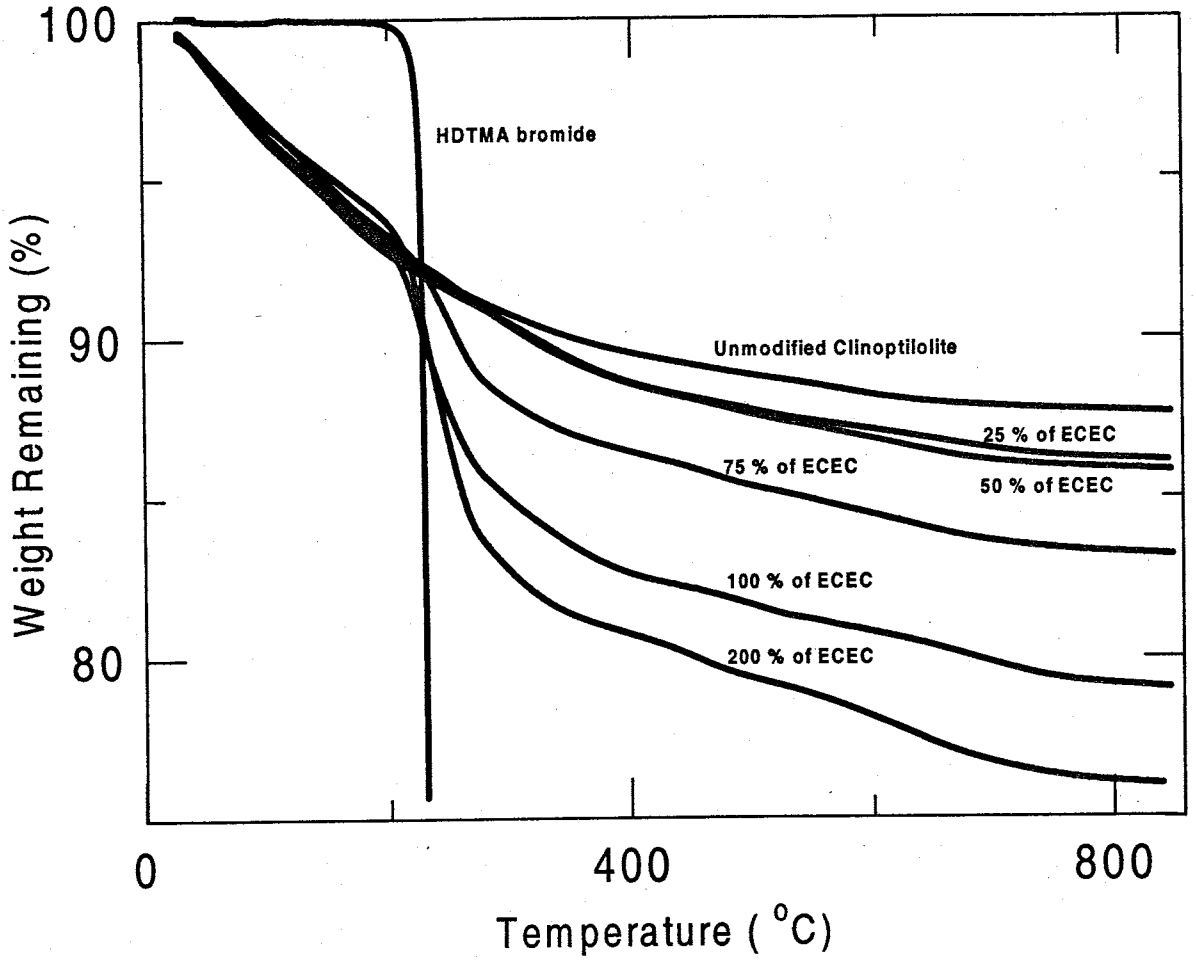

Figure 2.14. Weight-loss curves from HR-TGA analysis for unmodified clinoptilolite, HDTMA bromide, and a series of HDTMA-modified clinoptilolites from 25 % to 200 % of ECEC.

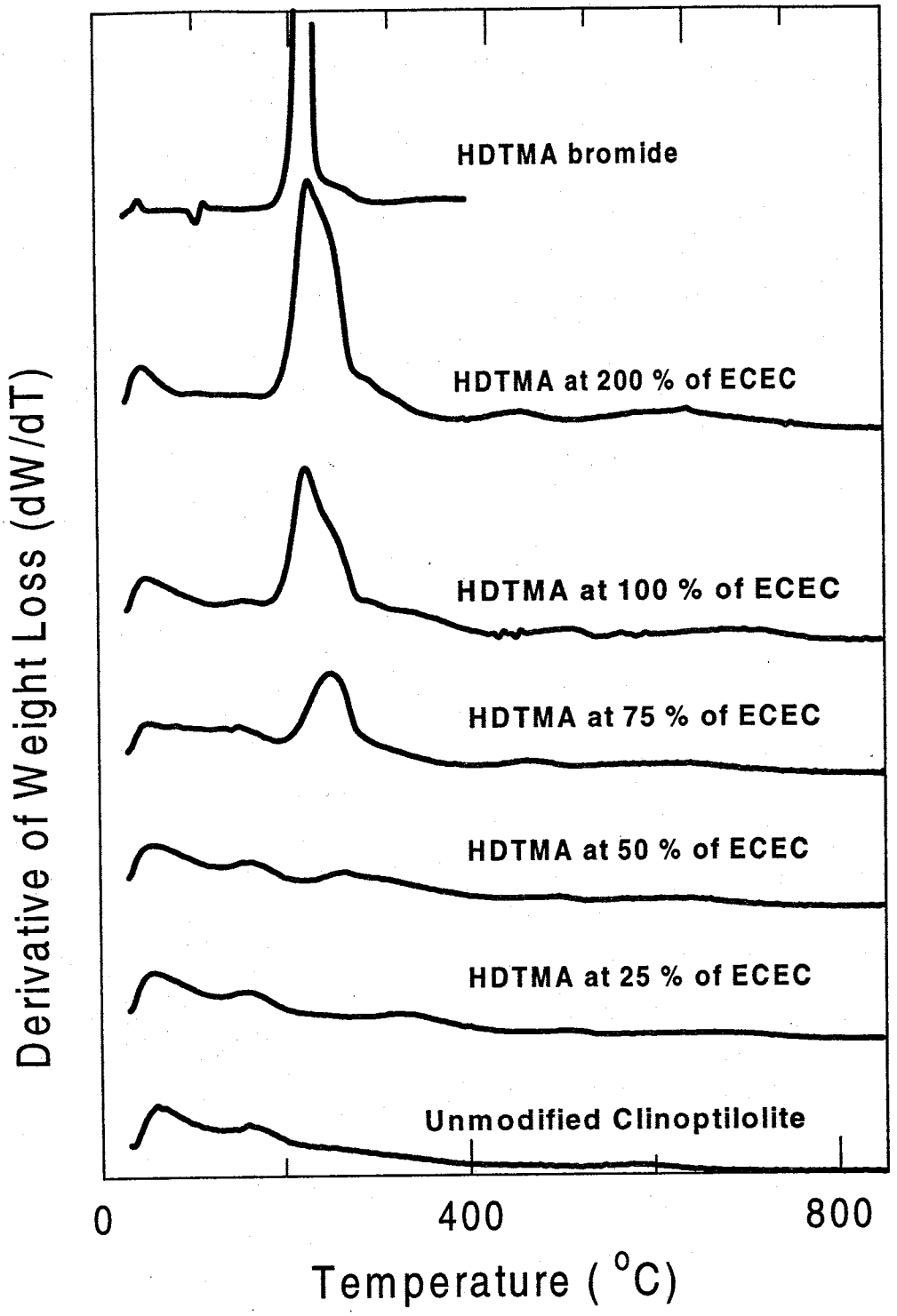

Figure 2.15. Derivative curves from the HR-TGA analysis for unmodified clinoptilolite, HDTMA bromide, and a series of HDTMA-modified clinoptilolites from 25 % to 200 % of ECEC.

treatments and TGA analyses yielded the same results. In the derivative curves of the modified zeolites (Figure 2.15), the first water-loss peak occurs at about 50°C, followed by a second water-loss peak at 159°C. Further water loss is the cause of the continued gradual slope of the baselines to 800°C (Bish 1988). No other peaks occur on the unmodified clinoptilolite curve. Weak, broad peaks at 265.6°C and 334°C are seen in the derivative curves for the 50 %- and 25 %-modified samples. These losses correspond to pyrolysis of HDTMA from higher-energy bonding sites, probably material that is closely bound to the clinoptilolite surface and is therefore stabilized with respect to pyrolysis. A stronger peak at 251.6°C is seen for the 75 %-treatment sample and is indicative of an intermediate bonding state of HDTMA, slightly less stabilized than seen for the lower loading levels. This peak underlies a shoulder evident in the two largest peaks, which correspond to HDTMA losses from the 100 %-and 200 %-modified samples. These large peaks are found at 230°C, with the shoulder at 253.6°C. The large peaks can be directly correlated with the unbonded HDTMA weight loss derivative, and correspond to removal of HDTMA from lower-energy or less-stabilized bonding sites such as the external portion of a bilayer or admicelle. The HDTMA is held in those sites with weaker hydrophobic or van der Waals forces. This difference in pyrolysis temperature and peak breadth between the low and high loading levels indicates stronger, more complex bonding of HDTMA at lower treatment levels, presumably because of cation exchange or other chemical bonding effects in combination with van der Waals forces.

The above evidence from the TMAFM and HR-TGA correlates well with the surfactant sorption model proposed by Chen et al. (1992). Thickening of the surfactant

layer beyond a monolayer and the presence of zones of surfactant coverage on the clinoptilolite surface at 25 % of the ECEC and above indicates the possibility of the presence of rearranged admicelles at the lower treatment levels. The pyrolysis energy differences between higher treatment levels (greater than 75 %) and lower treatment levels (less than 75 %) also indicate that admicelles or some form of a bilayer exist on the surface at less than 100 % of the ECEC. This is consistent with the TMAFM z-dimension measurements, which suggest multiple tail group buildup at as low as 25 % loading. It also appears that at low treatment levels, HDTMA sorption to the surface may be stablilized by van der Waals forces between the surfactant tail group and the clinoptilolite surface. This stabilization is probably very similar to that proposed for clays (Zhang et al. 1993).

SUMMARY AND CONCLUSIONS

TMAFM images were obtained in air for unmodified and surfactant-modified forms of microcrystalline clinoptilolite and for surfactant-modified muscovite. The molecular structure of the clinoptilolite is apparent in the higher-resolution images and compares well to previously reported fluid cell images of much larger, artificially-cleaved crystals. Features of the surfactant noted on the clinoptilolite surface include a dendritic, clustered sorption pattern, which corresponds to agglomerations of surfactant molecules, and extensive coverage of the surface at low loading levels with near complete coverage at 50 % of the ECEC. The z-dimension of the sorbed material is on the order of multiples of the average van der Waals diameter of a hydrocarbon chain. Overlap of

chains suggested some form of admicelle or bilayer formation with increased coverage. Comparisons with HDTMA sorbed onto muscovite showed similarities between HDTMA conformation on the two mineral surfaces and yielded comparable measurements of surfactant cluster length and z-dimension. Comparisons of surfactant size, loading, and available external surface area measurements show that the surfactant can cover the mineral surface extensively even when the equivalents of surfactant applied are less than 100 % of the ECEC. Setpoint voltage measurements indicated increased hydrophilicity of the surface at the 200 % loading level, suggesting charge reversal.

HR-TGA results showed significant stabilization of HDTMA sorbed at 75 % and lower loadings compared to that sorbed at higher loadings. This is due to the combined stabilization effects of coulombic and van der Waals forces between HDTMA and the clinoptilolite surface.

ACKNOWLEDGMENTS

This study was supported by a student research grant from The Clay Minerals Society, the Oak Ridge Institute for Science and Education research travel program, Waste-Management Education and Research Consortium (WERC) Grant No.01-4-23190, contract DE-AC09-76SROO-819 between the U.S. Department of Energy and The University of Georgia, and by ERDA/WSRC subcontract AA46420T. The generous support of the Advanced Analytical Center for Environmental Sciences at the Savannah River Ecology Laboratory, including Brian Teppen, John Seaman, and Paul Bertsch is

acknowledged. Kathy Nagy of Sandia National Laboratories provided valuable advice and review of the TMAFM images.

REFERENCES

Bish DL. 1988. Effects of composition on the dehydration behavior of clinoptilolite and heulandite. Occurrence, Properties, and Utilization of Natural Zeolites. Kalló D. and Sherry H.S. Budapest, Hungary: Akadémiai Kiadó. 565-576.

Bowman RS, Haggerty GM, Huddleston RG, Neel D, Flynn MM. 1995. Sorption of nonpolar organic compounds, inorganic cations, and inorganic oxyanions by surfactant-modified zeolites. Surfactant-Enhanced Subsurface Remediation. ACS Symposium Series 594, Sabatini DA, Knox RC, and Harwell JH. Washington, DC: American Chemical Society. 54-64.

Brunauer S, Emmett PH, Teller E. 1938. Adsorption of gases in multimolecular layers. J. Amer. Chem. Soc. 60: 309-319.

Chen YL, Chen S, Frank C, Israelachvili J. 1992. Molecular mechanisms and kinetics during the self-assembly of surfactant layers. J. Colloid and Interface Sci. 153 (1): 244-265.

Chipera SJ, Bish DL. 1995. Multireflection RIR and intensity normalizations for quantitative analyses: applications to feldspars and zeolites. Powder Diffraction 10: 47-55.

Gao F, Cadena F, Peters RW. 1991. Use of tailored zeolites for removal of benzene, toluene and xylenes from water. Proc. of the 45th Annual Purdue Ind. Waste Conf. 509-516.

Haggerty GM, Bowman RS. 1994. Sorption of chromate and other inorganic anions by organo-zeolite. Environ. Sci. and Technol. 28(3): 452-458.

Israelachvili J N. 1991. Intermolecular and Surface Forces. 2nd Ed. San Diego, CA: Academic Press, Inc. 450pp.

Komiyama M, Yashima T. 1994. Atomic force microscopy images of natural zeolite surfaces observed under ambient conditions. Jpn. J. Appl. Phys. 33(1,6B): 3761-3763.

MacDougall JE, Cox SD, Stucky GD, Weisenhorn AL, Hansma PK, Wise WS. 1991. Molecular resolution of zeolite surfaces as imaged by atomic force microscopy. Zeolites 11: 429-433.

Malliaris A, Lang J, Zana R. 1986. Micellar aggregation numbers at high surfactant concentration. J. Coll. Int. Sci. 110(1): 237-242.

Manne S, Gaub HE. 1995. Molecular organization of surfactants at solid-liquid interfaces. Science 270:1480-1482.

Maurice PA. 1995. Applications of atomic-force microscopy in mineral-water interface chemistry. American Chemical Society Preprint Extended Abstract, Division of Environmental Chemistry; 1995 April 2-7. Anaheim, CA: 521-524.

Ming DW, Dixon JB. 1987. Quantitative determination of clinoptilolite in soils by a cation-exchange capacity method. Clays & Clay Minerals 35: 463-468.

Ming DW, Mumpton FA. 1989. Zeolites in soils. Minerals in Soil Environments. 2nd Ed. Dixon JB, Weed SB. Madison, Wisconsin: Soil Sci. Soc. Am. 873-911.

Neel D, Bowman RS. 1991. Sorption of organics to surface-altered zeolites. Proc. 36th Annual New Mexico Water Conference; 1990 November 7-8. 57-61.

Ong SK, Lion LW. 1991. Effects of soil properties and moisture on the sorption of trichloroethylene vapor. Water Research 25: 29-36.

Petersen LW, Moldrup P, El-Farhan YH, Jacobsen OH, Rolston DE. 1995. The effect of moisture and soil texture on the adsorption of organic vapors. J. Environ. Qual. 24: 752-759.

Reiss-Husson F, Luzzati V. 1964. The structure of the micellar solutions of some amphiphilic compounds in pure water as determined by absolute small-angle X-ray scattering techniques. J. Phys. Chem. 68: 3504-3510.

Scandella L, Kruse N, Prins R. 1993. Imaging of zeolite surface structures by atomic force microscopy. Surface Science Letters 281: 331-334.

Smyth, JR, Spaid AT, Bish DL. 1990. Crystal structures of a natural and a Cs-exchanged clinoptilolite. American Mineralogist 75: 522-528.

Stipp SLS, Eggleston CM, Nielsen BS. 1994. Calcite surface structure observed at microtopographic and molecular scales with atomic force microscopy (AFM). Geochimica et Cosmochimica Acta 58(14): 3023-3033.

Sullivan EJ, Bowman RS, Haggerty GM. 1994. Sorption of inorganic oxyanions by surfactant-modified zeolite. Spectrum 94, Proc. Nuclear and Hazardous Waste Mgmt. International Topical Meeting Vol. 2.; 1994 August 14-18, Atlanta, Georgia, 940-945.

Weisenhorn AL, MacDougall JE, Gould AC, Cox SD, Wise WS, Massie J, Maivald P, Elings VB, Stucky GD, Hansma PK. 1991. Imaging and manipulating molecules on a zeolite surface with an atomic force microscope. Science 24: 1330-1333.

Xu S, Boyd SA. 1995. Cationic surfactant adsorption by swelling and nonswelling layer silicates. Langmuir 11: 2508-2514.

Zhang ZZ, Sparks DL, Scrivner NC. 1993. Sorption and desorption of quaternary amine cations on clays. Environ. Sci. and Technol. 27: 1625-1631.

Zhong Q, Inniss D, Kjoller K, Elings VB. 1993. Fractured polymer / silica fiber surface studied by tapping mode atomic force microscopy. Surface Science Letters 290: L688-L692.

CHAPTER 3

THERMODYNAMICS OF CATIONIC SURFACTANT SORPTION ONTO CLINOPTILOLITE

(Submitted to the Journal of Colloid and Interface Science, January 28, 1997)

ABSTRACT

Sorption enthalpies of hexadecyltrimethylammonium bromide (HDTMA) as monomers and micelles and of tetraethylammonium bromide (TEA) were used with surfactant, counterion, and co-ion sorption isotherms to infer the conformation, sorption mechanism, and relative stability of the sorbed surfactants on clinoptilolite. The average value of the sorption enthalpy was -10.375 ± 3.029 kJ/mol for HDTMA monomers, -11.980 ± 2.848 kJ/mol for HDTMA micelles, and +3.029 ± 1.790 kJ/mol for TEA. Sorption of monomers produced a lower sorption plateau than micelle sorption (maxima 145 mmol/kg, 225 mmol/kg). Analysis of the sorption data demonstrated a change in sorption mechanism at the external cation exchange capacity (ECEC) of clinoptilolite. Sorption data from below and above the ECEC were fit to a simple polynomial model and the Gibbs free energy of sorption (ΔG_m^0) and sorption entropies were calculated. Resultant values of ΔG_m^0 were -9.27 and -14.38 kJ/mol for HDTMA monomers and micelles, respectively, for sorption below the ECEC, and -16.11 and -23.10 kJ/mol, respectively, for sorption above the ECEC. The value for TEA was -1.04 kJ/mol, indicating weaker

sorption than for HDTMA. Monomer sorption to clinoptilolite exceeded the ECEC even when the solution concentration was below the critical micelle concentration. Hydrophobic (tail-tail) components of ΔG_m^0 were the driving force for sorption of HDTMA both below and above the ECEC. A significant kinetic effect was observed in the sorption isotherms with a period of rapid sorption followed by slow equilibration requiring 7 days to achieve steady state for HDTMA; TEA equilibration occurred within 24 hours.

INTRODUCTION

Surfactant modification of clay minerals is frequently studied because of the unique sorptive properties of the modified material (1-3). Modification of the zeolite clinoptilolite with surfactants such as hexadecyltrimethylammonium bromide (HDTMA) or tetraethylammonium bromide (TEA) is similar to modification of clay and produces a product which sorbs organic compounds, inorganic cations, and inorganic anions while retaining favorable hydraulic properties (4). Surfactant-modified clinoptilolite thus has potential for use in remediation systems such as permeable barriers. Understanding the mechanism of HDTMA sorption and its subsequent conformation on the clinoptilolite surface is crucial to understanding the interaction of sorbed HDTMA with organic and inorganic compounds in solution and predicting the stability of the sorbed surfactant.

Clinoptilolite has a two-dimensional channel system that allows the mineral to act as a molecular sieve (5). Large surfactant molecules such as HDTMA sorb only to the external surface of clinoptilolite. The external cation exchange capacity (ECEC) characterizes the exchange capacity of the mineral surface for HDTMA (6). The size of

the surfactant headgroup and the extent of interaction of the tail group with the surface or with other surfactant molecules are expected to be significant in determining the monolayer density on the surface at low solution concentrations. At greater solution concentrations, surfactant molecules with large tail groups may sorb via hydrophobic (tail-tail) interactions, forming a bilayer or admicelles (7) (Fig. 3.1).

In this study, the sorption mechanism of HDTMA to clinoptilolite was investigated using sorption isotherms and calorimetry. In previous studies of sorption of HDTMA to clinoptilolite, a Langmuir-type isotherm was observed (4,6). The data presented here show that more than one layer of surfactant occurs on the surface of clinoptilolite, counter to the assumptions of the Langmuir model. Observation of counterion and co-ion sorption is necessary to fully understand the surfactant sorption process. Sorption was studied from both monomer-bearing solutions at one-half of the critical micelle concentration (CMC) and micelle-bearing solutions at twice the CMC, to compare the sorption behavior of HDTMA as monomers and as micelles. TEA, which does not form micelles, was used to approximate the sorptive behavior of an amine headgroup, to further elucidate the effect of the HDTMA tail group on the sorption process. Kinetics were found to be a significant factor in sorption and in the calorimetric measurements.

A number of models have been developed in recent years to describe the sorption of ionic surfactants onto charged mineral surfaces such as silica (8-12, and others cited therein). These models recognize the complexity of the sorption process, particularly the ability of the surfactants to form admicelles or hemimicelles on the surface as well as the interactions which occur between surfactant molecules in these sorbed forms. While the

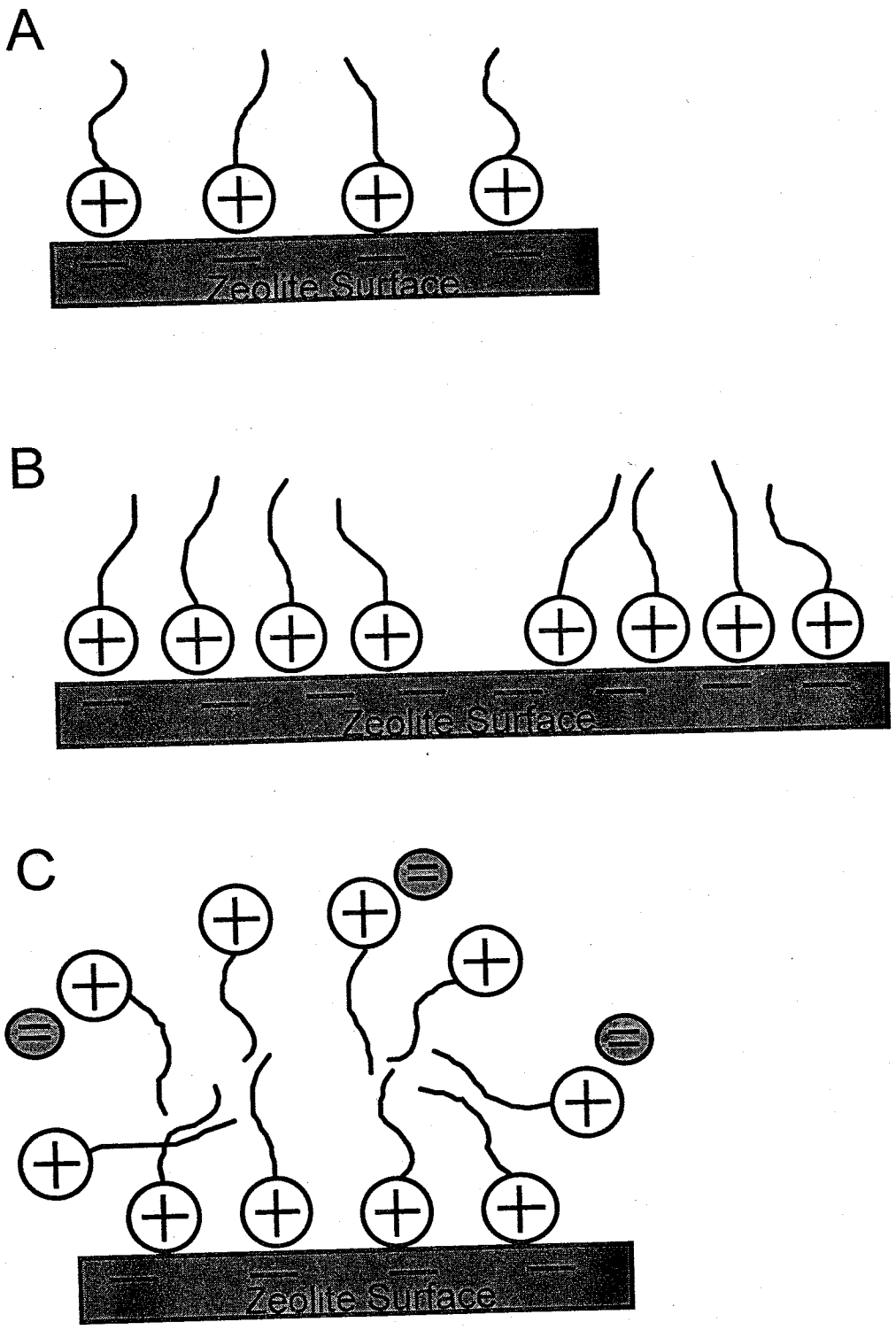

Figure 3.1. Monolayer (A), hemimicelle (B), and admicelle (C) formation by sorption of a long-chain cationic surfactant on a mineral surface.

models are useful in recognizing the details of the sorption process for particular systems, it is still difficult to extrapolate them to other systems and concentration ranges. For the clinoptilolite system, a generalized sorption equation with polynomial fitting terms similar in form to that of Cases and Villieras (9) was found to be useful for analysis of both HDTMA and TEA.

Microcalorimetry was used to investigate details of the sorption process not observable in the sorption isotherms (10). Very sensitive calorimetric methods have been used in this manner in recent surfactant-mineral sorption studies (13,14). The heat of sorption of HDTMA and TEA on clinoptilolite was measured for a range of surfactant coverages to elucidate the strength of the bond between the clinoptilolite surface and the surfactant. These data were used to develop a thermodynamic description of the sorption process.

THERMODYNAMICS

Sorption Equilibria

The sorption of surfactant molecules to clinoptilolite occurs as two distinct processes, depending upon the degree of sorption. Initially, surfactant is sorbed by cation exchange, and later, surfactant is sorbed by hydrophobic forces.

1. Exchange-Driven Surfactant Sorption

For sorbed quantities of surfactant less than the ECEC, sorption can be described as a cation-exchange reaction, as follows:

$$Z^- M^+ + S^+ \Leftrightarrow Z^- S^+ + M^+ \qquad [1]$$

or

$$\tfrac{1}{2}(Z_2^- M^{2+}) + S^+ \Leftrightarrow Z^- S^+ + \tfrac{1}{2} M^{2+} \qquad [2]$$

where Z^- is a unit-charge cation-exchange site on the external surface of the zeolite, M^+ or M^{2+} is an exchangeable cation on the clinoptilolite surface (primarily Ca^{2+}, but also Na^+, K^+, and Mg^{2+}), and S^+ is the monovalent, cationic surfactant. For the system studied here, the predominant exchangeable cations were divalent, and therefore Equation 2 was used to describe sorption below the ECEC. The thermodynamic equilibrium constant for reaction 2 takes the form:

$$K = \frac{(Z^- S^+)(M^{2+})^{0.5}}{(Z_2^- M^{2+})^{0.5}(S^+)} \qquad [3]$$

where ( ) denotes activities. If the system behaves ideally, then the activities in solution may be expressed as molalities and the activities on the zeolite exchange sites may be expressed as mole fractions as follows:

$$X_{S^+} = \frac{n_{S^+}}{n_{S^+} + n_{M^{2+}}} \qquad [4]$$

$$X_{M^{2+}} = \frac{n_{M^{2+}}}{n_{S^+} + n_{M^{2+}}} \qquad [5]$$

where n refers to the amount of material sorbed (in mol/kg clinoptilolite). These equations, when substituted into Equation 3, yield a relation for an ideal equilibrium constant (K_6):

$$K_6 = \frac{X_{S^+}[M^{2+}]^{0.5}}{[S^+]X_{M^{2+}}{}^{0.5}} \qquad [6]$$

where brackets [ ] indicate concentrations in solution (mg/kg solution).

2. *Van der Waals-Driven Surfactant Sorption*

Above the ECEC, sorption can occur via intermolecular or surfactant-surface interactions, and may be similar to organic partitioning or Henry's law mechanisms (8). The sorption process follows the general form:

$$Z^- S^+ + S^+ R^- \Leftrightarrow Z^- S_2^+ R^- \qquad [7]$$

where R^- is the counterion associated with the surfactant in solution. An equilibrium constant for reaction 7 is

$$K = \frac{(Z^- S_2^+ R^-)}{(S^+ R^-)(Z^- S^+)} \qquad [8]$$

An ideal equilibrium constant (K_9) for this sorption can be formulated as follows (15):

$$K_9 = \frac{n_{S^+}}{[S^+]} \qquad [9]$$

This is equivalent to a simple partitioning model.

Thermodynamic Model

For the case where there are no data for solution or surface activities, non-ideality in the system can be represented by the following expression (9,12,16):

$$\ln K = \ln K_{ideal} + f(n_{S^+}) \qquad [10]$$

where $f(n_{S^+})$ is a function of the amount of surfactant sorbed, n_{S^+}. Ln K_{ideal} is equal to ln K_6 or ln K_9, depending upon whether sorption is below or above the ECEC. In general, $f(n_{S^+})$ can be expressed in a polynomial form. Isotherm data may be regressed in terms of

ln K_{ideal} as a function of n_{s^+} (Equation 10) to produce a value of ln K and the coefficients of the polynomial function $f(n_{s^+})$. For example, a first-order polynomial yields the Frumkin isotherm (12,16). This formulation combines non-ideality from all sources, such as solution, intermolecular, steric, chemical, or electrostatic interactions, into the polynomial coefficients. Note, however, that Blandamer et al. (17) argue that HDTMA solution properties are approximately ideal.

At constant pressure, the standard molar free energy change ΔG_m^0 of the sorption reaction may be calculated from:

$$\Delta G_m^0 = -RT \ln K \qquad [11]$$

where R is the gas constant and T is the absolute temperature (K). The subscript m and superscript 0 refer to molar quantities and standard conditions, respectively.

In this study, the enthalpy of sorption was measured directly to estimate ΔH_m^0 and the entropy of sorption was calculated from the relation:

$$\Delta S_m^0 = \frac{-\left(\Delta G_m^0 - \Delta H_m^0\right)}{T} \qquad [12]$$

using values of ΔG_m^0 obtained in the sorption isotherm experiments.

The approach taken in this analysis is independent of assumptions regarding the atomistic origin of the thermodynamic terms. However, previous work suggests that contributions to the free energy of sorption can be split into electrostatic (ΔG_{elec}) and specific sorption (ΔG_{spec}) interactions, where specific interactions include contributions such as chain-chain, chain-substrate, and headgroup-substrate interactions (16,18).

MATERIALS AND METHODS

Clinoptilolite was supplied by the St. Cloud Mine in Winston, New Mexico. It was used as provided, after sieving to a size range between 2 mm and 150 μm. It consists of about 74% clinoptilolite, 5% smectite, 10% quartz and cristobalite, 10% feldspar, and 1% illite, based on internal standard X-ray diffraction analysis (19). The ECEC of the clinoptilolite was 90 meq/kg as determined by a method modified from Ming and Dixon (20) and described previously (19). The zeolite has a measured surface area of about 15.7 m^2g^{-1} (19). The surfactants HDTMA (Baker Chemicals) and TEA (Sigma Chemical Company) were supplied as Br^- salts of greater than 99% purity and were used as provided. Two HDTMA solutions were used, 0.45 meq/L and 1.8 meq/L. These are, respectively, one-half and two times the CMC of HDTMA at 25°C (21) and will be referred to here as the monomer system and the micelle system. A TEA solution of 1.8 meq/L was used. Type I water (ASTM) from a Milli-Q system (Millipore Corp.) was used for all solutions.

Sorption isotherms were prepared in 50-ml Oak Ridge centrifuge tubes for each surfactant system using the initial solution concentrations described above. Aqueous surfactant solutions were spiked with [^{14}C-methyl]HDTMA iodide or [^{14}C-methyl]TEA iodide (American Radiochemicals Inc.) as appropriate. The clinoptilolite was treated with amounts of surfactant equivalent to a range from 0% to 600% of its ECEC by adjusting the amount of clinoptilolite added to a constant volume of solution. Measured quantities (from 0.05 g to 3.2 g) of clinoptilolite were shaken mechanically with 40 ml of each of the

two HDTMA solutions for a series of time steps between 24 hours and 28 days, and with the TEA solution for times from 2 to 24 hours, at 25°C. Quantities of clinoptilolite were measured so that the ratio of exchange capacity to moles of surfactant in solution was the same among the batches. Each sample was prepared in duplicate or triplicate with appropriate blanks. After shaking, the tubes were centrifuged at 14500 x g for 20 minutes and the excess surfactant solution decanted. Solution concentrations of ^{14}C-labeled surfactant were measured using a Packard Tri-Carb liquid scintillation counter. Solution concentrations of exchanged cations Na^+, Ca^{2+}, and Mg^{2+} were measured using atomic absorption spectrophotometry. Solution concentrations of the counterion, Br^-, were measured by high-performance liquid chromatography (HPLC).

The calorimeter used was a Tronac 558 isothermal solution calorimeter (Tronac, Inc., Orem, Utah). The same surfactants, surfactant concentrations, and solution:clinoptilolite ratios were used as in the sorption experiments, except the range of treatment varied from 0% to 400% of ECEC. Clinoptilolite weights used ranged from 0.03 to 1.5 g. Each unmodified clinoptilolite sample was weighed and placed into a 1-ml borosilicate glass ampoule (Tronac, Inc.). A small quantity (35 μl) of Type I water was added to the ampoule before sealing to wet the clinoptilolite. This amount of water was found by calorimeter measurement to be sufficient to remove enthalpy of hydration effects for the amounts of clinoptilolite used. Each ampoule was sealed and mounted on the stirring rod of the calorimeter containing 25 ml of surfactant solution and operated at 25°C. Following thermal equilibration, the calorimeter was electrically calibrated, the ampoule was broken remotely, and the enthalpy of sorption was measured by integration

of the heat of the sorption reaction over time. After the reaction was complete, post-calibration was performed. Enthalpy changes over time were integrated and a single value for heat lost or gained was recorded. Blanks containing 35 μl of Type I water and no clinoptilolite were also measured and the subsequent enthalpy of mixing between this volume of water and the HDTMA or TEA solutions was subtracted from the final results. These values were: -0.0238 J, -0.02035 J, and -0.0556 J for the monomer, micelle, and TEA systems, respectively. Each surfactant solution remaining in the reaction vessel was decanted, centrifuged at 10500 x g for 20 minutes, and analyzed for HDTMA content by HPLC. Concentrations of TEA remaining after reaction were estimated by correlation with the sorption isotherms.

RESULTS AND DISCUSSION

Sorption Isotherm Results

A time dependence was observed for the sorption of surfactants to the clinoptilolite surface. A 7-day experiment in the HDTMA micelle system resulted in essentially complete sorption, when compared with the results of 28-day experiments. Monomer HDTMA sorption was complete after 24 hours, showing little change when compared with 7-day results. Therefore, the 7-day HDTMA sorption data for both monomers and micelles were used in the data analysis for consistency. Twenty-four hours were found to be sufficient for TEA sorption, although preliminary tests showed near complete sorption at two hours.

Surfactant sorption data for the HDTMA and TEA systems were normalized to the ECEC of 90 meq/kg. This degree of sorption is significant because beyond this point surfactant sorption must be multilayer because all available cation exchange sites are likely to be filled. Sorption above this level is expected to be in the form of a bilayer, patchy bilayer, or admicelles, while sorption below this point is likely in the form of monomers or hemimicelles (Fig. 3.1).

The s-shaped isotherm of the HDTMA monomer system reached an observed maximum at about 160% of the ECEC (Fig. 3.2). The maximum equilibrium solution concentration was near 0.31 meq/kg solution, much less than the CMC of HDTMA. In the micelle system, the Type I (concave-down) isotherm reached a plateau at 250% of the ECEC, similar to previous maxima determined at solution concentrations much above the CMC (4,6). The maximum equilibrium solution concentration from the micelle system was just above the CMC of 0.9 meq/L, at 1.0 meq/kg solution. The amount sorbed from the 100% of ECEC treatment level was 97% of the ECEC, as expected. The surfactant TEA sorbed to a much lower extent than either HDTMA system. This is typical of smaller surfactant molecules and reflects the slightly larger headgroup size and lack of tail group. The maximum sorption level of TEA observed was 46% of the ECEC.

The isotherms for the HDTMA monomer and micelle systems differ in shape and quantity sorbed, indicating that there is some difference in the sorption mechanism between monomer- and micelle-bearing solutions. The monomer isotherm is s-shaped and lies below that for micelles. The s-shape of some long-chain surfactant isotherms has been interpreted to mean that hemimicelles are forming on the surface above a monomer

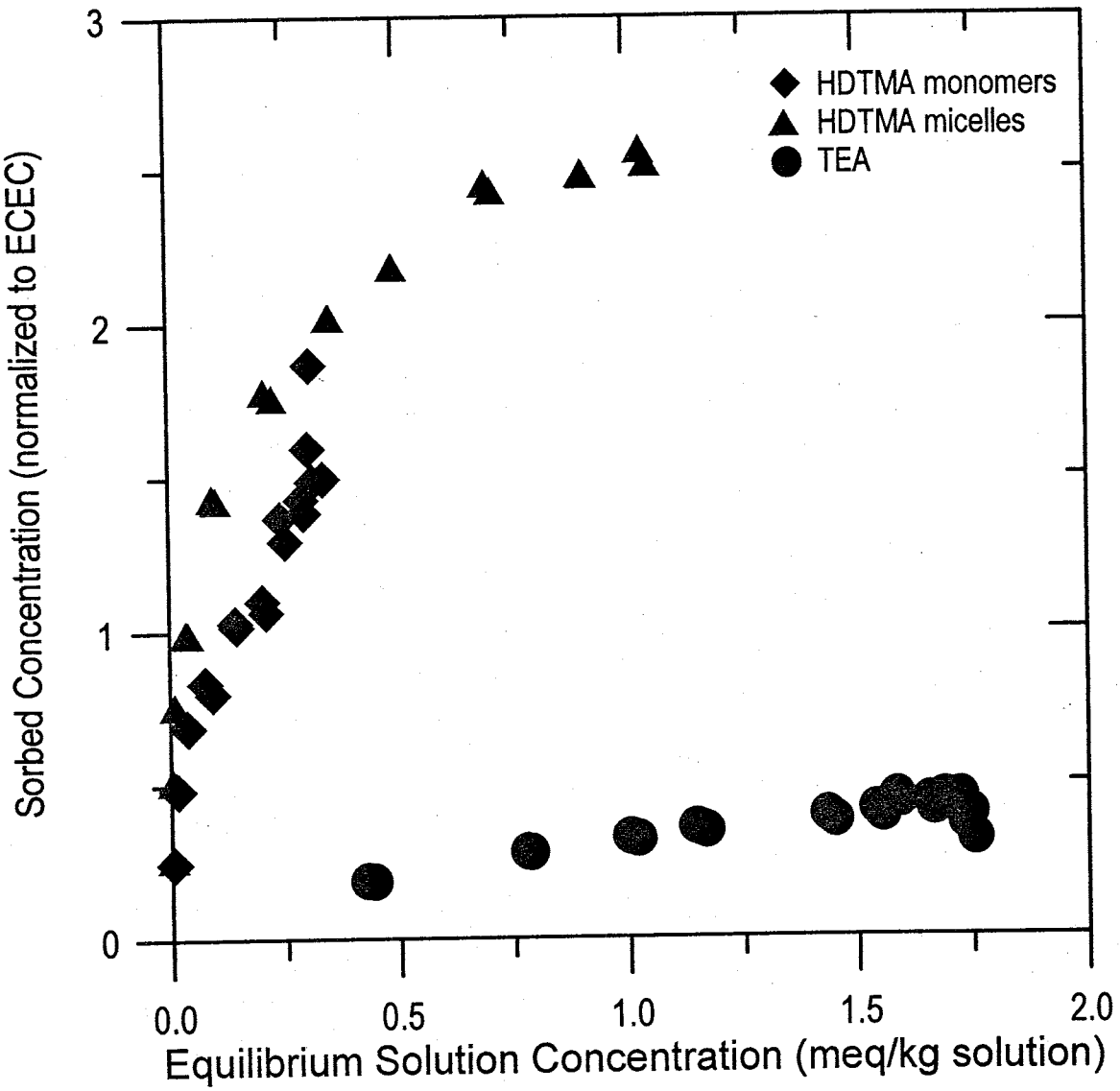

Figure 3.2. Sorption isotherms for TEA (24 hours), HDTMA monomers (7 days), and HDTMA micelles (7 days) on clinoptilolite. The ECEC equals 90 meq/kg.

sorption threshold (16, and others cited therein). This isotherm could also indicate a lack of equilibration. The lack of change between the 24-hour and 7-day data sets, however, does not support this, unless the equilibration time is quite long. If so, this may indicate a metastable equilibration state for monomers, in which case an equilibrium constant can still be calculated for comparative purposes.

Bromide counterion sorption can be used to distinguish between monolayer or hemimicelle sorption versus bilayer or admicelle sorption, as the counterion should only be sorbed with the latter two forms. In calculating the degree of Br^- sorption, the data were corrected to account for anion exclusion using the method described by Israelachvili (21) using the measured surface area (19).

For the HDTMA monomer system, no Br^- sorption was measured up to 100% of the ECEC treatment level (Fig. 3.3), indicating monomer or hemimicelle sorption only. The maximum Br^- sorption was 45 meq/kg or one-half of the ECEC. This correlates with the amount of HDTMA sorbed in excess of the ECEC, approximately 45 meq/kg. This bilayer sorption occurred even though the solution concentration remained below the CMC.

For the micelle system, there was also little Br^- sorption up to the 100% of ECEC treatment level (Fig. 3.3). Above the ECEC, Br^- sorption increased sharply and was nearly linear with HDTMA sorption. The maximum amount of Br^- sorbed was 105 meq/kg, equivalent to 45% of the maximum HDTMA sorption of 225 meq/kg. The Br^- data show that below the ECEC sorbing micelles rearrange to a monolayer or hemimicelles; while above the ECEC admicelles or bilayers occur at the surface. The equilibrium HDTMA

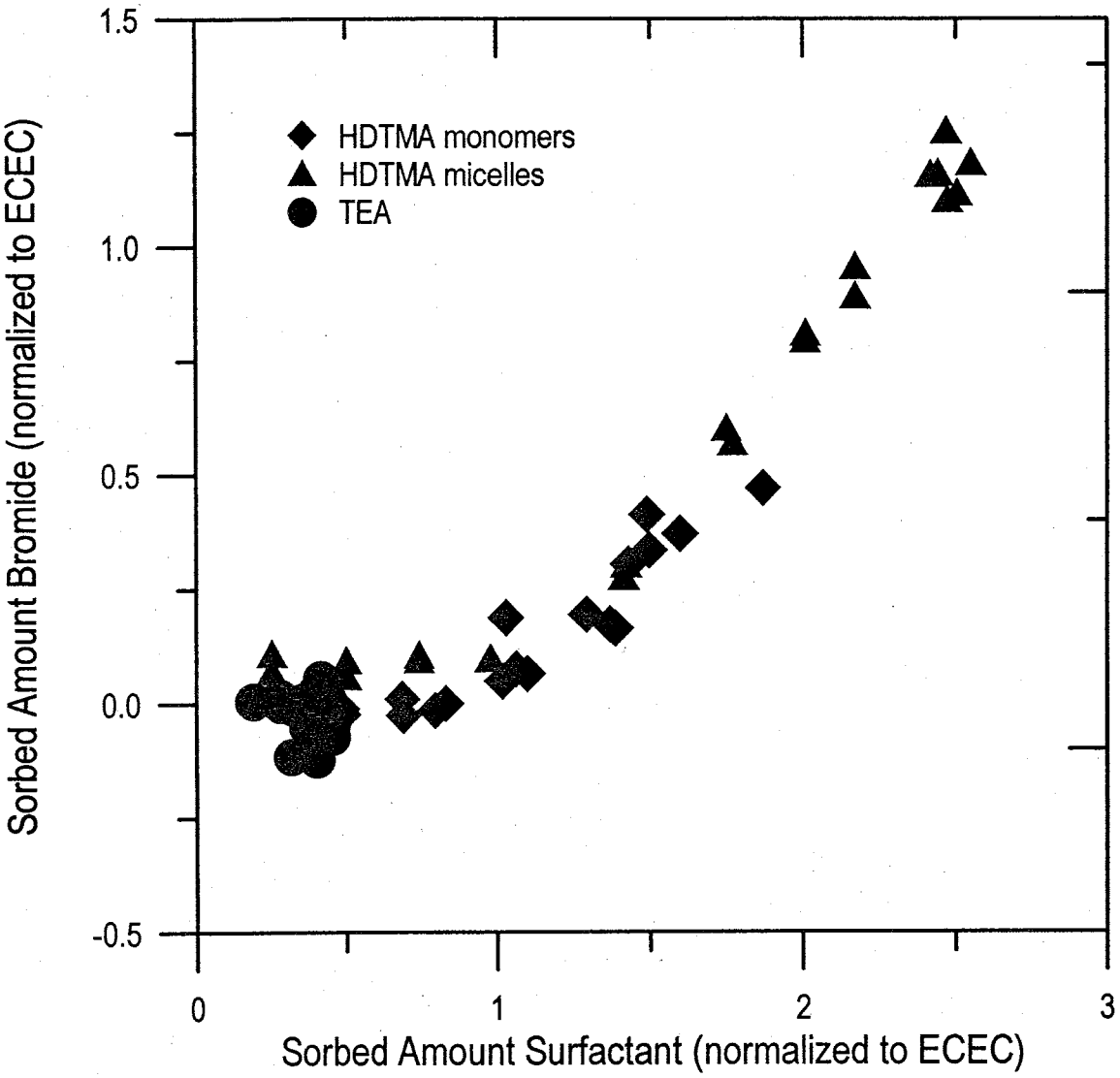

Figure 3.3. Sorbed amount of bromide counterion versus sorbed amount of surfactant for HDTMA monomers, HDTMA micelles, and TEA.

solution concentration fell below the CMC for all the micelle experiments except at the highest treatment levels (400% to 600%). The sorption data indicate that the sorbed bilayers or admicelles are stable in solutions at or below the CMC at least for observations extending to 28 days. Sufficient time, however, is needed for the rearrangement from admicelles to a monolayer. The maximum Br^- sorption amount for the 24-hour batch at 400% of ECEC was 135 meq/kg versus 105 meq/kg at 7 days, indicating that time is needed for HDTMA rearrangement, desorption of the bromide-surface co-ion pair, and subsequent equilibration with the solution.

No sorption of Br^- was noted in the TEA system (Fig. 3.3). This was expected because TEA cation exchanges but does not form admicelles or bilayers.

Equilibrium solution concentrations of Na^+, Ca^{2+}, and Mg^{2+} were measured and are plotted in Fig. 3.4 as meq of desorbed cations versus sorbed surfactant amount for all three systems. The monomer system produced a maximum desorption of about 60% of the ECEC. Cation desorption was less than HDTMA monomer sorption for each initial condition. Cation desorption continued even when HDTMA sorption exceeded the ECEC and Br^- was sorbing (Figs. 3.3 and 3.4). This may indicate some lack of equilibration in the time allotted, perhaps because of a slow release of the co-ion from the surface. Cations have been noted to release from lipid layers at slower rates than anions (21).

The desorbed cation curve in the micelle system rose linearly with HDTMA sorption and reached a plateau between 80 and 100% of ECEC. This is approximately the same point at which Br^- sorption begins to rise in this system, and supports the hypothesis that admicelles or a bilayer form at loading levels at and above the ECEC.

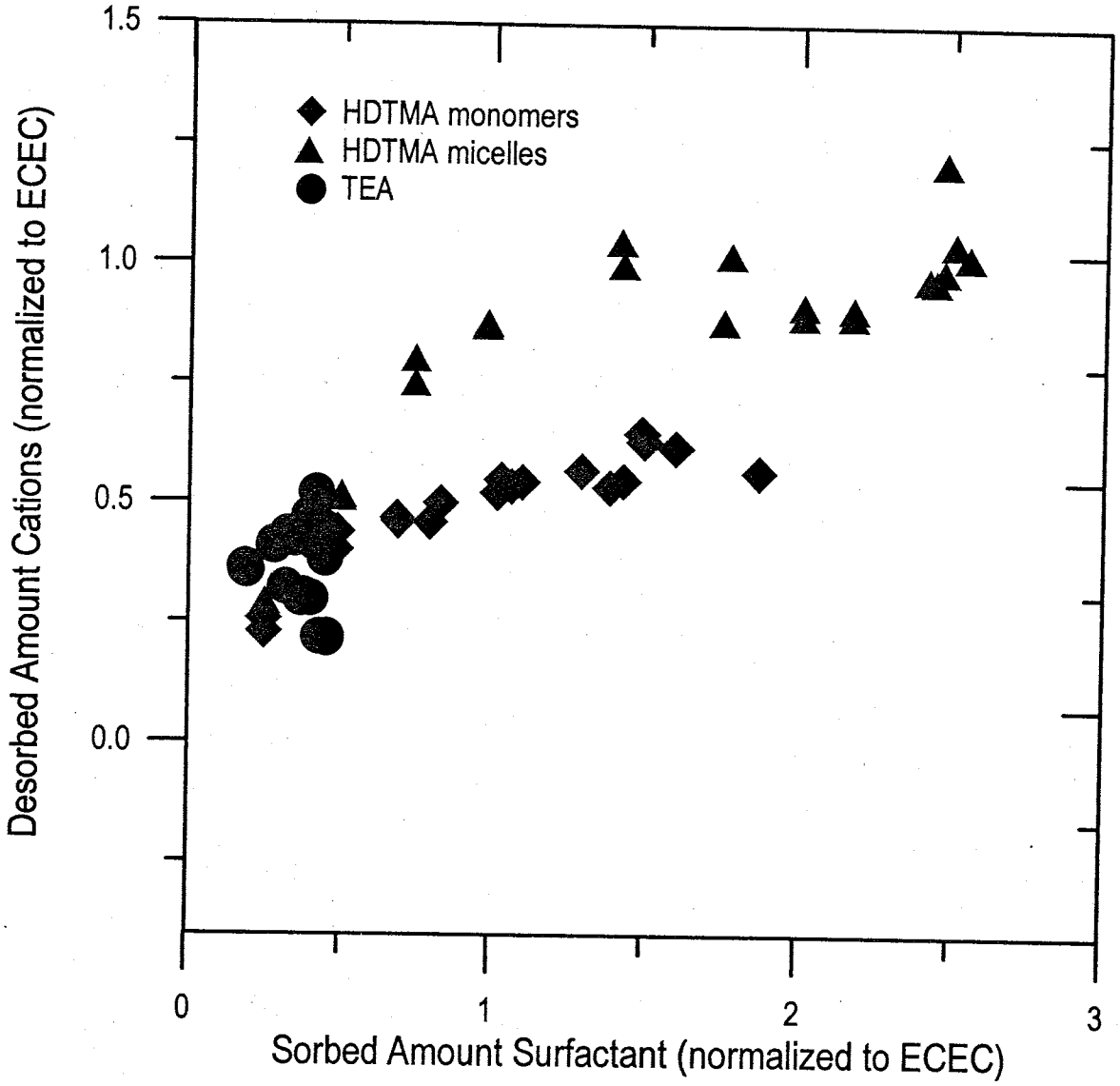

Figure 3.4. Total meq desorbed cations (Mg^{2+}, Ca^{2+}, and Na^{+}) versus sorbed amount of HDTMA monomers, HDTMA micelles, and TEA.

Maximum desorption of cations for the TEA system was almost 50% of ECEC and was for the most part linear with TEA sorption (Fig. 3.4).

HDTMA as both monomers and micelles was observed to sorb to a greater extent than TEA. This difference between long- and short-chain surfactants is observed frequently in clay-surfactant systems (22-24) and is attributed to the presence of the hydrophobic tail group of length greater than C-8. The TEA headgroup is roughly 30 percent larger in diameter than the HDTMA headgroup (21). Size may limit the effective interaction of a molecule with specific surface site geometries (24). Native cation competition may also limit the TEA exchange with the surface.

Sorption Model Results

Surfactant sorption was analyzed by first comparing the observed behavior to the simplest, ideal equilibrium constant (Equation 9) in plots of the logarithm of the ratio of sorbed and solution concentration as a function of the amount sorbed (Fig. 3.5). This allowed the identification of possible changes in the sorption mechanism below and above the ECEC and has been found useful in previous studies (16, 25, 26).

A distinct break in the slope was observed in the HDTMA monomer system at the ECEC; a less-distinct change occurred in the micelle system. Using the results of the sorption experiments, the data below the ECEC were modeled using Equation 6, which accounts for cation exchange in the equilibrium constant. The occurrence of Br^- sorption in the remaining data from 150% to 250% of the ECEC indicates that a partitioning model (Equation 9) is appropriate.

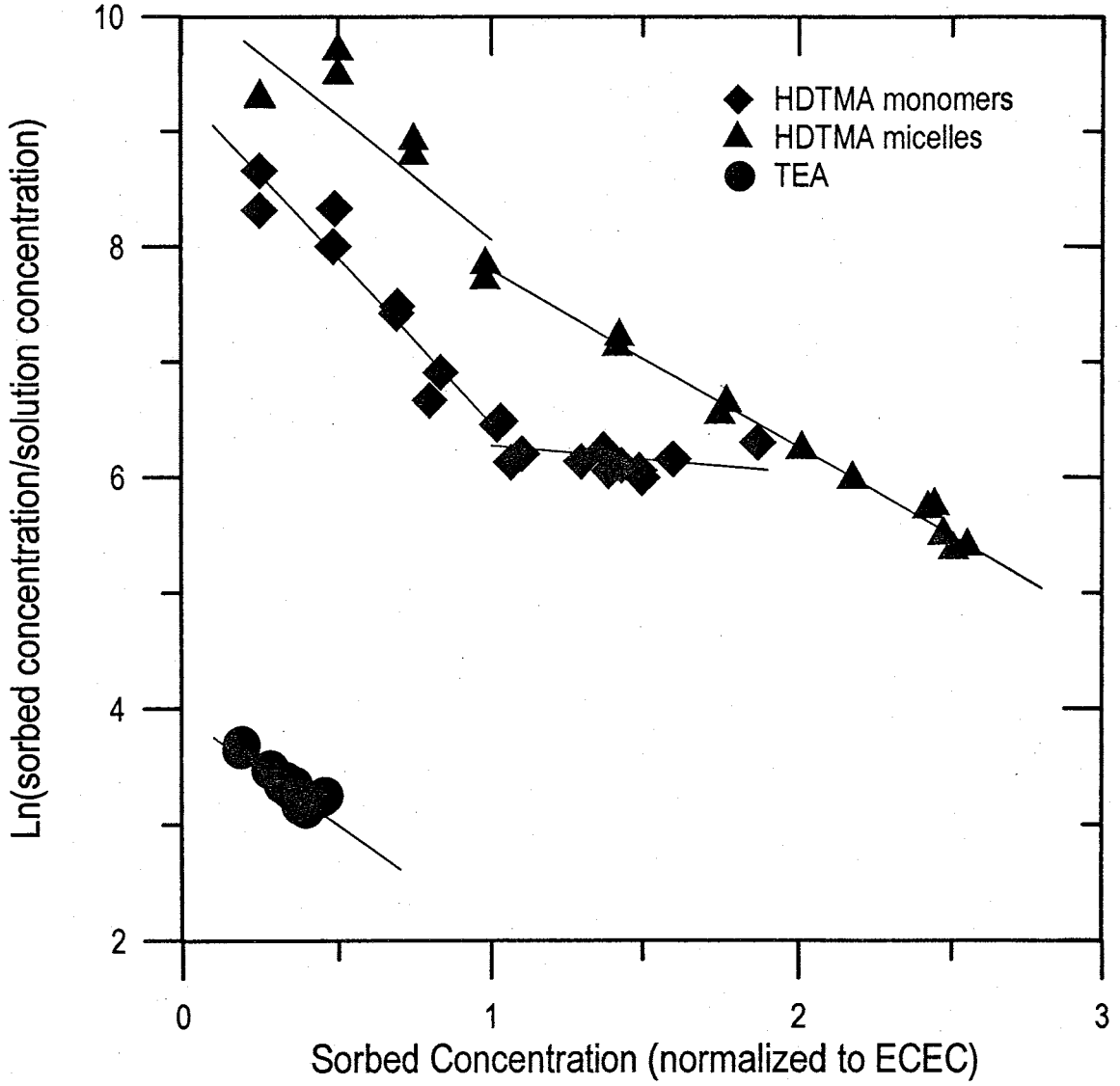

Figure 3.5. Ln($n_{s^+}/[S^+]$) versus sorbed surfactant concentration (symbols) and linear regression of the data (solid lines).

Below the ECEC, values of ln K_6 (resulting values from Equation 6) for the micelle system were approximately constant, indicating nearly ideal conformity to the cation-exchange model (Fig. 3.6). The ln K_6 values for the monomer system were not constant and were best fit by a second-order polynomial in the amount sorbed. This behavior may reflect a lack of attainment of equilibrium in the monomer system, or there may be sorption hysteresis. It is not uncommon for ion exchange constants to vary with the ratios of the competing species sorbed on the solid. This produces a change in affinity (ln K) as monomers displace original cations. In contrast, micelle exchange affinity is higher because it acts as a large, multivalent cation which displaces a number of surface cations simultaneously.

Above the ECEC, the ln K_9 values (values from Equation 9) for monomers are nearly ideal for partitioning-type sorption as indicated by their near constant values. The compositional range covered in the monomer system is not great above the ECEC and may be consistent with the results for the micelle system. Ln K_9 values for the micelle system depend linearly on the amount sorbed (Fig. 3.6). The slight non-ideality may reflect monomer/micelle processes in the solution or interaggregate interactions on the clinoptilolite surface. For an HDTMA micelle to insert itself into a bilayer, much rearrangement must take place and K decreases with micelle loading. It is much easier for a monomer to insert itself into a bilayer, producing less change in K.

TEA sorption was modeled with Equation 6, because sorption was not greater than the ECEC and equivalent cation exchange was found (Fig. 3.4). The data required a second-order polynomial fit, and the non-ideality may have resulted from steric

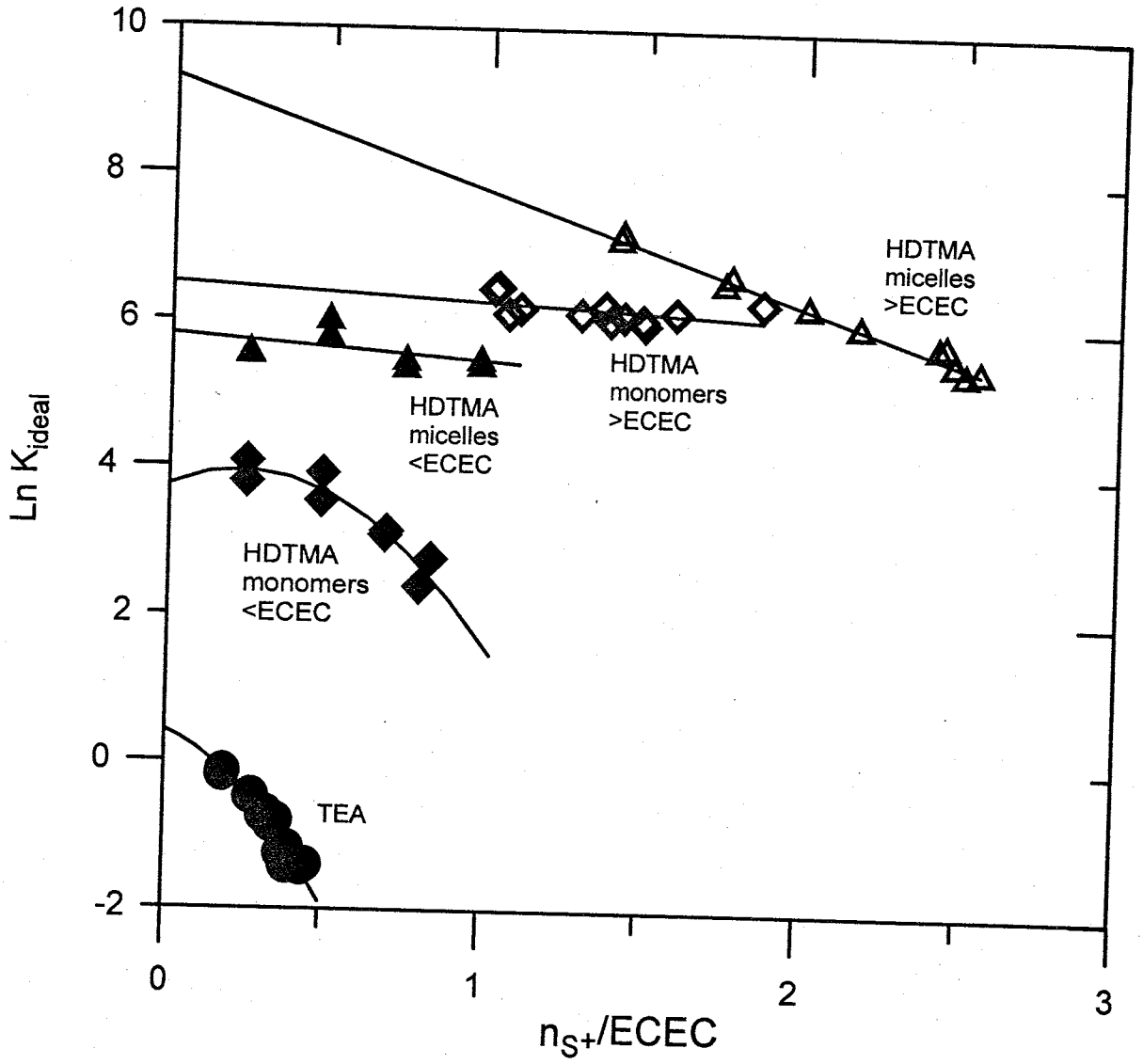

Figure 3.6. Model fits based on Equation 10 (solid lines) to plotted ln K_{ideal} data (symbols) for sorbed HDTMA monomers, HDTMA micelles, and TEA. Ln K_{ideal} values for data below the ECEC were calculated with Equation 6 and incorporate cation exchange effects (K_6). Ln K_{ideal} values for data above the ECEC were calculated with Equation 9 (K_9). Model fits were extrapolated to $n_{S^+}/ECEC = 0$ to obtain the value of ln K for each system.

interference or other sorbent-sorbate effects. As for HDTMA monomer sorption at less than the ECEC, the exchanging cation ratios vary with sorption causing ln K to vary.

Results of the isotherm models are given in Table 3.1. Values of ln K were found as the zeroth order term (y-intercept) in the fitting procedure using Equation 10. Interestingly, the >ECEC system is characterized by a stronger partitioning of surfactant than the <ECEC for both monomer and micelle HDTMA systems. The micelle system sorbed more strongly than the monomer system, and the TEA system was characterized by near neutral sorption.

Microcalorimetry Results

The enthalpy of sorption of HDTMA from both monomer and micelle solutions was moderately exothermic, while TEA was weakly endothermic (Fig. 3.7). The enthalpy measurement includes the effect of the displacement of native cations including Na^+, Ca^{2+}, and Mg^{2+} from the surface and any micelle/monomer reactions in solution. All systems showed an essentially constant enthalpy of sorption as a function of the amount sorbed. The enthalpy of sorption of HDTMA from the micelle solution was slightly greater in magnitude than for the monomer solution, but the difference is not statistically significant (t-test of means at 95% confidence level).

The calorimetric measurements demonstrated that a measurable heat of reaction ceased after approximately ½ hour (Fig. 3.8). The measured amount of sorption of HDTMA in the calorimeter experiments was less than that observed in the isotherm experiments. These results are consistent with a rapid and energetic sorption rate for an

Table 3.1. Fitted data from HDTMA and TEA sorption models.

Batch[a]	Fit Method	Polynomial Terms		
		ln K (a_1)	a_2	a_3
HDTMA monomers, <ECEC	2^0 fit	3.74±0.55[b]	2.32	-6.43
HDTMA monomers, >ECEC	1^0 fit	6.50±0.15[c]	-2.99	N/A
HDTMA micelles, <ECEC	1^0 fit	5.80±0.20[b]	-0.32	N/A
HDTMA micelles, >ECEC	1^0 fit	9.32±0.59[c]	-5.15	N/A
TEA	2^0 fit	0.42±0.45[b,d]	-0.89	-1.43

[a]HDTMA=7 day equilibration, TEA=24 hour equilibration.
[b] Based on Eq. 6.
[c] Based on Eq. 9.
[d]The full set of TEA data was analyzed for the <ECEC case.
N/A: not applicable.

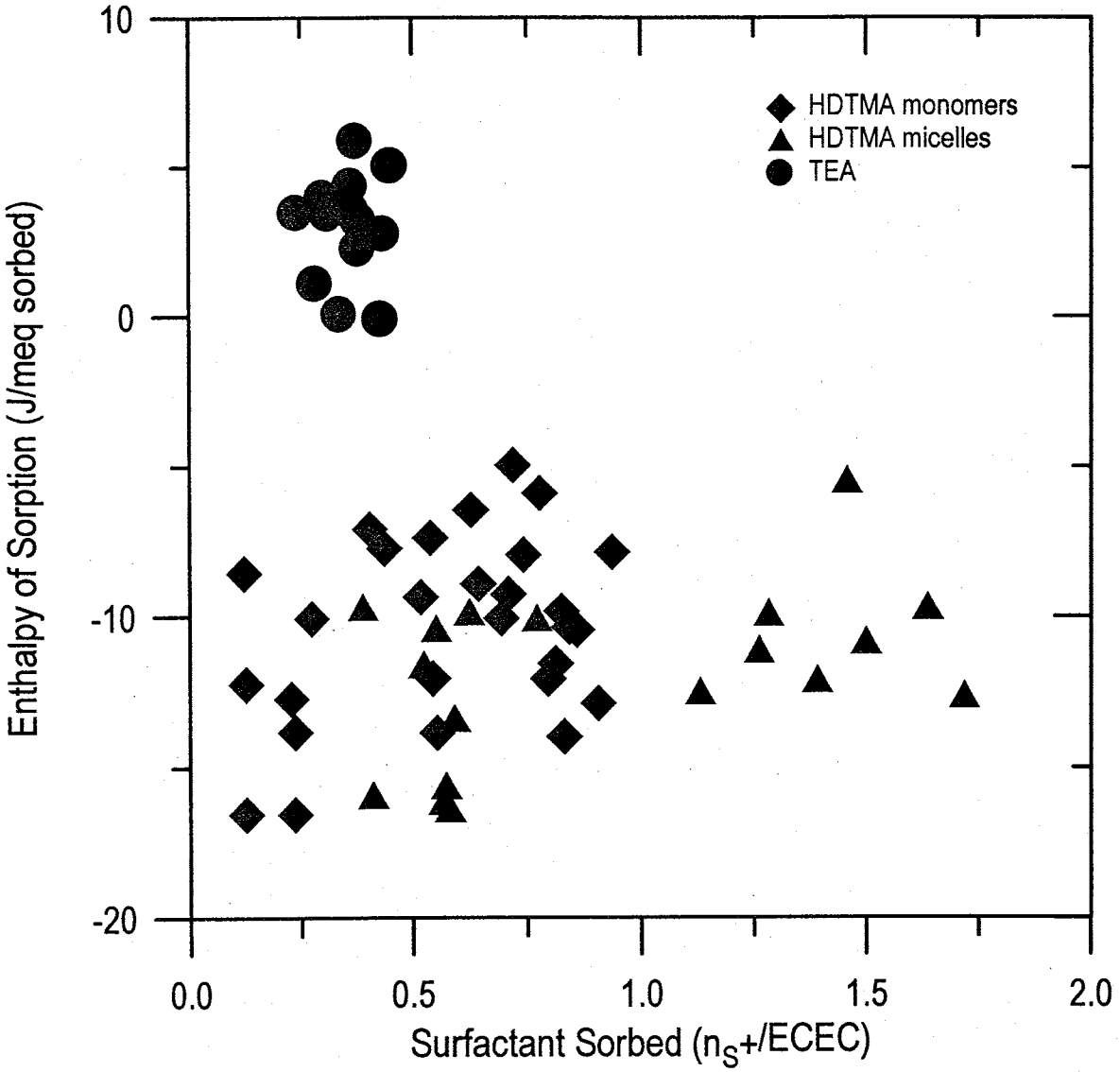

Figure 3.7. Enthalpy of sorption (per meq of surfactant sorbed) versus surfactant sorbed, for HDTMA monomers, HDTMA micelles, and TEA. Sorption equilibration times for all systems were 2 hours.

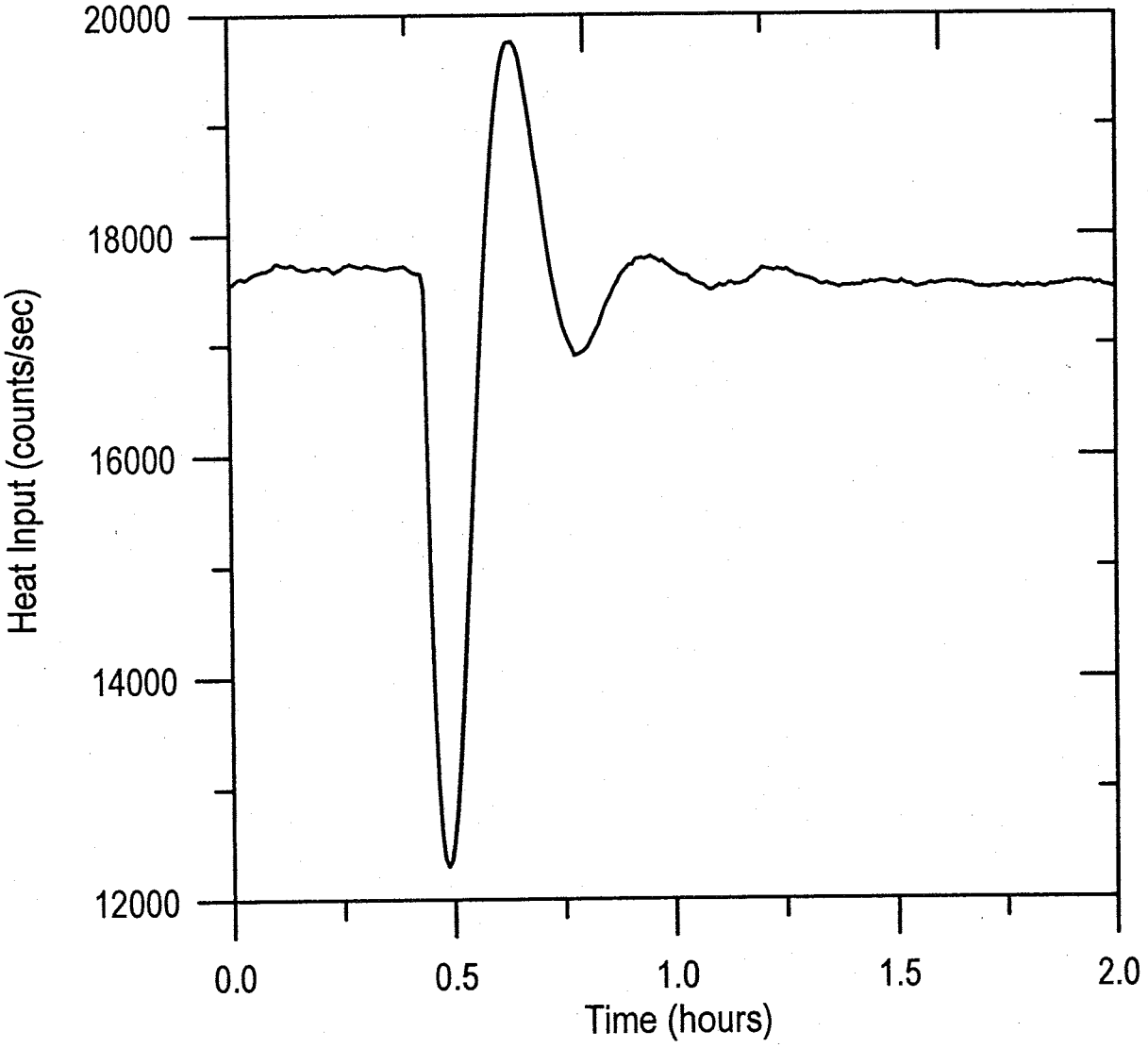

Figure 3.8. Typical plot of a calorimetric measurement: Heat input in counts versus time. The heat input counts are the electrical units for heat added to the system to maintain thermal equilibrium in the calorimeter vessel at 25°C. Decreasing heat input means an exothermic reaction is occurring. Total heat input is determined from integration of the curve across a baseline.

initial quantity of HDTMA. Subsequent sorption occurs at a slower rate, although possibly with the same enthalpy per mole of surfactant if the constant values illustrated in Fig. 3.7 can be extrapolated to higher coverage. The HDTMA micelle system showed a large decrease in sorption rate with increasing time over 72 hours. Sorption at 2 hours was 17 times greater than at 48 hours, for example. Thus the energy released per unit time decreases significantly at longer equilibration times and may not have been detectable with our apparatus.

Assuming that the molar enthalpy values remain constant for surfactant sorption beyond 2 hours, the partial molar enthalpy of sorption is independent of composition ($\Delta H_m^0 = \Delta H_m$). The enthalpy data can then be combined with the isotherm results to calculate the entropy of sorption (Table 3.2). Values of ΔG_m^0 were calculated using Equation 11 and the data in Table 3.1, and the $T\Delta S_m^0$ values were obtained from Equation 12 at T = 298 K.

Discussion

Enthalpy of Sorption

Similar enthalpies of sorption were measured for both the monomer and micelle HDTMA systems. The enthalpy data from the micelle system did not reflect an additional contribution from demicellization as HDTMA sorbed below the ECEC. The enthalpy of micellization, about -9.7 kJ/mol (27,28,29), is close to the measured enthalpies of sorption. This suggests that the dominant enthalpic effect is the transfer of HDTMA from the water phase to the bound phase, regardless of the HDTMA structure on the surface or

Table 3.2. Thermodynamic parameters (± standard deviations) for the exchange of HDTMA or TEA on clinoptilolite.

Batch	ln K (ref. Table 3.1)	ΔG_m^0 (kJ/mol) [a]	ΔH_m^0 (kJ/mol), mean values, (total number of measurements)	$T\Delta S_m^0$ (kJ/mol), T = 298K, mean values[b]
HDTMA monomers, <ECEC	3.74±0.55	-9.27	-10.375±3.029 (28)	-1.10
HDTMA monomers, >ECEC	6.50±0.15	-16.11		+5.74
HDTMA micelles, <ECEC	5.80±0.20	-14.38	-11.980±2.848 (18)	+2.40
HDTMA micelles, >ECEC	9.32±0.59	-23.10		+11.12
TEA[c]	0.42±0.45	-1.041	+3.029±1.790 (13)	+4.07

[a] Calculated from Equation 11.
[b] Calculated from Equation 12.
[c] Values calculated from full data set. All sorption was at less than the ECEC.
N/A: not applicable.

in solution. This is valid for either monomers or intact micelles in the 2-hour measurement time frame for enthalpy. Because the sorption during the enthalpy measurement was generally less than the ECEC, it appears that rearrangement of micelles to a monolayer must occur later, and possibly more slowly than the initial adsorption process. This is consistent with the slow release of desorbed co-ions observed in the sorption isotherms.

The enthalpy of sorption for TEA was slightly endothermic, while that of HDTMA was moderately exothermic. The endothermic character of the sorption of TEA has been attributed to the disruption of the interfacial water structure and release of water molecules from the surface (14, 30). As discussed previously, TEA was used to investigate the sorption energy of a simple polar headgroup. The difference in the enthalpy of sorption of TEA and HDTMA is then an approximate measure of the sorption energy of the tail groups. Most of the exothermic character of the sorption of HDTMA is due to the non-polar part of the molecule and is thus attributable to van der Waals, tail-tail interactions, or tail-surface interactions. Lajtar et al. (10) found that an increasing enthalpy of sorption of cationic surfactants on polar silica corresponds with monomers sorbing as hemimicelles on the surface, a process normally associated with tail-tail interactions (partial micellization). This corresponds to the s-shaped isotherm noted for monomers. However, the enthalpy of sorption of HDTMA on clinoptilolite here is independent of coverage. This seems to indicate independent HDTMA monomer sorption at early times and low coverages. Van der Waals interactions between the tail groups and the surface may be more significant

than tail-tail interactions at those times. This effect has been noted in other systems with large cationic surfactants (30).

Free Energy of Sorption

Values of ΔG_m^0 for HDTMA monomer and micelle sorption versus that of TEA (Table 3.2) reflect stronger sorption of the long-chain hydrocarbon molecules. This is consistent with other studies which found that ΔG_m^0 generally becomes more negative with increasing tail length (Table 3.3). The presence of the HDTMA tail group here makes a considerable difference to the sorption process and thermodynamic stability in this system, both above and below the ECEC. Micelles sorbing above the ECEC present the most negative value of ΔG_m^0 and the strongest forward reaction.

As discussed previously, ΔG_m^0 can be broken into electrostatic (ΔG_{elec}) and specific (ΔG_{spec}) additive components. The polar headgroup dominates ΔG_{elec}, while chain-chain interactions usually dominate ΔG_{spec} (16). In this study, TEA, which lacks a tail group, was used as an indicator of the effect of the polar headgroup on sorption. The value of ΔG_m^0 for TEA then should be approximately equal to ΔG_{elec} for HDTMA. The value of ΔG_m^0 for TEA is small and indicates that ΔG_{spec} is the driving force for sorption of HDTMA. This provides insight into why HDTMA monomers sorb as admicelles or a bilayer even where the solution concentration is less than the CMC.

Israelachvili (21) presented data for the hydrophobic energy associated with the transfer of surfactant chains from water into a bulk phase such as micelles or a bilayer. Generally this varies between 1.7 to 2.8 kJ/mol per CH_2-CH_2 bonding unit added to the

Table 3.3. Literature values of thermodynamic constants for sorption of alkylammonium compounds[a].

Compound	K (ln K)	ΔG_m^0 (kJ/mol)	ΔH_m^0 (kJ/mol)	$T\Delta S_m^0$ (kJ/mol)	Method (*sorption interface*)	Reference
$(C_4H_9)_4N^+I$	NR	-15.68	+ 4.22	+19.89	Calculated (*aqueous solution/air*)	34
$(CH_3)_4N^+$ $C_{14}H_{29}(CH_3)_3N^+$ C_{17}(pyridinium)$^+$	NR	NR	-8.63 -10.37 -13.61	NR	Microcalorimetry (*solution/ montmorillonite*)	35
n-$C_3H_7NH_3^+$	NR	-1.38	NR	NR	Isotherm (*solution/ clinoptilolite*)	23
n-$C_4H_9NH_3^+$	NR	-3.96	assumed zero	+3.99	Isotherm (*solution/ montmorillonite*)	36
n-$C_4H_9NH_3^+$	NR	NR	+5.35	NR	Isotherm (*solution/calcium montmorillonite*)	37
n-$C_8H_{17}NH_3^+$ *n*-$C_{10}H_{21}NH_3^+$	9.2 (2.22) 35.7 (3.58)	-5.39 -8.78	NR NR	NR NR	Isotherm (*solution/ montmorillonite*)	22
n-$C_{14}H_{29}NH_3^+$ *n*-$C_{18}H_{37}NH_3^+$	64±5.9 (4.16±0.09) 102±5.3 (4.62±1.67)	-10.25 -11.46	-10.46 NR	-0.25 NR	Isotherm (*solution/ bentonite*)	38
BDDOAB[b]	NR	NR	-15[d]	NR	Calorimetry (*solution/quartz*)	14
BDOAB[c]	NR	NR	+2[d]	NR	Calorimetry (*solution/silica*)	32

[a]all values determined at 298 K. The counterion is indicated when specified by the authors.
[b]benzyldimethyldodecylammonium bromide
[c]benzyldimethyloctylammonium bromide
[d]maximum value with maximum coverage, enthalpy of displacement varied with coverage.
NR: not reported

tail group. For the 15 CH_2-CH_2 bonds in the HDTMA molecule, the predicted transfer energy is then between 25.5 and 42 kJ/mol. A total value for micellization of HDTMA also can be calculated or measured to be about -32 kJ/mol (17,27,28,29). The ΔG_{spec} values for sorption above the ECEC (obtained using TEA as a measure of ΔG_{elec}) are -18.26 and -25.5 kJ/mol, respectively, for the monomeric and micellar HDTMA systems. These values are just at and above the referenced values for micellization and may thus reflect fewer CH_2 groups actively participating in hydrophobic bonding when the bulk phase is a sorbed bilayer or admicelle rather than a solution micelle. This might occur because of variable tail group conformations when sorbed, or interaction of the tails with water still bound on the surface. The roughness and hydrophilicity of the clinoptilolite surface may also contribute to reduced energetics of transfer.

Entropy of Sorption

Changes in system entropy ($T\Delta S_m^0$) here involve a number of processes. The largest contributors to the total entropy change include the "mobility" of the sorbing surfactant, which is large for HDTMA because of the long, flexible tail group; and the degree of water destructuring (cavity collapse) upon removal of the hydrophobic part of the molecule from solution, because of the high cohesion energy density of water (32, 33). The entropy of the surfactant generally decreases upon sorption because of fixation on the mineral surface, while the water phase gains entropy because of destructuring. Actual structural effects of sorption on the surfactant molecules are difficult to extract from these data (Table 3.2), but some relative comparisons can be made between the HDTMA systems and the less hydrophobic and less mobile TEA molecule.

Sorption of TEA produced a moderately small positive value of $T\Delta S_m^0$ (+4.07 kJ/mol, Table 3.2). The molecule undergoes a small loss of entropy due to sorption in addition to the larger gain in water entropy from cavity collapse.

Sorption of monomers at less than the ECEC showed a small net loss of entropy (-1.10 kJ/mol). The loss of entropy from surfactant fixation is thus slightly greater than the increase in water entropy (cavity collapse). This is consistent with the idea that tail groups may interact with the surface at low loading levels, or that cavity collapse around the monomers is minimal. Above the ECEC, a net increase in monomer entropy is measured (+5.74 kJ/mol), likely because of a greater cavity collapse as the monomers condense into patchy bilayers. A value of about +18.5 kJ/mol was reported for the entropy of micellization of HDTMA in solution (27), indicating the large potential effect of the cavity collapse as the monomers sorb.

The values of $T\Delta S_m^0$ for micellar HDTMA sorption were larger than for monomers below and above the ECEC (+2.40 and + 11.12 kJ/mol, respectively). There was little time for admicelle rearrangement to a monolayer, so the degree of mobility of the sorbed molecules is likely less important than the degree of cavity collapse. The smaller value for the less-than-ECEC admicelle sorption suggests only a small amount of cavity collapse upon removal of the micelles from solution. This may also suggest limited mobility of the hydrocarbon chains in the hemimicelles or patchy bilayers. A much larger $T\Delta S_m^0$ value for the greater-than-ECEC system indicates more extensive cavity collapse, or possibly greater tail freedom of movement as the individual admicelles begin to coalesce into a complete bilayer.

Conceptual Sorption Model

As a result of the above observations, we propose the following conceptual model for the sorption of HDTMA onto clinoptilolite. Early sorption is fast for all systems, then slows some time after the first half hour. For the monomer system, it appears that sorption below the ECEC is in the form of individual monomers, which may either interact with the surface, or form coiled tail groups with a limited interaction with the solution. In any event, it is likely that they undergo little further interaction with each other during sorption at low coverages. As available surfactant increases, a monolayer forms and tail group interactions increase as a small amount of surfactant is sorbed as a bilayer, probably in the form of patchy bilayers (disperse admicelles).

For the micellar system below the ECEC, sorption is in the form of admicelles which later rearrange to a monolayer (disperse hemimicelles). Above the ECEC, micelles sorbing initially may rearrange to the extent of the ECEC, with the remainder forming patchy bilayers or admicelles on the surface. At high loading levels, sorbed micelles are stable and later may coalesce to a full bilayer.

In view of energy of the system and prediction of thermodynamic stability, modified clinoptilolite prepared with surfactant solutions above the CMC and above the ECEC seems to be the most stable (ΔG_m^0=-23 kJ/mol for micelles above the ECEC versus -16 kJ/mol for monomers) and has the fastest sorption time. When solution concentrations fall below the CMC, HDTMA sorbed as a bilayer will still be stable as evidenced by negative values of ΔG_m^0 for sorption.

ACKNOWLEDGMENTS

This study was supported by the U.S. Department of Energy under contract DE-AR21-95-MC32108 through the Morgantown Energy Technology Center. We thank MST-11 Group at Los Alamos National Laboratory, particularly Eric Brosha and Fernando Garzon. Emily Keene and Jeanne Verploegh of New Mexico Tech provided valuable assistance with the laboratory studies.

REFERENCES

1. Zhang, Z.Z., Sparks, D.L., and Scrivner, N.C., Sorption and desorption of quaternary amine cations on clays. *Environ. Sci. Technol.* **27**, 1625 (1993).

2. Xu, S., and Boyd, S.A., Cationic surfactant sorption to a vermiculitic subsoil via hydrophobic bonding. *Environ. Sci. Technol.* **29**, 2, 312 (1995a).

3. Xu, S., and Boyd, S.A., Alternate model for cationic surfactant adsorption by layer silicates. *Environ. Sci. Technol.* **29**, 12, 3022, (1995b).

4. Bowman, R.S., Haggerty, G.M., Huddleston, R.G., Neel, D., and Flynn, M.M., Sorption of nonpolar organic compounds, inorganic cations, and inorganic oxyanions by surfactant-modified zeolites. *in* "Surfactant-Enhanced Subsurface Remediation" (D.A. Sabatini, R.C. Knox, and J.H. Harwell, Eds.), p. 54. ACS Symposium Series 594, American Chemical Society, Washington, DC, 1995.

5. Barrer, R.M., "Zeolites and Clay Minerals as Sorbents and Molecular Sieves." Academic Press Inc., New York, 1978.

6. Haggerty, G.M., and Bowman, R.S., Sorption of chromate and other inorganic anions by organo-zeolite. *Environ. Sci. and Technol.* **28**, 3, 452 (1994).

7. Chen, Y.L., Chen, S., Frank, C., and Israelachvili, J., Molecular mechanisms and kinetics during the self-assembly of surfactant layers. *J. Colloid Interface Sci.* **153**,1, 224 (1992).

8. Harwell, J.H., Hoskins, J.C., Schechter, R.S., and Wade, W.H., Pseudophase separation model for surfactant adsorption: Isomerically pure surfactants. *Langmuir* **1**, 251 (1985).

9. Cases, J.M. and Villieras, F., Thermodynamic model of ionic and nonionic surfactant adsorption-abstraction on heterogeneous surfaces. *Langmuir* **8**, 1251 (1992).

10. Lajtar, L., Narkiewicz-Michalek, J., and Rudzinski, W., A new theoretical approach to adsorption of ionic surfactants at water/oxide interfaces: studies of the mechanism of cationic surfactant adsorption. *Langmuir* **10**, 3754 (1994).

11. Hayakawa, K., Morita, T., Ariyoshi, M., Maeda, T., and Satake, I., Adsorption of cationic surfactants on hydrophobic mordenites of different Si/Al ratio. *J. Colloid Interface Sci.* **177**, 621 (1996).

12. Tamura, H., Noriaki, K., and Ryusaburo, F., Modeling of ion-exchange reactions on metal oxides with the Frumkin isotherm. *Environ. Sci. Technol.* **30**, 4, 1198 (1996).

13. Seidel, J., Application of calorimetric methods to the adsorption of surfactants from solution. *Thermochim. Acta* **229,** 257 (1993).

14. Zajac, J., Trompette, J.L., and Partyka, S.,. Calorimetric studies of cationic surfactant adsorption at low surface coverages on different silica samples. *J. Thermal Anal.* **41,** 1277 (1994).

15. Lyman, W.J., Reehl, W.F., and Rosenblatt, D.H., "Handbook of Chemical Property Estimation Methods." American Chemical Society, Washington, DC, 1990.

16. Hough, D.B., and Rendall, H.M., *in* "Sorption from Solution at the Solid/Liquid Interface" (G.D. Parfitt and C.H. Rochester, Eds.), p. 247. Academic Press Inc., New York, 1983.

17. Blandamer, J., Cullis, P.M., Soldi, L.G., Engberts, J.B.F.N., Kacperska, A., Van Os, N.M., and Subha, M.C.S., *Adv. Colloid Interface Sci.* **58**, 8, 171 (1995).

18. Fuerstenau, D.W., and Herrera-Urbina, R., *in* "Cationic Surfactants-Physical Chemistry" (D.N. Rubingh and P.M Holland, Eds.), p. 407. Surfactant Science Series Vol. 37, Marcel Dekker, Inc., New York, 1991.

19. Sullivan, E.J., Hunter, D.B., and Bowman, R.S. Topological and thermal properties of surfactant-modified clinoptilolite studied by Tapping-Mode™ atomic force microscopy and high-resolution thermogravimetric analysis. *Clays and Clay Minerals* **45,** 1, in press (1997).

20. Ming, D.W. and Dixon, J.B., Quantitative determination of clinoptilolite in soils by a cation-exchange capacity method. *Clays & Clay Minerals* **35**, 463 (1987).

21. Israelachvili, J. N., "Intermolecular and Surface Forces." 2nd Ed. Academic Press, Inc., San Diego, California, 1991.

22. Cowan, C.T., and White,D., The mechanism of exchange reactions occurring between sodium montmorillonite and various *n*-primary aliphatic amine salts. *Trans. Faraday Soc.* **54,** 691 (1957).

23. Barrer, R.M., Papadopoulos, R., and Rees, L.V.C., Exchange of sodium in clinoptilolite by organic cations. *J. Inorg. Nucl. Chem.* **29,** 2047 (1967).

24. Theng, B.K.G., "The Chemistry of Clay-Organic Reactions." John Wiley & Sons, Inc., New York, 1974.

25. Wakamatsu, T., and Fuerstenau, D.W., "Adsorption from Aqueous Solution." Adv. Chem. Series Vol. 79. American Chemical Society, Washington D.C. 1968.

26. Connor, P. and Ottewill, R.H. *J. Colloid Interface Sci.* **37**, 3, 642 (1971).

27. Paredes, S., Tribout, M., and Sepulveda, L., Enthalpies of micellization of quaternary tetradecyl- and cetyltrimethylammonium *J. Phys. Chem.* **88**, 1871 (1984).

28. Bach, J., Blandamer, J., Burgess, J., Cullis, P.M., Soldi, L.G., Bijma, K., Engberts, J.B.F.N., Dooreman, P.A., Kacperska, A., Rao, K.C., and Subha, M.C.S., *J. Chem. Soc. Faraday Trans.* **91**, 8, 1229 (1995).

29. Bashford, J.T., and Woolley, E.M., *J. Phys. Chem.*, **89**, 3173 (1985).

30. Zajac, J., Trompette, J.L., and Partyka, S., Adsorption of cationic surfactants on a hydrophilic silica surface at low surface coverages: Effects of the surfactant alkyl chain and exchangeable sodium cations at the silica surface. *Langmuir* **12**, 1357 (1996).

31. Sepulveda, L., and Cortes, J., *J. Phys. Chem.* **89**, 5322 (1985).

32. Kronberg, B., Costas, M., and Silveston, R., Thermodynamics of the hydrophobic effect in surfactant solutions-micellization and adsorption. *Pure & Appl. Chem.* **67**, 6, 897 (1995).

33. Costas, M., Kronberg, B., and Silveston, R., General thermodynamic analysis of the dissolution of non-polar molecules into water. *Chem. Soc. Faraday Trans.* **90**, 11, 1513 (1994).

34. Rosen, M.J., "Surfactants and Interfacial Phenomena", John Wiley & Sons, New York, 1978.

35. Chong, F.Y., Seol, Y., Paker, P.E., and Johnson, C.T., *in* "Proceedings of the 33rd Annual Meeting of the Clay Minerals Society", p. 36. Clay Minerals Society, Gatlinburg, Tennessee, 1996.

36. Vansant, E.F., and Uytterhoeven, J.B., Thermodynamics of the exchange of n-alkyl ammonium ions on Na-montmorillonite. *Clays and Clay Minerals* **20**, 47 (1972).

37. Slabaugh, W.H., and Kupka, F., Organic cation exchange properties of calcium montmorillonite. *J. Phys. Chem.* **62**, 599 (1958).

38. Slabaugh, W.H., Cation exchange properties of bentonite. *J. Phys. Chem.* **58**, 162 (1954).

CHAPTER 4

FOURIER-TRANSFORM RAMAN SPECTROSCOPY OF SORBED HDTMA AND THE MECHANISM OF CHROMATE SORPTION TO SURFACTANT-MODIFIED CLINOPTILOLITE

(Submitted to Environmental Science and Technology, March 19, 1997)

ABSTRACT

We examined sorption of hexadecyltrimethylammonium bromide (HDTMA) to clinoptilolite zeolite and subsequent sorption of the chromate anion to the surfactant-modified zeolite (SMZ) with Fourier-transform (FT) Raman spectroscopy and batch sorption methods. At high loading levels (above the external cation exchange capacity, ECEC) the sorbed HDTMA was similar in conformation to solution micelles, with some decreased structuring of tail groups and decreased headgroup hydration states. At these loading levels HDTMA has available anion exchange sites. At lower loadings, the HDTMA tended to exhibit more disorder as monomers than sorbed or solution micelles, and lacked potential anion exchange sites. Chromate sorption was observed to high-loading SMZ, with equivalent Br^- counterion exchange. Sorption data indicated that chromate sorbed best to zeolite modified to greater than 100% of the ECEC. The FT-Raman spectrum of the sorbed chromate showed a shift and split in the chromate peak, indicating the potential for more than one type of binding environment on the surface. Based on the sorption data, anion exchange was indicated as a probable mechanism for

the chromate sorption. Based on the FT-Raman spectra, however, enhanced Lewis acid-base interactions are also a potential mechanism.

INTRODUCTION

Surfactant-modified zeolite (SMZ) has potential use as a sorbent for toxic compounds from contaminated waters, in subsurface permeable barriers or *ex-situ* water treatment systems. SMZ can sorb organic compounds as well as inorganic cations and oxyanions from water (1,2,3). Partitioning is responsible for organic sorption by SMZ while transition metal cation sorption is generally unaffected (1). The conformation and quantity of surfactant on the surface as well as complex interactions between the surface and the surfactant are potentially responsible for the ability of the surface to retain oxyanions (2). One proposed mechanism is retention of the oxyanions via anion exchange with counterions on the external portion of a surfactant bilayer or on admicelles (4). The presence of admicelles versus a monolayer is thus important because admicelles imply the presence of anion exchange sites.

The Raman spectrum arises from changes in molecular polarizability, while the infrared (IR) spectrum arises from changes in dipole moment during visible, infrared, or ultraviolet-induced molecular vibrations (5). Peaks can be recorded for both IR and Raman at some frequencies while other vibrations may be mutually exclusive. Changes in the chemical environment which affect the polarizability of a bond will shift or remove a band in a Raman spectrum. Low concentrations of the bond type also can cause apparent removal of a band because of low signal-to-noise ratios. Previously, Fourier-

transform IR (FTIR) methods have been used to characterize surfactant structure in micelles and on surfaces (6-8), and interpretations of this data have relevance to FT-Raman spectral interpretation. A number of atomic groups in organic compounds produce vibrations at characteristic wavenumbers for both Raman and IR methods (9,10). These include, for example, the CH_2 stretching modes between 3000 and 2800 cm^{-1} and the CH_2 bending modes between 1470 to 1400 cm^{-1}.

In biological and chemical systems, FT-Raman spectroscopy has been used successfully to characterize the structural conformation, functionalities, and molecular composition of lipid bilayers and surfactant mono- and bilayers, including the interdigitization of lipid and surfactant chains or tail groups in bilayers (11-14). Integrated band intensities, peak height ratios, and peak shifts were used to measure these properties. Particularly, the region between 3,100-2,800 cm^{-1} was used to examine the acyl or alkyl chain C-H stretching mode region to show bilayer perturbations (11,12). This spectral region is also accepted in IR spectroscopy as a means of determining *trans* to *gauche* transitions based on band frequency shifts, such as during thermotropic phase transitions of sorbed fatty acids (7), and surfactant conformation changes at different coverages and wetting states on silica (8). These vibrations are important in that they can help measure the order/disorder, compactness, and crystallinity of the alkyl chain (8, 13). Comparable band shifts in the FT-Raman spectrum have been noted (13-14).

Oxyanions such as chromate can produce strong peaks which exhibit band shifts and variations in intensity and height ratios depending upon the chemical environment before and after sorption. FT-Raman spectroscopy was chosen to probe surface

interactions between zeolite, surfactant, and chromate because it can give information about binding between SMZ and chromate. Anion exchange sites for potential chromate sorption have been demonstrated to occur on surfactant bilayers on HDTMA-modified zeolite (15). Alternately, hexavalent chromate may act as a Lewis base by donating an electron pair to acid sites present on the zeolite surface. The presence of Lewis acid sites on zeolites has been demonstrated (16, 17). These sites on adsorbates are known to affect the polarizability and dipole moment of the conjugate acid or base and, thus, the Raman and IR band frequencies (10, 16, 18, and others cited therein). Lewis acid sites occur when the zeolites have been completely alkali-exchanged and dried under vacuum (16, 18). The presence of the surfactant may substantially reduce the amount of near-surface water, enhancing the relative acidity of such sites and subsequently promoting chromate sorption. One goal of this study was to determine which, if any, chromate sorption process is most important.

Near-infrared FT-Raman spectroscopy holds a number of advantages over conventional Raman techniques, including avoidance of sample fluorescence (13). The broad adsorption bands of water in IR spectra at 1640 cm^{-1} and 3,000 to 4,000 cm^{-1} can obscure data from other sorbed compounds. This problem is eliminated in the near-IR FT-Raman spectrum, expanding the range of absorbance information. FT-Raman techniques can be used on wet surface-adsorbed samples, particularly because the Raman spectrum is principally a result of the sorbed material only (5, 10). This allows examination of the sorbed surfactant under *in-situ* conditions.

This paper describes spectroscopic and macroscopic methods used to determine the type of interaction between a surfactant, hexadecyltrimethylammonium bromide (HDTMA), and a clinoptilolite zeolite surface, the subsequent form and relative thickness of the HDTMA on the surface, and the type of interaction occurring between the SMZ and chromate. FT-Raman spectroscopy was used to examine the structural characteristics of HDTMA sorbed to zeolite, solid HDTMA, HDTMA solutions, and the SMZ-chromate system. Sorption isotherms were used to quantify the amounts of HDTMA, HDTMA counterion (Br^-), and chromate retained by the SMZ, to account for potential chromate sorption mechanisms.

MATERIALS AND METHODS

Zeolite and Reagents

The zeolite used is a clinoptilolite-rich tuff from the St. Cloud mine in Winston, New Mexico. It consists of about 74% clinoptilolite, 5% smectite, 10% quartz and cristobalite, 10% feldspar, and 1% illite, based on internal standard X-ray diffraction analysis (19, 20). We measured an external cation-exchange capacity (ECEC) of 70 to 90 meq/kg for the St. Cloud zeolite using the method of Ming and Dixon (21). We also measured an external surface area of 15.7 m^2/g on a sample dried for 24 hours at 200°C (15). The zeolite was sieved to a size range of 2 mm to 150 μm prior to use.

The HDTMA-Br^- was used as received (Sigma Chemicals, >99% purity). Reagent-grade K_2CrO_4 was also used as received (Baker Chemicals). All aqueous solutions were made with 18.2 Mohm cm^{-1} (ASTM Type I) water.

Sorption Experiment

For the sorption experiment, variable quantities (0.1 to 4 g) of zeolite were placed in 500 ml polyallomer centrifuge bottles with 100 ml of one of two surfactant solutions. One solution was made up to 0.45 mmol/L, which is one-half of the critical micelle concentration (CMC) of 0.9 mmol/L (at 25°C) (22), and therefore contained predominantly HDTMA monomers. The other solution was 2 times the CMC or 1.8 mmol/L, where the HDTMA was predominantly in micellar form. Each surfactant solution was spiked with [^{14}C-methyl]HDTMA (American Radiolabelled Chemicals, Inc., St. Louis, MO). The zeolite was treated with HDTMA to 50%, 100%, and 400% of ECEC, where 100% was assumed equal to 90 meq/kg zeolite. Each sample was prepared in duplicate, and appropriate blanks were included in each batch. The solutions were shaken with the zeolite for 7 days at 25°C, then the SMZ was centrifuged at 14500 x g for 30 minutes. Preliminary experiments showed that up to 7 days were required to obtain sorption equilibrium for the low-concentration solutions used. After the centrifuging step, 5 ml of supernatant were removed from each bottle for analysis of HDTMA and Br^-. ^{14}C-HDTMA was determined using a Packard Tri-Carb liquid scintillation counter. The supernatants were analyzed for Br^- by high-performance liquid chromatography (HPLC). The surface tension was also measured to determine if the supernatants were above or below the CMC.

To measure chromate sorption, the samples were then spiked with 5 ml of either a 0.19 mmol/L solution (for the more dilute monomer system) or 1.9 mmol/L solution (for the micelle system) of K_2CrO_4 (Baker Chemicals). The chromate-spiked SMZ was

shaken for 24 hours, then centrifuged and an aliquot of supernatant removed as above. Samples were analyzed for Br^- and chromate by HPLC.

FT-Raman Sample Preparation

The unmodified zeolite was first saturated with sodium by shaking 40 g with 120 ml of 1 *N*, pH 5 sodium acetate buffer for 15-min in a 500-ml polyallomer centrifuge bottle. The samples were centrifuged at 14500 x g for 20 minutes, the supernatant discarded, and the entire sequence repeated two more times. This was followed by three rinses with Type I water and three rinses with 95% ethanol, then air drying.

The sodium-saturated zeolite was modified with HDTMA to a range of coverages from 0% to 310% of the ECEC. Surfactant modification consisted of shaking 5 g of zeolite with 20 ml of the selected HDTMA solution (between 0-70 mmol/L) for 12 hr at 25°C in a 50-ml polyallomer Oak Ridge centrifuge tube. This amount of time was shown to be sufficient for complete reaction of HDTMA on zeolite for these solution concentrations (23). All solutions were well above the CMC. The SMZ was centrifuged at 14500 x g for 30 minutes and excess HDTMA solution decanted. The samples were then washed with 20 ml of Type I water, centrifuged, and decanted as above.

The various samples of SMZ were then shaken for 24 hours in 50-ml polyallomer centrifuge tubes with 0.04 mmol/L K_2CrO_4 in the ratio of 1 g of zeolite to 4 ml of solution. The samples were allowed to settle for 1 hour and excess solution was removed with a pipette. The SMZ-chromate was then rinsed for 30 seconds with 5 ml of the chromate solution and the excess solution removed with a pipette. This step was repeated

two more times and was intended to reduce the concentration of HDTMA in the supernatant to prevent interference. A background check revealed that the 0.04 mmol/L chromate solution was below the FT-Raman detection limit. Each SMZ-chromate sample was packed as a wet slurry into a non-fluorescing Nicolet NMR glass tube for FT-Raman analysis.

FT-Raman Spectroscopy

Solid HDTMA-Br^- powder, a solution of 70 mmol/L K_2CrO_4, solutions of 0.45 mmol/L and 70 mmol/L HDTMA, and wet slurries of SMZ and SMZ-chromate were analyzed using a Nicolet 910 Fourier Transform Raman spectrometer with a diode-pumped solid state laser emitting at 1064 nm. Samples were loaded as a dry powder, solution, or wet slurry into 5 mm non-fluorescing Nicolet NMR tubes. The laser power was adjusted to 1.1 W. There were 3,000 scans co-added for each spectrum at 1 cm^{-1} resolution. Wavenumber accuracy was ± 1 cm^{-1} and the range of operation was 4000-50 cm^{-1}. Background scans were taken of a 70 mmol/L K_2CrO_4 solution to determine if solution chromate would interfere with the sorbed chromate spectrum, which it did not. A 200 mmol/L K_2CrO_4 solution therefore was used to produce a chromate spectrum. The signal-to-noise criterion for peak existence was 3 standard deviations above the mean value of the noise. Band shifts of greater than 2 cm^{-1} were considered to be real changes in vibration energy values.

RESULTS AND DISCUSSION

Sorption Data

Sorption of HDTMA monomers versus HDTMA micelles can produce different conditions on the surface of the zeolite, depending upon whether the amount of available surfactant exceeds the ECEC. The samples treated to 50 or 100% of the ECEC should exhibit an absence of a bilayer (i.e., a monolayer) of surfactant whether or not the surfactant is applied as monomers or micelles (15). The samples treated to 400% of ECEC were expected to produce a surfactant bilayer. Previous sorption studies showed that monomer solutions produce stable monolayers at less than the ECEC, but above the ECEC produce less extensive bilayers than do micelle systems. Micelle systems readily form complete bilayers or extensive admicelles when treated above the ECEC (15). Both systems were examined here for completeness.

Data for HDTMA sorption to zeolite for three treatment levels, 50%, 100%, and 400% of ECEC, and subsequent chromate sorption to the SMZ are shown in Figures 4.1a and 4.1b. The plots also show sorption of the original Br^- counterion, the remaining Br^- sorbed after CrO_4^{2-} treatment, and CrO_4^{2-} sorbed. All data were calculated in terms of meq. Chromate was assumed to be sorbing predominantly as CrO_4^{2-}, based on previous experiments which showed pH values of about 7. Surface tension measurements (not shown) indicated that all of the solutions fell at or below the CMC after the HDTMA sorption step, a condition expected to correlate with HDTMA bilayer sorption (15). Results were similar to those found in previous studies (15).

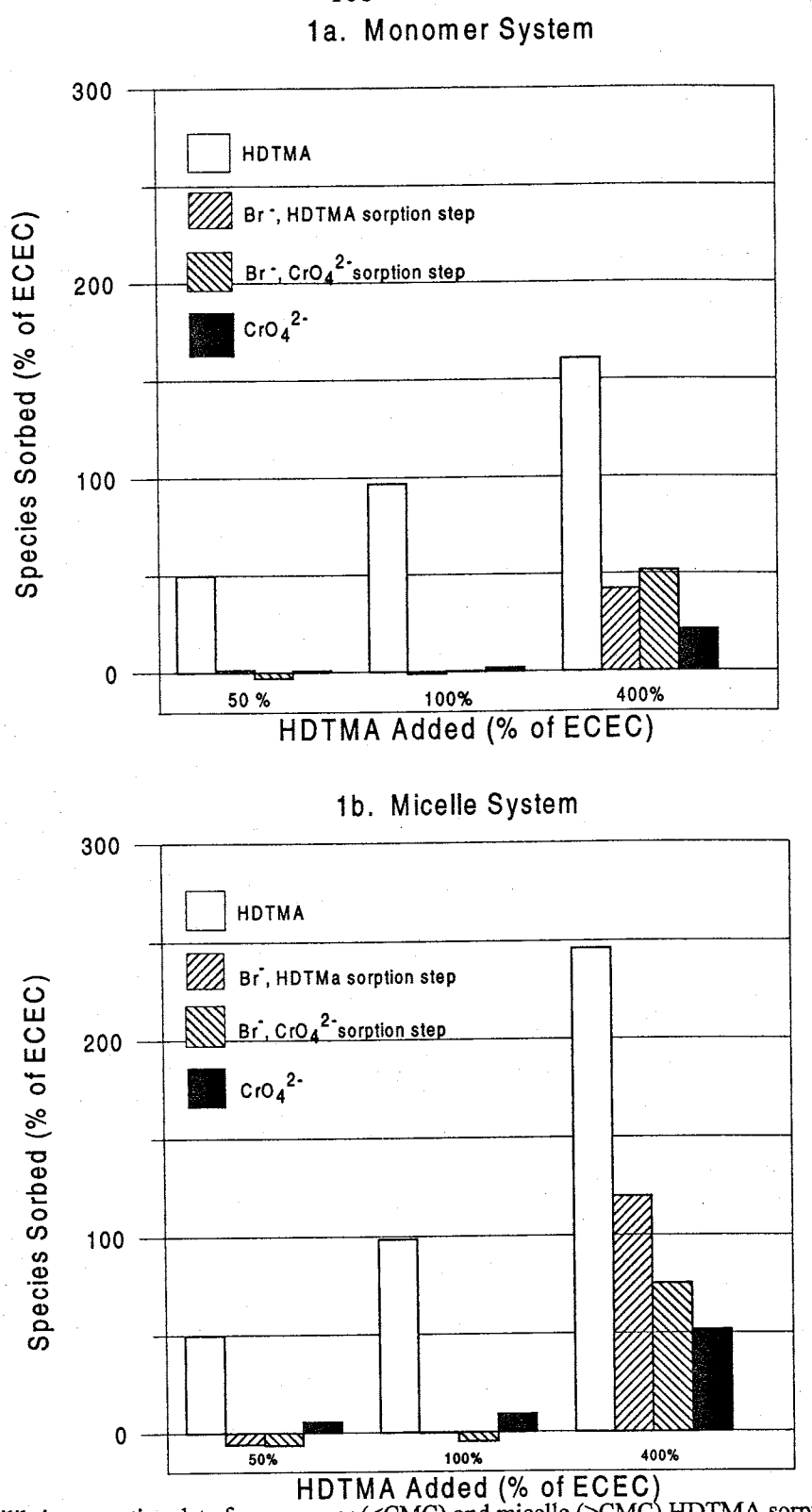

Figure 4.1. Equilibrium sorption data for monomer (<CMC) and micelle (>CMC) HDTMA sorption to clinoptilolite zeolite, with Br^- counterion data for the initial sorption step. Sorbed CrO_4^{2-} and Br^- concentrations are also shown for the subsequent chromate spike step.

For the monomer and micelle systems, similar results were measured for HDTMA and Br^- sorption at the 50% and 100% treatment levels. HDTMA sorbed only up to the ECEC, while Br^- sorption was very low, indicating that no bilayer exists on the surface. Subsequent CrO_4^{2-} sorption was also extremely low, indicating that SMZ with a monolayer conformation does not readily adsorb CrO_4^{2-}. It was shown previously that unmodified zeolite also does not sorb CrO_4^{2-} (2).

For the 400% treatment samples, HDTMA sorbed to 160 and 250% of ECEC for the monomer and micelle systems, respectively. Bromide sorbed to about half the HDTMA amount in the micelle system and slightly less than half in the monomer system. This indicates admicelle or bilayer formation in both systems, however, the monomer system bilayer is less complete and is probably in the form of patchy bilayers. Subsequent CrO_4^{2-} treatment produced chromate sorption to about 20 and 50% of ECEC for the monomer and micelle systems, respectively. This was almost the same as the amount of desorbed Br^- (in meq) in the micelle system, with a variation of about ±6%. A slight gain in Br^- sorption was noted in the CrO_4^{2-} sorption step of the monomer system, possibly from dissociation of HDTMA-Br^- caused by uncommon anion or other solution effects. The total sorbed anion equivalents were very close to the quantity of surfactant adsorbed above the ECEC. This indicates that anion exchange is a reasonable mechanism for CrO_4^{2-} sorption, and that CrO_4^{2-} sorption is most favored in those samples where a bilayer or admicelles can sorb directly from a micelle-containing solution with available quantities of HDTMA well above the ECEC.

FT-Raman Spectra Assignment of HDTMA Monomer, Micelle, and Solid Band Shifts

Figure 4.2 shows the higher-frequency range of the FT-Raman spectra for HDTMA in a solution below the CMC (0.45 mmol/L), above the CMC (70 mmol/L), and as a solid. Peak assignments are shown in Table 4.1. The spectra differ significantly among all three states. These spectra show HDTMA in solid and solution states, so that comparisons with sorbed HDTMA can be made.

Changes in bands associated with the HDTMA tail groups indicated more disorder in solution species tail groups than in the solid form. In previous studies, higher-frequency band shifts were associated with increased *gauche* conformers and increased disorder after surfactant phase changes from solids or liquid crystals to liquids (7,8,24). For example, the shift from 2847 cm^{-1} to 2852 cm^{-1} for the CH_2 s-stretch (symmetrical stretch for chain carbon bonds) between solid and solution species (Table 4.1) indicates an increase in the number of *gauche* versus *trans* conformers in the solution system. The appearance of a peak at 2869 cm^{-1} in the monomer solution may also be related to this change in tail group conformation. A similar shift occurs in the various CH_2 a-stretch (asymmetrical stretch) bands between solid (2881 cm^{-1}) and solution (2888-2898 cm^{-1}). *Gauche* bonds in the surfactant chain produce increased chain bending, greater disorder, and less rigidity in chain forms (14).

Using these band shift comparisons, there appears to be more order in solution micelle tail groups when compared to solution monomer tail groups. This is expected because monomer tail groups are free to rotate in solution while micellized surfactant

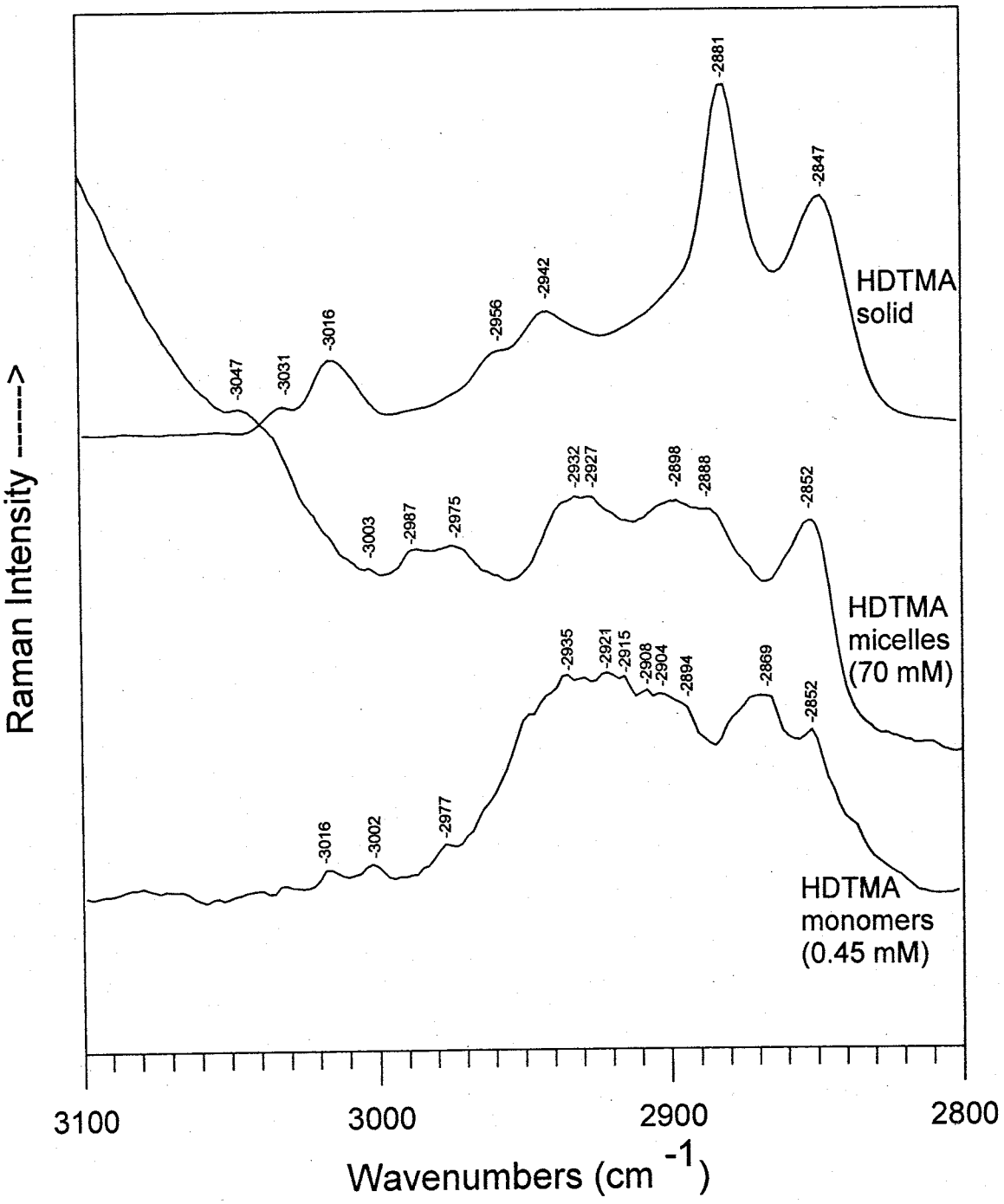

Figure 4.2. FT-Raman spectra for HDTMA in the monomer, micelle, and solid forms, showing the higher-frequency portion of the spectra.

Table 4.1. FT-Raman high-frequency data for HDTMA as monomers, micelles, and solid for the spectra shown in Fig. 4.2.

	HDTMA Form				
	HDTMA 0.45 mM (monomers)	HDTMA 70 mM (micelles)	HDTMA solid	Reference[a,b] 100 mM (micelles)	Reference[b] (solid)
Tentative Assignment	Raman Bands, cm^{-1}				
CH_2 s-stretch[a,b]	2852	2852	2847	2854	2850
	2869				
CH_2 a-stretch[b,d]	2894 sh 2904 b 2908	2888 sh 2898 b	2881	2890[d]	2873 2883 2900
	2915 2921			2930[e]	
CH_2 a-stretch[a,b,c]	2935	2927 2932	2942	2935	2945[c]
CH_3-R a-stretch[a,e]			2956 sh		2961
CH_3-N^+ s-stretch[a,d]	2977 sh	2975		2974	2974
		2987		2987	3009
	3002	3003			
CH_3-R a-stretch[a] ?	3016		3016		
CH_3-N^+ a-stretch[b]		3047	3031	3042	3020 3029 3034

[a] Suga et al. 1993.
[b] Dendramis et al. 1983.
[c] Dendramis et al. characterize this as a CH_3-R s-stretch.
[d] Suga et al. characterize this as a CH_3-R s-stretch.
[e] Suga et al. characterize this as a SERS band.
w = weak; sh = shoulder, b = broad peak, a-stretch = asymmetrical stretch, s-stretch = symmetrical stretch

tails tend to associate with each other through van der Waal's forces. For example, chain (11), or terminal carbon stretches (14) at 2888 to 2898 cm^{-1} for micelles shifted to a broad set of peaks at 2894 to 2921 cm^{-1} in the monomer solution.

Figure 4.3 (7) shows a schematic diagram applicable to both sorbed and solution species, depicting the distortion which occurs to the chain when these *gauche* conformations arise. This is significant in the interpretation of sorbed surfactant band shifts because less rigidity in tail groups forming bilayers or admicelles corresponds with a lower degree of interdigitization and a larger bilayer or admicelle volume than for solution micelles (13). This also provides a means for distinguishing between adsorbed monolayers and bilayers.

Higher-frequency band shifts in FTIR CH_2 stretch modes occur with an increasingly hydrophilic environment, for example, from solid to solution species (6,8). This shift is apparent in the data here (Table 4.1). Monomers, which can have extensive contact with the water structure, show less relative difference from the micelles than from the solid. This interpretation of the molecular environment may be more clear when head group data, which can show indications of hydration, are included in the analysis. There is a trend in the referenced data (14) and here (Table 4.1) which indicates a higher-frequency shift in head group CH_3-N^+ bond vibrations with an increasingly hydrophilic environment. For example, the CH_2-N^+ a-stretch shifts from 3031 cm^{-1} for the solid to 3047 cm^{-1} for the micelle solution. Bands corresponding to the CH_3-N^+ (head group methyl) s-stretch in the monomer and micelle systems (2977, 2975 cm^{-1}) are missing in

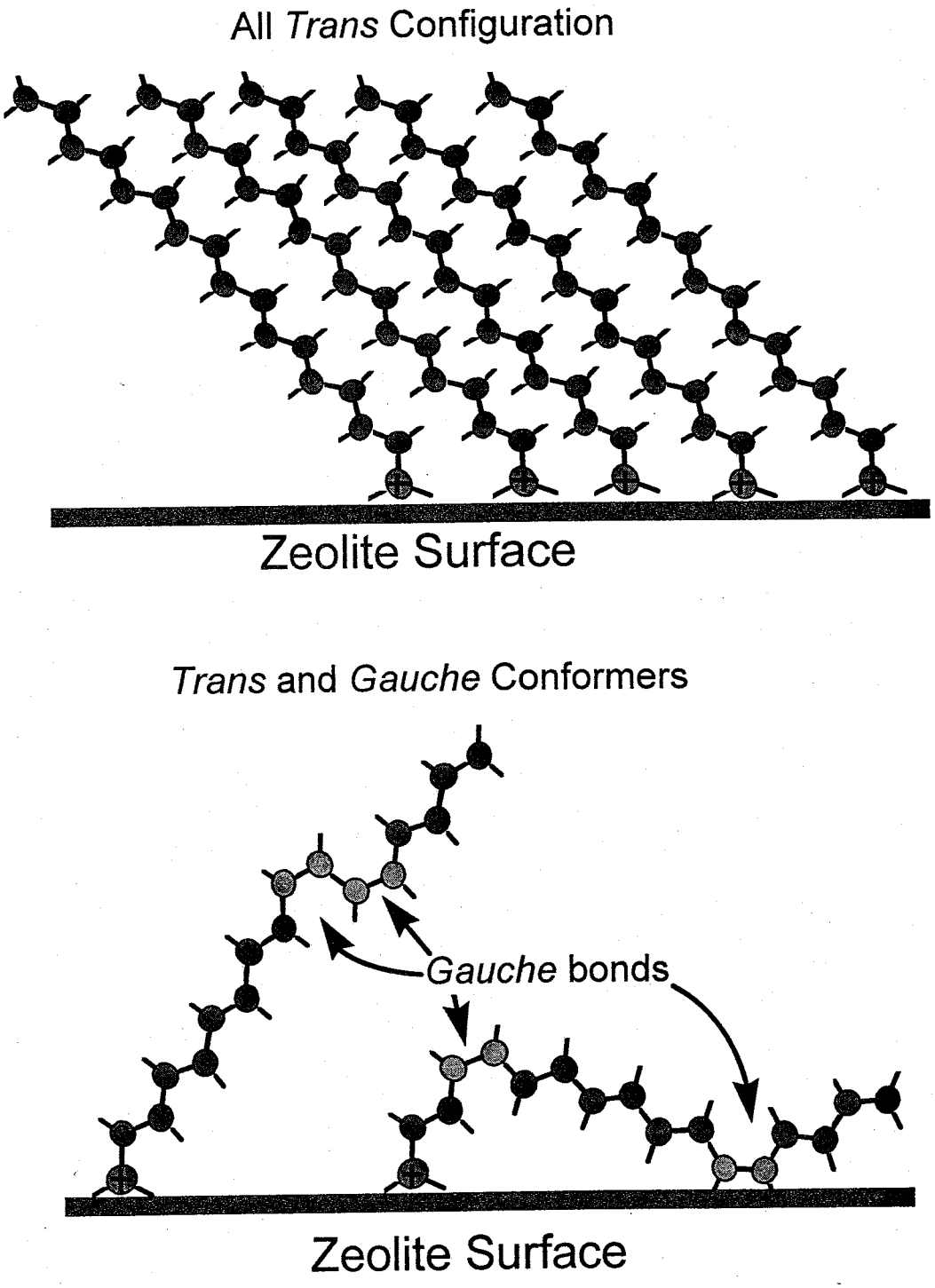

Figure 4.3. Depiction of *trans* and *gauche* conformers of sorbed HDTMA (adapted from Kellar, 1990).

the solid spectrum. This was interpreted to result from hydration of the head group in the solution versus the solid (11).

FT-Raman Spectra Assignment of Sorbed HDTMA Band Shifts

The higher-frequency bands corresponding to the CH_3-N^+, CH_3-R, and CH_2 stretching regions are shown in Fig. 4.4 and listed in Table 4.2 for a range of coverages of HDTMA sorbed onto zeolite. Also shown is the spectrum for the HDTMA micelle solution. The results correlate well with reported literature values (11,14). Band intensity is reduced with reduced surface coverage, and so the lowest treatment levels are not shown (5). Some peaks related to CH_3-N^+ stretching (head group interactions), CH_3-R stretching, and CH_2 stretches (chain interactions) were not detected at lower treatment levels because of insufficient signal-to-noise ratios. Interestingly, parallel vibrations did not always disappear with reduced loading. For example, the CH_3-N^+ a-stretch is retained, but shifts to 2985 cm^{-1} for the 60% treatment level, while the CH_3-N^+ s-stretch was not detected. The CH_2 a-stretch at 2926 cm^{-1} was retained, but the CH_2 a-stretch at about 2930 cm^{-1} was not.

Lower-frequency spectra for various HDTMA treatment levels are shown in Fig. 4.5 and the band assignments are listed in Table 4.3. Also listed in Table 4.3 are the lower-frequency band assignments for a reference 100 mM HDTMA micelle solution (11,14). Loss of band resolution occurred with reduced coverage, but to a lesser extent than for the higher-frequency portion of the spectrum. Bands for adsorbed chromate also are visible in this range; these will be discussed in greater detail below. Band

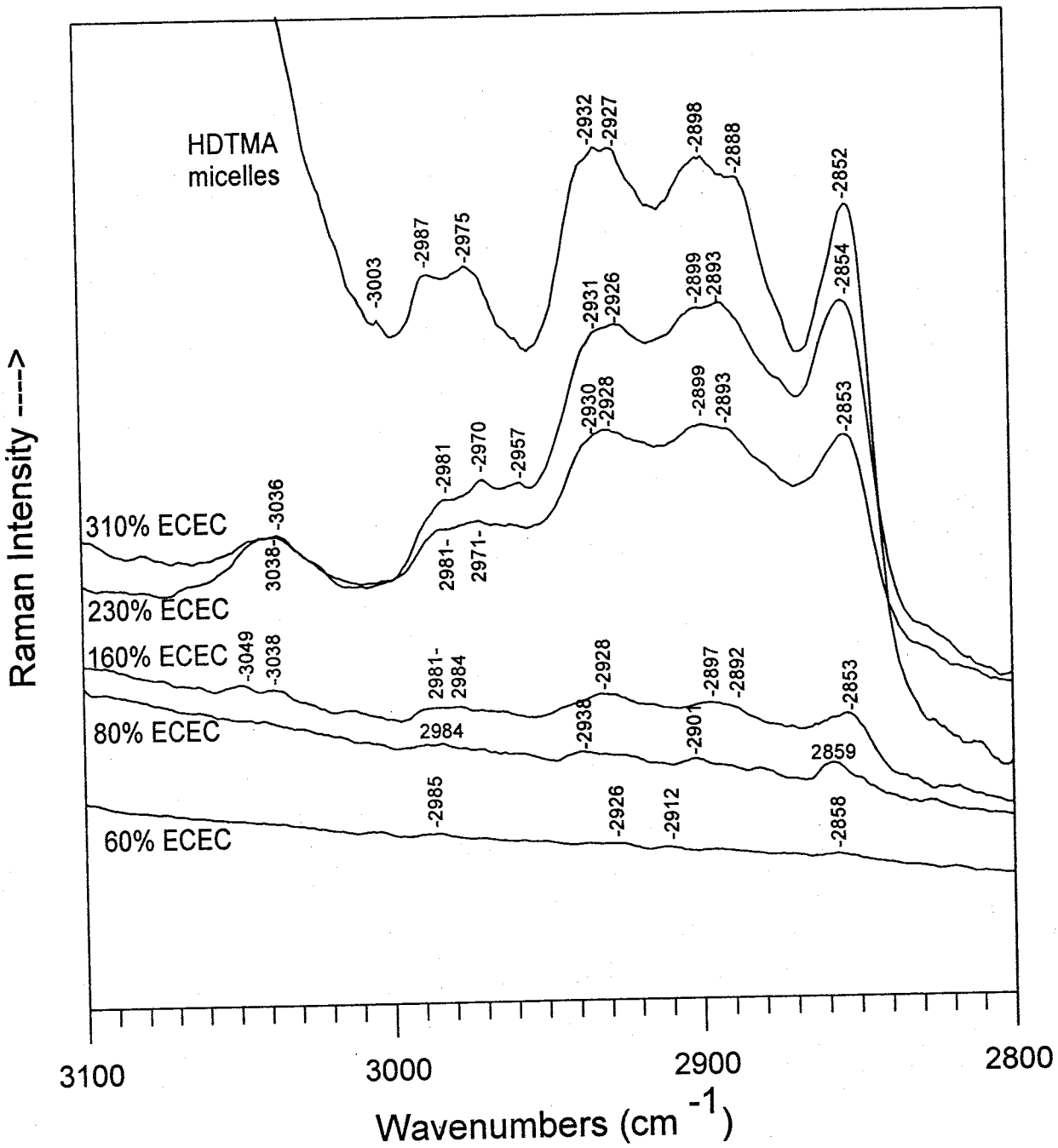

Figure 4.4. FT-Raman spectra of HDTMA sorbed on clinoptilolite zeolite for a series of treatment levels and for an HDTMA micelle solution, showing the higher-frequency portion of the spectra.

Table 4.2. FT-Raman high-frequency data for sorbed HDTMA at various treatment levels for the spectra shown in Fig.4.4.

	HDTMA Treatment Level (percentage of ECEC)						
	60%	80%	160%	230%	310%	HDTMA 70 mM (micelles)	Reference[a,b] 100 mM (micelles)
Tentative Assignment	Raman Bands, cm^{-1}						
CH_2 s-stretch[a,b]	2858 w	2859	2853	2853	2854	2852	2854
CH_3-R s- stretch ?			2892 sh	2893 sh	2893 sh	2888 sh	
CH_2 a-stretch[b,c]	2912	2901 w	2897	2899	2899	2898 b	2890[c]
CH_2 a-stretch[d] ?	2926 w	2926 w	2928 sh	2928	2926	2927	2930[d]
CH_2 a-stretch[a,c]		2938	2930	2930 sh	2931 sh	2932	2935
					2957		
CH_3-N^+ s-stretch[a,b]			2971 sh	2971	2970	2975	2974
CH_3-N^+ a-stretch[a]	2985	2984	2981-2984 b	2981 sh	2981	2987	2987
						3003	
CH_3-N^+ a-stretch[b]			3038 3049	3038 b	3036	3047	3042

[a] Suga et al. 1993.
[b] Dendramis et al. 1983.
[c] Suga et al. characterize this as a CH_3-R s-stretch.
[d] Suga et al. characterize this as a surface-enhance Raman band.
w = weak; sh = shoulder, b = broad peak, a-stretch = asymmetrical stretch, s-stretch = symmetrical stretch

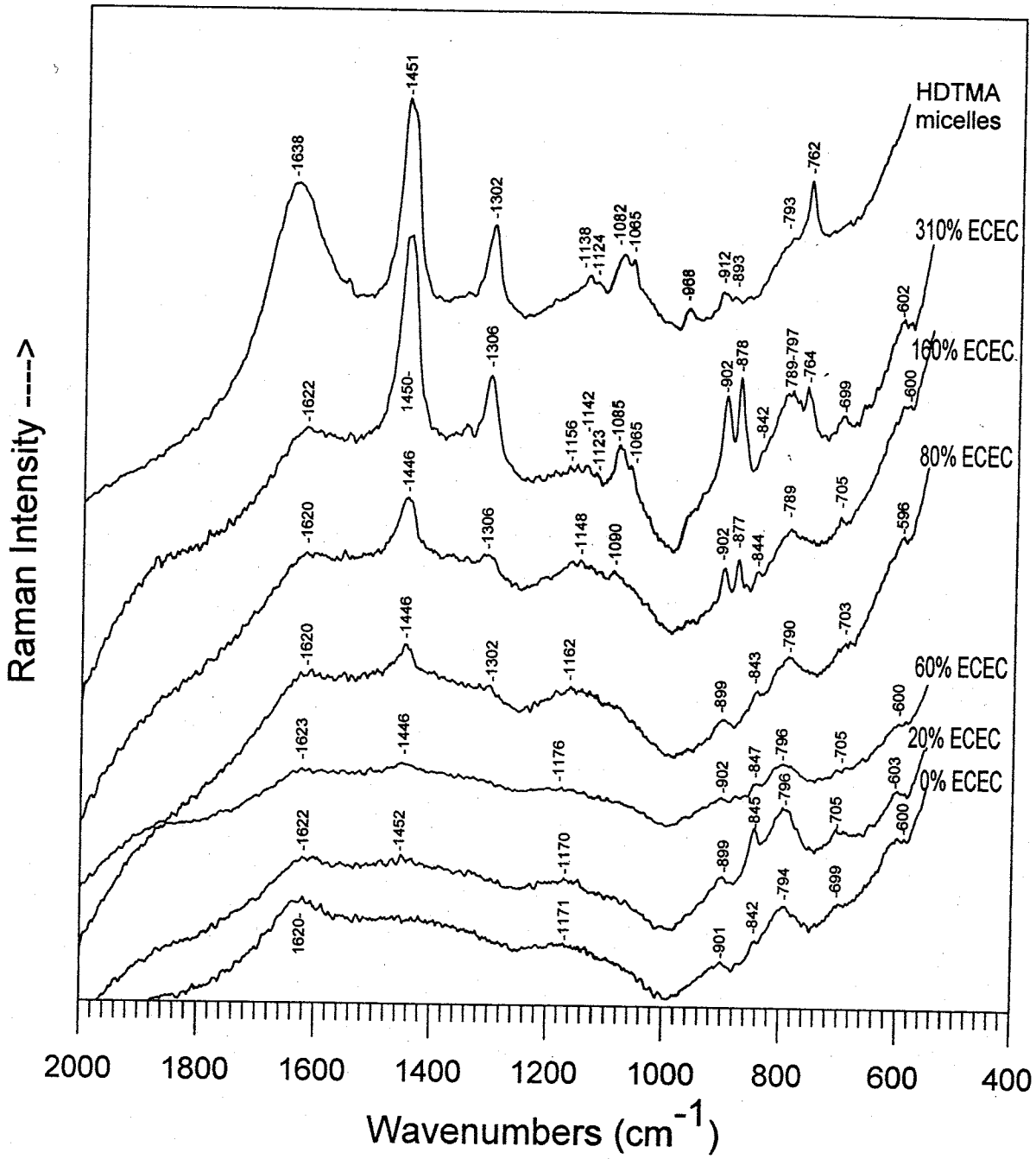

Figure 4.5. FT-Raman spectra of HDTMA sorbed on clinoptilolite zeolite for a series of treatment levels and for unmodified clinoptilolite zeolite, showing the lower-frequency portion of the spectra.

Table 4.3. FT-Raman low-frequency data for sorbed HDTMA, unmodified clinoptilolite zeolite, and sorbed chromate at various treatment levels for the spectra in Figs. 4.5 and 4.7.

	HDTMA Treatment Level (percentage of ECEC)								
	0%	20%	60%	80%	160%	230%	310%	HDTMA 70 mM (micelles)	Reference[b] 100 mM micelles
Tentative Assignment	Raman Bands, cm^{-1}								
zeolite	600	603	600	596	600	597	602		
zeolite	699	705	705	703	705	698	699		
C-N^+ stretch[a,b]						763	764	762	760
zeolite	794	796	796	790	789	786 794	789-797		
						815 sh		793 sh	
zeolite	842 sh	845	847	843 sh	844 sh		842 sh		
chromate					877	878	878		
								893	891
chromate or zeolite	901	899	902	899	902[c]	904[c]	902[c]		
CH_3 rock, CN^+ stretch[b]								912 968	912 970
C-C stretch[b,d]					1090	1092	1065 sh 1085 1123	1065 1082 1124	1064 1084 1122
							1142	1138	
zeolite and /or water	1171 b	1170 b	1176 b	1162 b	1148 b	1144 1164 1199	1156 b		
CH_2 twist				1302	1306	1306	1306	1302	1302
CH_2 scissor[a,b]		1452	1446	1446	1446	1451	1450	1451	1450
zeolite and /or water	1620 b	1622 b	1623 b	1620 b	1620 b	1621	1622 b	1638	

[a]Suga et al. 1993 for sorbed HDTMA (surface-enhanced Raman spectrum).
[b] Dendramis et al. 1983.
[c] due to chromate overwhelming zeolite peak.
[d] Sun et al. (1990) assign a peak at 1065 cm^{-1} as a C-C symmetric stretch, and a peak at 1121 cm^{-1} as a C-C antisymmetric stretch.
w = weak; sh = shoulder, b = broad peak, a-stretch = asymmetrical stretch, s-stretch = symmetrical stretch

assignments for the alkyl (tail group) chain, the methyl head group, and other pertinent spectral features in both the high and low frequency ranges are discussed below by group.

Alkyl Chain Assignments—Solution Micelles and Admicelles

There is a strong correlation between many peaks for the micellar HDTMA solution and the 160%, 230%, and 310% treatment-level samples (Figs. 4.4 and 4.5), which indicates structural similarities between micelles in solution and admicelles. Based on peak shift comparisons pertinent to the alkyl chain, it is interpreted that the tail groups in admicelles are only slightly less structured and interfingered than those in solution micelles. High-frequency bands which illustrate this similarity are the CH_2 s-stretch (2852 cm^{-1}) the CH_2 a-stretch (2899 cm^{-1}), and the CH_2 a-stretch (2932 cm^{-1}) which are essentially the same for both sorbed bilayers/admicelles (160-310%) and the solution systems (Fig. 4.4, Table 4.2). The largest difference occurs in the CH_3-R s-stretch (tentative identification, this has also been identified as another CH_2 stretch (15)) which shifts from 2888 cm^{-1} for the micelle solution to 2893 cm^{-1} for the 310% treatment level. This may indicate more *gauche* conformers, where micelles on the surface have less ordered or structured tail groups than in solution. Because this shift only occurs for one of the bands, this is potentially a minor effect which may occur only for the terminal part of the tail group. The peak disappears with reduced loading, so no correlation with adsorbed monomers can be made.

In the lower frequency range (Fig. 4.5, Table 4.3), four bands listed for the 310% treatment level (admicelles) corresponded very closely to those found for solution

micelles, including one band at 1138 cm^{-1} in solution, which was listed but not assigned in the literature (14). These bands include the C-C stretch (1065-1082 cm^{-1}), the CH_2 twist (1302-1306 cm^{-1}), and the CH_2 scissor (1450-1451 cm^{-1}) for tail group assignments, as well as a tentative assignment of the head group C-N^+ stretch (head group-tail group bond, 762-764 cm^{-1}). Few significant shifts were noted for HDTMA bands between treatment levels in this range of the spectrum. All of the bands disappeared at some reduced loading level, e.g., below 60% ECEC coverage.

Alkyl Chain Assignments—Sorbed Admicelles and Monolayers

In Fig. 4.4, we see a shift to higher frequency with lower coverage for the CH_2 s-stretch between the highest and lowest treatment levels. This is evident also in Table 4.2, in the change from 2853 cm^{-1} to 2858 cm^{-1} between the 160% and the 80% and lower treatment levels. A similar change is noted for the CH_2 a-stretch at 2898-2912 cm^{-1}. These changes may be associated with increased twisting or bending of the chain when the admicelle structure is disassembled below the 160% level. This describes a disorganized monolayer at lower treatment levels, quite different from the organized *trans*-conforming monolayer described by Sun et al. (25) for HDTMA sorbed on a silver electrode. This interpretation corresponds well with previous atomic force microscope observations of disorganized HDTMA monomers on the zeolite surface (4). Disorganization may be enhanced by the molecularly rough zeolite surface, as opposed to the relatively smooth metal surfaces used by others (11, 14).

A number of bands indicating tail group orientation and conformation in the lower frequency range between 500 and 2000 cm^{-1} are clearly visible in Fig. 4.5. These include C-C stretch, CH_2 twist, and CH_2 scissor bands. The C-C stretch (1085 cm^{-1}) in the 310% treatment level shifted to 1090 cm^{-1} and weakened in the 160% treatment level before disappearing entirely at lower treatment levels (Table 4.3). Another C-C band at 1065 cm^{-1} also disappears below 310% ECEC. This shift as an indication of the C-C bonds paralleling the surface, in conjunction with weakening of the CH_2 twist and scissor bands (14). The CH_2 twist (1302-1306 cm^{-1}) disappears below the 80% treatment level, while the CH_2 scissor (1446-1452 cm^{-1}) persists weakly down to the 20% treatment level. This indicates disordered chains lying near the surface in the monolayer form, a conformation associated with dry, not wet, systems (8). Surfactant orientation may depend upon the quantity of surfactant on the surface (4, 26, 27, 28), with close horizontal contact (less ordering) between the surfactant and surface at low loading levels, and with a perpendicular orientation (greater ordering) at higher loading levels.

Figure 4.6 shows a schematic of the resulting structural changes during HDTMA sorption interpreted from the above data. Sorbed micelles exhibit slightly more tail group disorder and less interfingering of tail groups than do solution micelles, based on peak shift data. This is interpreted to result from interaction with the rough zeolite surface. Sorbed monolayers at higher loading levels are more structured than monomers sorbed at low coverages. Monomers at any loading level exhibit more disorder than admicelles. These monomers may interact with the zeolite surface or perhaps "coil up" when other tail groups are not available for interactions.

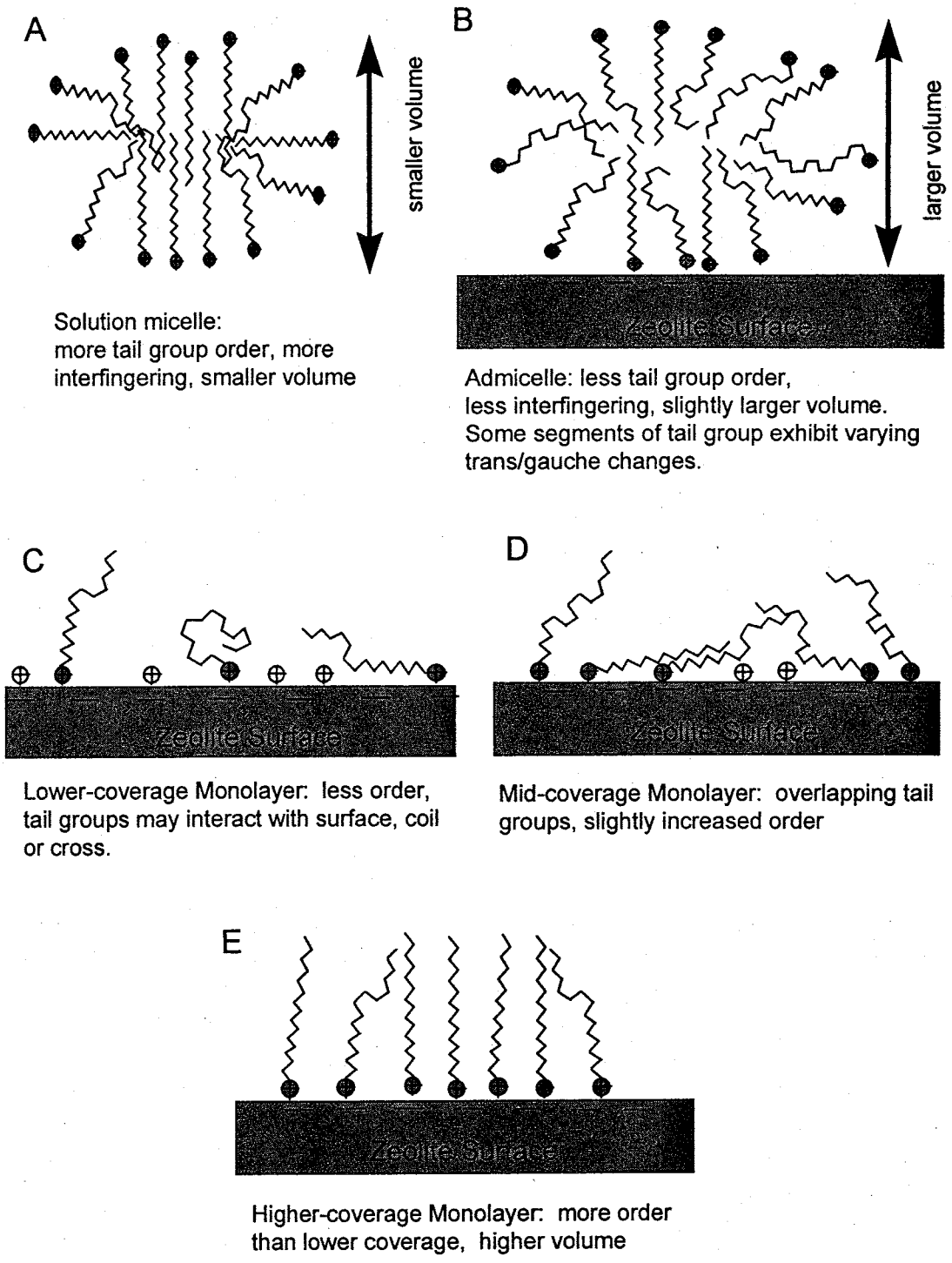

Figure 4.6. Two-dimensional schematic of HDTMA sorbed as micelles or monomers on zeolite surface, describing the effects of sorption on tail group disorder. Although not illustrated, the third dimension of the surfactant structure, surface roughness, and time also affect the structure and amount of disorder in the surfactant tail groups.

Head Group Assignments

The bands associated with the symmetrical and asymmetrical CH_3-N^+ stretches (Fig. 4.4, Table 4.2) show distinct differences between solution and adsorbed HDTMA (310% treatment level). Two of the three bands become indistinct below the 160% treatment level. The loss of the symmetrical stretch (2970 cm^{-1}), with retention of the asymmetrical stretch in the CH_3-N^+ group (2970 to 2985 cm^{-1}) may indicate an alteration of some of the head group bonds on the surface between lower and higher loading levels.

The sorbed head group CH_3-N^+ a-stretch and s-stretches all shift to a lower frequency at the 310% loading level when compared with solution head group bands. This indicates less hydration for sorbed headgroups than for those in solution. This same lower-frequency shift occurs between solution HDTMA and wet films (11, 14). Interestingly, a reversal in the trend then occurs from the 80% to 60% treatment levels, where the peaks shift higher again. The corresponding peak in the 160% level is broad, so this relative shift is indistinct, but may indicate more water available to the headgroups as monolayer density is decreased. Nitrogen bands in pyridine-water mixtures also shift to higher frequencies upon hydration (5,18). Water has been noted to exist between headgroups and silver island surfaces in previous studies of sorbed HDTMA monolayers (11).

The C-N^+ stretch at 764 cm^{-1} was noted in reference solutions (14), in solutions in this experiment (Table 4.3, Fig. 4.5), and in the 310% and 230% loading levels. It is not clear whether this band disappears at lower treatment levels because of some change in head group character or because of decreased loading. Peaks assigned to a CH_3 rock or

C-N^+ stretch mode (912 and 968 cm^{-1}) noted in solution micelles were obscured in the higher levels (310% and 160% ECEC) by adsorbed CrO_4^{2-}; these peaks were not measurable at lower loading levels because of detection limits.

FT-Raman Band Assignments for Chromate

Figure 4.7 shows a comparison among the chromate bands in the CrO_4^{2-}-SMZ (310% treatment level) spectrum, a K_2CrO_4 solution (20 mM) and an HDTMA-chromate solution (70 mM $HDTMA_2$-CrO_4). The spectra for an unmodified zeolite equilibrated with 20 mM K_2CrO_4 solution is also shown. Chromate adsorbed to SMZ is visible in the spectrum as two strong bands at about 902 and 878 cm^{-1} (Fig. 4.7, Table 4.3). These bands were seen only in the 310% through 160% treatment levels, the levels where admicelles or a bilayer were expected to occur (Fig. 4.5).

Chromate in solution is visible as a strong band at 847 cm^{-1}. The adsorbed chromate bands (878 and 902 cm^{-1}) are very clearly shifted and split compared to the solution chromate band. These bands are unrelated to zeolite, HDTMA, or water. The nearest band in the HDTMA-water solution at 912 cm^{-1} is close to but does not underlie the 902 cm^{-1} chromate peak. The broad band in the K_2CrO_4 solution spectrum (Fig. 4.7) at about 887 cm^{-1} is related either to water or chromate. It is interesting to note that the presence of chromate as a counterion versus Br^- (in the HDTMA-water solution) has no effect on bands related to head group or tail group conformation.

Based on the observed spectra, chromate exhibits two different vibration shifts or two different binding states upon sorption to SMZ in the hydrated system. Huang and

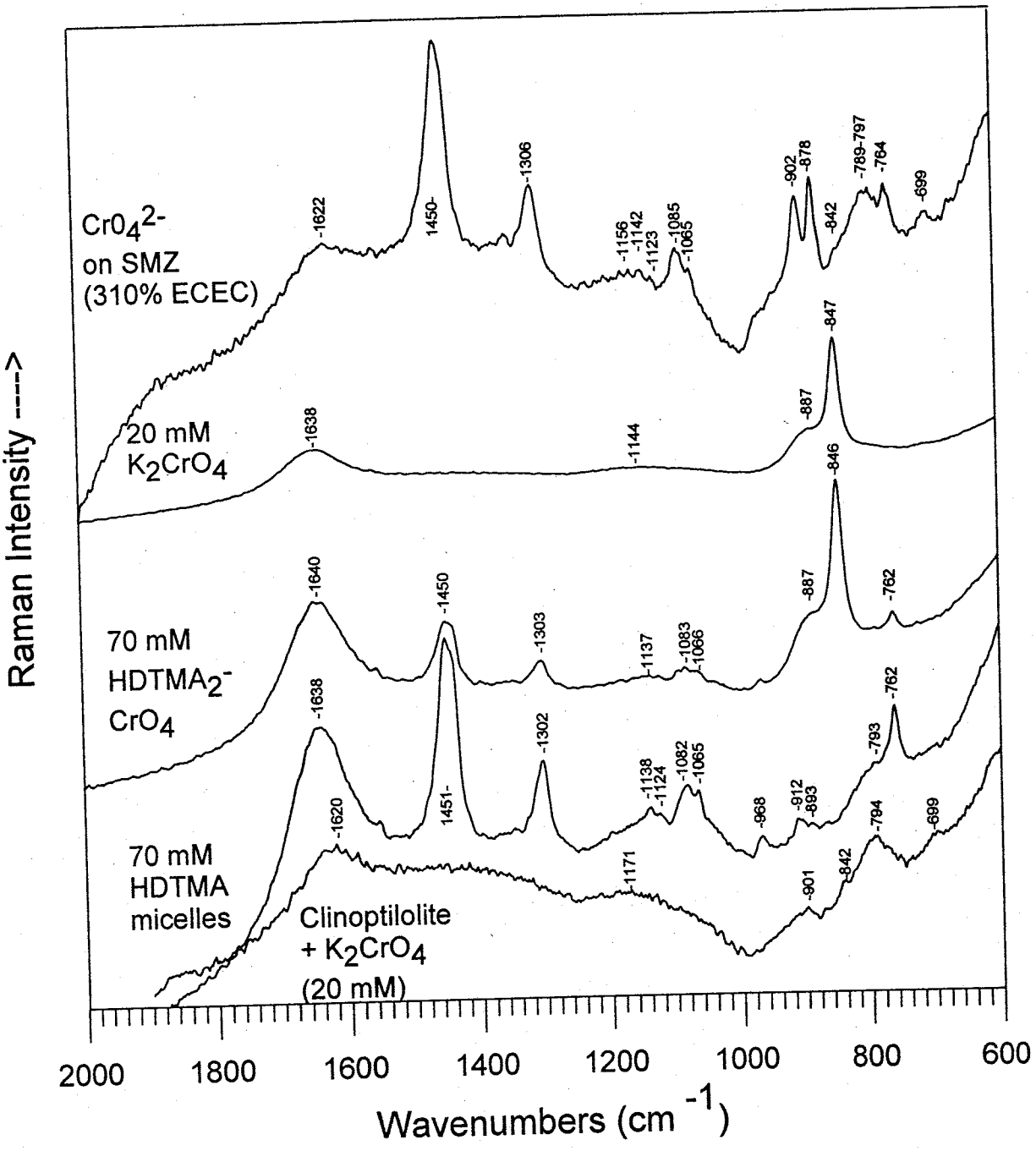

Figure 4.7. FT-Raman spectra for chromate sorbed on SMZ, aqueous K_2CrO_4 (20 mM), aqueous $HDTMA_2$-CrO_4 (70mM), aqueous HDTMA-Br^- (70 mM), and unmodified clinoptilolite zeolite which was equilibrated with chromate, showing the lower-frequency portion of the spectra.

Butler (29) list bands at 854 cm^{-1}(ν_1), 880 cm^{-1} (ν_3), and 907 cm^{-1} (ν_3) for solid K_2CrO_4, while Bostic et al. (30) list a ground-state vibration at 853 cm^{-1} for aqueous K_2CrO_4. It appears that adsorbed chromate exhibits the two ν_3 vibrations much like solid chromate. Reduction of Cr(IV) to Cr(III) does not occur with sorption, as shown in previous studies (2). Chromate does not sorb well to unmodified zeolite (2, Figure 4.7). As shown here, CrO_4^{2-} does not sorb to SMZ at HDTMA treatment levels below 100% of the ECEC (Figs. 4.1 and 4.5). All of these observations point to anion exchange on HDTMA bilayer headgroups as the dominant mechanism for CrO_4^{2-} sorption.

In the presence of the excess surfactant, the relative acidity of Lewis acid sites on the zeolite surface may be enhanced through reduction of the amount of water present at the surface. When CrO_4^{2-} penetrates the bilayer, it may act as an electron donor to these sites. This is a reasonable sorption mechanism. Both electron donation and anion exchange require the presence of sufficient sorbed surfactant, making it difficult to distinguish between the two possibilities. The split in the SMZ-CrO_4^{2-} peak may mean that two environments for sorbed CrO_4^{2-} exist. The strong shift in the peak is typical of other Lewis bases such as pyridine (18,19). There are some problems, however, with this acid site mechanism. First, the counterion data above indicates that anion exchange has occurred during chromate sorption for micelles, an effect which need not occur with acid site interactions. Second, the time needed for a chromate anion to penetrate the bilayer could be a limiting step, even though chromate sorption was found to be quite rapid (2).

Alternatively, interpretation of the data should include the potential effect of hydration on the sorbed chromate, and the possibility that other chromate species, such as

$HCrO_4^-$, might affect the spectra. Hydration of the chromate might be facilitated by the zeolite surface. Hydration affects the polarizability of nitrogen species, and, thus, may also affect the chromate anion. A previous study of a similar zeolite-surfactant-chromate system (2) presented the FT-Raman spectra of SMZ-chromate, $HDTMA_2$-CrO_4 precipitate, and SMZ. These spectra were taken of the dry powdered material. In that study, a single peak was noted for the $HDTMA_2$-CrO_4 precipitate, at 905 cm^{-1}. A single sharp peak at 895 cm^{-1} was noted for the SMZ-chromate. The peak at 905 is probably related to the peak noted here at 846 cm^{-1} (Fig. 4.7), while the sharp band at 895 cm^{-1} is probably related to the broad band noted here at 878 cm^{-1}. The most important difference between the system of Haggerty and Bowman (2) and the present system is the effect of hydration on near-surface CrO_4^{2-}. This most likely causes the split peaks noted here, which are also strongly shifted to a lower frequency from the previous data.

The above sorption information also indicated that chromate did not sorb significantly at treatment levels at or less than 100%. This data has implications for low loading as a reason for the chromate bands to disappear in spectra of samples treated to less than 100%. The bands disappear because there is no chromate on the surface at any significant loading level when HDTMA cannot form admicelles. Thus, the lack of the chromate bands is due to limitations on chromate sorption, not a lack of Raman resolution.

ACKNOWLEDGMENTS

This study was supported by a student research grant from The Clay Minerals Society, the Oak Ridge Institute for Science and Education research travel program, the U.S. Department of Energy (DOE) under contract DE-AR21-95-MC32108 through the Morgantown Energy Technology Center, Financial Assistance Award Number DE-FC09-96SR18546 from DOE to the University of Georgia Research Foundation, and by ERDA/WSRC subcontract AA46420T. The generous support of the Advanced Analytical Center for Environmental Sciences at the Savannah River Ecology Laboratory, including Brian Teppen, John Seaman, and Paul Bertsch, is acknowledged. Emily Keene of New Mexico Tech performed the sorption studies.

REFERENCES

(1) Bowman R.S.; Haggerty G.M.; Huddleston R.G.; Neel D.; Flynn M.M. Sorption of nonpolar organic compounds, inorganic cations, and inorganic oxyanions by surfactant-modified zeolites. In *Surfactant-Enhanced Subsurface Remediation*, Sabatini, D.A, Knox, R.C., and Harwell, J.H., Eds., 1995, ACS Symposium Series **594**, 54-64.

(2) Haggerty, G.M.; Bowman, R.S. Sorption of chromate and other inorganic anions by organo-zeolite. *Environ. Sci. Technol.*, **1994,** 28(3), 452-458.

(3) Neel, D.; Bowman, R.S. Sorption of organics to surface-altered zeolites. In *Proc. New Mexico 36th Annual Water Conference*, 1992, November 7-8 1991, Las Cruces, New Mexico, 57-61.

(4) Sullivan, E.J.; Hunter, D.B.; Bowman, R.S. Topological and thermal properties of surfactant-modified clinoptilolite studied by Tapping-Mode™ atomic force microscopy and high-resolution thermogravimetric analysis. *Clays Clay Miner.*, **1997,** 45, in press.

(5) Burch R.; Passingham, C.; Warnes, G.M.; Rawlence, D.J. The use of Fourier transform Raman spectroscopy in the characterization of catalysts. *Spectrochimica Acta*, **1990**, 46A (2), 243-251.

(6) Umemura, J.; Cameron, D.G.; Mantsch, H.H. An FT-IR study of micelle formation in aqueous sodium n-hexanoate solutions. *J. Phys. Chem.*, **1980**, 84, 2272-2277.

(7) Kellar, J.J.; Young, C.A.; Knutson, K.; Miller, J.D. Thermotropic phase transition of adsorbed oleate species at a fluorite surface by in situ FT-IR/IRS spectroscopy. *J. Colloid Interface Sci.*, **1990**, 144(2) 381-389.

(8) Kung, K.S.; Hayes, K.F. Fourier transform infrared spectroscopic study of the adsorption of cetyltrimethylammonium bromide and cetylpyridinium chloride on silica. *Langmuir,* **1993**, 9, 263-267.

(9) Grasselli, J.G.; Snavely, M.K.; Bulkin, B.J. *Chemical Applications of Raman Spectroscopy*. John Wiley & Sons, New York, 1981, 198 pp.

(10) Hendra, P.J.; Jones, C.; Warnes, G.M.. *Fourier Transform Raman Spectroscopy, Instrumentation and Chemical Applications*. Ellis Horwood, New York, **1991**, 259 pp.

(11) Suga, K.; Bradley, M.; Rusling, J.M. Probing the interface of cast surfactant films and an underlying metal by surface-enhanced Raman scattering spectroscopy. *Langmuir,* **1993**, 9, 3063-3066.

(12) Vincent, J.S.; Levin, I.W. Raman spectroscopic studies of dimyristoylphosphatidic acid and its interaction with ferricytochrome c in cationic binary and ternary lipid-protein complexes. *Biophys. J.,* **1991**, 59, 1007-1021.

(13) Levin, I.W.; Lewis, E.N. Fourier transform Raman spectroscopy of biological materials. *Anal. Chem.*, **1990**, 62(21), 1101-1111.

(14) Dendramis, A.L.; Schwinn, E.W.; Sperline, R.P. A surface-enhanced Raman scattering study of CTAB adsorption on copper. *Surface Science,* **1983**, 134, 675-688.

(15) Sullivan, E.J.; Carey, J.W.; Bowman, R.S. Thermodynamics of cationic surfactant sorption onto clinoptilolite. Submitted to *J. Colloid Interface Sci.,* **1997.**

(16) Hendra, P.J.; Passingham, C.; Warnes, G.M.; Burch, R.; Rawlence, D.J. Fourier transform Raman spectroscopy in the study of species adsorbed on catalyst surfaces. *Chem. Phys. Letters,* **1989**, 164, 178-184.

(17) Farmer, V.C. The characterization of adsorption bonds in clays by infrared spectroscopy. *Soil Science,* **1971**, 112(1), 62-68.

(18) Jakupca, M.R.; Dutta, P.K. Ultraviolet resonance Raman spectroscopy of 4-aminopyridine adsorbed on zeolite Y. *Anal. Chem.*, **1992**, 64, 953-957.

(19) Chipera S.J.; Bish D.L. Multireflection RIR and intensity normalizations for quantitative analyses: applications to feldspars and zeolites. *Powder Diffraction,* **1995**, 10, 47-55.

(20) J. W. Carey, Los Alamos National Laboratory, personal communication, **1995**.

(21) Ming, D.W.; Dixon J.B. Quantitative determination of clinoptilolite in soils by a cation-exchange capacity method. *Clays Clay Miner.*, **1987**, 35(6), 463-468.

(22) Israelachvili, J. N. *Intermolecular and Surface Forces.* 2nd ed. Academic Press, Inc., San Diego, CA., 1991, 450 pp.

(23) Sullivan, E.J.; Bowman, R.S.; Haggerty, G.M. Sorption of inorganic oxyanions by surfactant-modified zeolite. In *Spectrum 94, Proc. Nuclear and Hazardous Waste Mgmt. International Topical Meeting*, August 14-18, 1994, Atlanta, Georgia, vol. 2, 940-945.

(24) Diem, M.. *Introduction to Modern Vibrational Spectroscopy.* John Wiley & Sons, New York, 1993, 285 pp.

(25) Sun, S.; Birke, R.L.; Lombardi, J.R. Surface-enhanced Raman spectroscopy of surfactants on silver electrodes. *J. Phys. Chem.*, **1990**, 94, 2005-2010.

(26) Ter-Minassian-Saraga L. *Advan. Chem. Ser.*, **1964**, 43, 232.

(27) Bijsterbosch, B.H. Characterization of silica surfaces by adsorption from solution. Investigations into the mechanism of adsorption of cationic surfactants. *J. Coll. Int. Sci.*, **1974**, 47(1), 186-198.

(28) Chen Y.L.; Chen S.; Frank C.; Israelachvili J. Molecular mechanisms and kinetics during the self-assembly of surfactant layers. *J. Colloid Interface Sci.*, **1992**, 153(1), 244-265.

(29) Huang, Y.; Butler, I.S. *Applied Spectroscopy,* **1990**, 44(8), 1326-1328.

(1) Bostic, J.M.; Carriera, L.A.; Antcliff, R.R. *J. Raman Spectroscopy,* **1990**, 21, 601-605.

CHAPTER 5

SUMMARY AND RECOMMENDATIONS

This dissertation has produced new information with regard to HDTMA sorption and conformation on clinoptilolite surfaces and the subsequent mechanism of sorption of anions to surfactant-modified clinoptilolite. Both the instrumental methods of discovery and the findings from these methods have relevance to other systems utilizing surfactants and mineral surfaces.

Although atomic force microscopy has been in use for several years for nano-scale measurement, the tapping-mode method had never been used before on a zeolite surface. Although "dry" clinoptilolite was investigated, the surface retains enough water that the surfactant conformation information may approximate fully-hydrated conditions. Significant observations included the striated conformation of HDTMA clusters at high surface loading levels, clustering of HDTMA molecules at low loading levels, and what appeared to be coiled HDTMA monomers on the surface. The thickness and size of the clusters and individual HDTMA molecules were easily measured using the tapping-mode technique. The clustering patterns noted suggested a "tube-like" conformation for admicelles, and some control on the orientation of admicelle sorption by the mineral surface. The clustering also indicated the importance of tail-tail interactions between HDTMA molecules. The close association of the HDTMA molecules with the surface indicated the importance of tail-surface interactions in the sorption process. This interaction was further quantified in Chapter 3. Finally, the coiled monomer

APPENDIX I

This appendix describes experimental methods and results of characterization of the clinoptilolite and HDTMA. These experiments were conducted to obtain specific background information about the samples used. For example, ion exchange values of clinoptilolite from the St. Cloud mine were determined previously for other batches of clinoptilolite (Bowman et al. 1995; Haggerty and Bowman, 1994; Neel et al. 1992). The results were not consistent and the methods may have varied. This section documents the experimental methods used for a specific batch of clinoptilolite and HDTMA which were then used throughout the course of this project.

X-Ray Diffraction

X-ray diffraction of the clinoptilolite was performed at Los Alamos National Laboratories using an internal standard analysis method (J. W. Carey, Los Alamos National Laboratory, personal communication, 1995). This method uses an internal standard of 20 weight % of corundum and determines mineral abundances based upon the reference-intensity-ratio method using integrated peak areas (Chipera and Bish 1995). The sample was found to consist of 74 (± 4) % clinoptilolite, 5 (± 2) % smectite, 10 (± 1) % quartz, 2 (± 1) % cristobalite, 12 (± 2) % feldspar, and 1 (± 1) % mica. The complete results are shown in Table I.1.

Surface Area

The clinoptilolite surface area was measured with an ASAP 2000 gas sorption analyzer (Micromeritics, Inc., Norcross, GA) using the BET nitrogen adsorption method (Brunauer et al. 1938). A multiple-point method was used. The samples tested were held at ambient temperature and humidity or dried for 12 hours at 100°C and 200°C prior to testing. The only pre-treatment was sieving to a size range of between 2 mm and 150 μm. An alumina standard from the National Institute of Standards Batch No. 8571 (Gaithersburg, Md) was also measured. The known surface area of the standard was 158 m^2/g and the measured surface area was 154.1 m^2/g (-2.5%).

Surface areas for the undried, 100° C dried, and 200° C dried zeolite were 7.5, 14.1, and 15.7 m^2/g, respectively. Copies of the data printouts are attached. The variability in results is likely due to the loss of water from the zeolite surface with increasing temperature. Peterson (1980) found that the amount of nitrogen which can sorb onto NaA, CaA, NaX, and NaY zeolites is directly related to the amount of water remaining on the surface. The final number is a measure of the external surface area outside of the micropores. Remy and Poncelet (1995, and others cited therein) indicate that the BET analysis of the liquid nitrogen method used here yields an external surface area measurement for zeolites.

Cation Exchange Capacity

The clinoptilolite external and internal cation exchange capacities (ECEC and ICEC, respectively) were measured using the method of Ming and Dixon (1987), with

some modifications. Two different measurements were made, one using tert-butylammonium chloride (TBAC, mwt. 109.6) and one using HDTMA for the external exchanging cation.

TBAC Synthesis

The TBAC was synthesized using a method by D.C. Golden (NASA Johnson Space Center, Houston, TX, personal communication, 1994). Tert-butyl amine was used as received in liquid form from Aldrich Chemicals. The amine was dissolved in absolute ethanol to form a 1:1 (w/v) solution. A titration solution of 2M HCl was also made by dissolving concentrated HCl in absolute ethanol. The amine and the HCl were then combined in a 1:1 molar ratio to make the ammonium chloride by titrating the amine solution to a pH of 7 with the 2M HCl solution. For this experiment, 0.5 mole each of tert-butyl amine and HCl were used. A pH meter was used to test the pH. The resultant slurry was evaporated for several hours over gentle heat. The white crystals were then rinsed in the beaker with cold acetone, scraped onto filter paper in a Buchner funnel, rinsed two more times with cold acetone, and allowed to dry over vacuum. No recrystallization was performed because of the insolubility of the crystals in either warm acetone or ethanol. The purity of the TBAC was checked by NMR spectroscopy (J. Smith, New Mexico Tech, personal communication, 1995) (Figure I.1) where a single peak attributable to TBAC (NMR peak library search match) was observed. A melting point determination was unsuccessful due to sublimation of the material below the

melting point. The TBAC solutions made for the exchange experiments were filtered with an 0.45 μm Whatman filter prior to use.

External Cation Exchange Capacity Method

Samples of clinoptilolite from a previous batch which had been pre-saturated with Na^+ (Haggerty and Bowman, 1994), and from the current sample (not pre-saturated) were used. The clinoptilolite samples were freeze-dried using a lyophilizer prior to weighing. For each sample, 1.0 g of clinoptilolite was weighed into a 50-ml polyallomer Oak Ridge centrifuge tube. Each sample was analyzed in duplicate with appropriate blanks and background solution checks. Samples were then washed four times with 1N NaOAc buffered with HOAc to pH 5 to promote complete Na^+-saturation. All aqueous solutions were made with 18.2 Mohm·cm^{-1} (ASTM Type I) water. Washes were accomplished by adding 20 ml of NaOAc solution, ultrasonicating for 1 minute, then centrifuging at 14500 x g for 20 minutes and decanting the excess solution. Excess Na^+ was then removed from the clinoptilolite by rinsing each sample with Type I water three times and with 90% ethanol three times. Rinses were accomplished in the same manner as the NaOAc washes.

External CEC exchanges were performed for 24 and 48 hours to determine if time was a factor for the exchange. Both TBAC and HDTMA were used to measure external exchange capacity (2 or 3 duplicates each). The HDTMA-Br^- salt was used as received (Sigma Chemicals). Aqueous HDTMA solutions were spiked with [^{14}C-methyl]HDTMA iodide (American Radiochemicals Inc.). For each sample, either 25 ml

of 0.5 N TBAC solution or 25 ml of 0.04 N HDTMA solution were used. The higher concentration of TBAC was used to promote sorption of the cation, while the lower concentration of HDTMA was necessary to prevent liquid crystal formation. Samples were heated in a 60°C water bath for either 24 or 48 hours to facilitate the exchange of Na^+. Following the heating process, the samples were washed two more times with the exchanging solution using the above washing process. All wash solutions were saved for each sample, decanted into a 100-ml volumetric flask, and made up to 100 ml with Type I water. Solution concentrations of ^{14}C-labeled HDTMA were measured using a Packard Tri-Carb liquid scintillation counter. Solution Br^- concentrations were analyzed by high-performance liquid chromatography (HPLC). The decanted water was analyzed for the exchanged ions Na^+ and Ca^{2+} by atomic absorption spectrophotometry. Previous experiments indicated that Mg^{2+} and K^+ accounted for less than 3% of exchangeable cations and these cations were therefore not analyzed. It should be noted that previous work by others apparently only included the measurement of Na^+, which probably accounts for some of the difference between the current and previous data.

Internal Cation Exchange Capacity Method

The internal exchange capacity was determined by a subsequent exchange of the TBAC and HDTMA samples with 0.5 M CsCl. The clinoptilolite samples were rinsed of excess TBAC and HDTMA solutions by washing once with 90% ethanol. Each sample was then rinsed with three washes of 0.5 M CsCl using the above ultrasonication wash method. The washes were again decanted to a 100-ml volumetric flask and brought to

volume with Type I water. These solutions were analyzed as before for exchanged cations. No interference from Cs^+ was noted during the spectrophotometry.

ECEC and ICEC Results

Both internal and external capacities were measured based upon the cations released from the clinoptilolite surface. The external cation-exchange capacity (ECEC) was measured to be between 73 and 93 meq/kg using HDTMA as the exchanging cation. The current (J. Sullivan) sample exhibited higher exchange values than the previous (G. Haggerty) sample. Internal exchange capacity varied between 635 and 952 meq/kg using Cs^+. There was little difference noted between the two methods used (TBAC versus HDTMA) for the internal and external capacities and between the different times (24 and 48 hours). The shorter time appears to be sufficient for determination of the ECEC with this method. All results are shown in Table I.3.

A discrepancy was noted in the ICEC results for the Na^+ measurement in this experiment. The J. Sullivan samples were significantly lower in Na^+ than the G. Haggerty samples. This may result from an error in the AA analysis, because the internal exchange capacity should be much larger than the ECEC. The results for J. Sullivan samples appear to be about 1 order of magnitude too low.

Surface Tension

Surface tension of a series of HDTMA solutions was measured using a Fisher Model 20 Surface Tensiometer. During the measurement, a platinum ring is allowed to

contact the solution surface and is slowly lifted while the force necessary to pull the test ring free from the surface film is measured. Readings give apparent surface tension. The following relationship is used to convert apparent to true surface tension (Fisher Model 20 manual):

$$S = P \times F \tag{1}$$

where S is the true value, P is the apparent value, and F is a correction factor. The correction factor is dependent upon the size of the ring and the size of wire used in the ring, the apparent surface tension, and the densities of the two phases. F is calculated by:

$$F = 0.7250 + \sqrt{\left(\frac{0.01452P}{C^2(D-d)}\right) + 0.04534 - \frac{1.679r}{R}} \tag{2}$$

where: F = correction factor

R = ring radius

r = radius of the wire of the ring (0.007 inches)

P = the apparent value or dial reading

D = the density of the lower phase

d = the density of the upper phase

C = the circumference of the ring (6 cm)

The surface tension is calculated and plotted versus solution concentration to yield the critical micelle concentration of the surfactant, which is the point on the curve where surface tension ceases to be a function of concentration. The data for HDTMA are shown in Table I.4 and the results plotted in Figure I.2.

REFERENCES

Bowman, R.S., Flynn, M., Haggerty, G.M., Huddleston, R.G., and Neel, D. 1995. Organo-zeolites for sorption of nonpolar organics, inorganic cations, and inorganic anions. In: Surfactant-Enhanced Subsurface Remediation, Sabatini, D.A., Knox, R.C., Harwell, J.H., Eds., 1995, ACS Symposium Series 594, 54-64.

Brunauer S, Emmett P.H., Teller E. 1938. Adsorption of gases in multimolecular layers. *J. Amer. Chem. Soc.* **60**: 309-319.

Chipera SJ, Bish DL. 1995. Multireflection RIR and intensity normalizations for quantitative analyses: applications to feldspars and zeolites. *Powder Diffraction* **10**: 47-55.

Haggerty GM, Bowman RS. 1994. Sorption of chromate and other inorganic anions by organo-zeolite. *Environ. Sci. and Technol.* **28**(3): 452-458.

Ming DW, Dixon JB. 1987. Quantitative determination of clinoptilolite in soils by a cation-exchange capacity method. *Clays & Clay Minerals* **35**: 463-468.

Neel D, Bowman RS. 1992. Sorption of organics to surface-altered zeolites. Proc. 36th Annual New Mexico Water Conference; 1990 November 7-8. 57-61.

Peterson, D. 1980. Influence of presorbed water on the sorption of nitrogen by zeolites at ambient temperatures. In: Adsorption and Ion Exchange with Synthetic Zeolites, Principles and Practice. W.H. Flank, Ed. ACS Symposium Series 135, ACS, Washington, DC.

Remy, M.J. and Poncelet, G., 1995. A new approach to the determination of the external surface and micropore volume of zeolites from the nitrogen adsorption isotherm at 77 K. *J. Phys. Chem.*, **99**: 773-779.

I-9

QUANT5.05 XRD RESULTS
INTERNAL STANDARD METHOD

ANALYST Bill Carey
DATE 6-FEB-96
SAMPLE CowChow raw material 20% crn

PERCENTAGES		INPUT INTENSITIES	
SMECTITE (6.0)	= 5 +/- 2.	SMECTITE (6.0)	= 114.9
MICA (8.8)	= 1 +/- 1.	MICA (8.8)	= 26.6
QUARTZ (26.6)	= 9.57	QUARTZ (26.6)	= 233.8
QUARTZ (20.8)	= 10.14	QUARTZ (20.8)	= 51.3
TOTAL =	10 +/- 1.		
CLINOPTILOLITE(9.8)	= 72.53	CLINOPTILOLITE(9.8)	= 519.0
CLINOPT (22.1-23.0)	= 75.09	CLINOPT (22.1-23.0)	= 465.3
CLINOPTILOLITE(30.0)	= 0.00	CLINOPTILOLITE(30.0)	= 0.0
CLINOPTILOLITE(11.1)	= 0.00	CLINOPTILOLITE(11.1)	= 0.0
TOTAL =	74 +/- 4.		
CRISTOBALITE (21.9)	= 1.59	CRISTOBALITE (21.9)	= 52.4
CRISTOBALITE (36.1)	= 0.00	CRISTOBALITE (36.1)	= 0.0
TOTAL =	2 +/- 1.		
FELD (SUM 13.4-14.0)	= 0.00	FELD (SUM 13.4-14.0)	= 0.0
FELDSPAR (23.6)	= 12.48	FELDSPAR (23.6)	= 74.7
FELD (27.0-28.75)	= 11.38	FELD (27.0-28.75)	= 280.6
TOTAL =	12 +/- 3.		
		CORUNDUM (43.3)	= 154.3
		PERCENT CORUNDUM	= 20.0
		SMECTITE RIR	= 3.85

TOTAL= 104. +/- 6.

Table I. 1 X-ray diffraction results for clinoptilolite, internal standard analysis method.

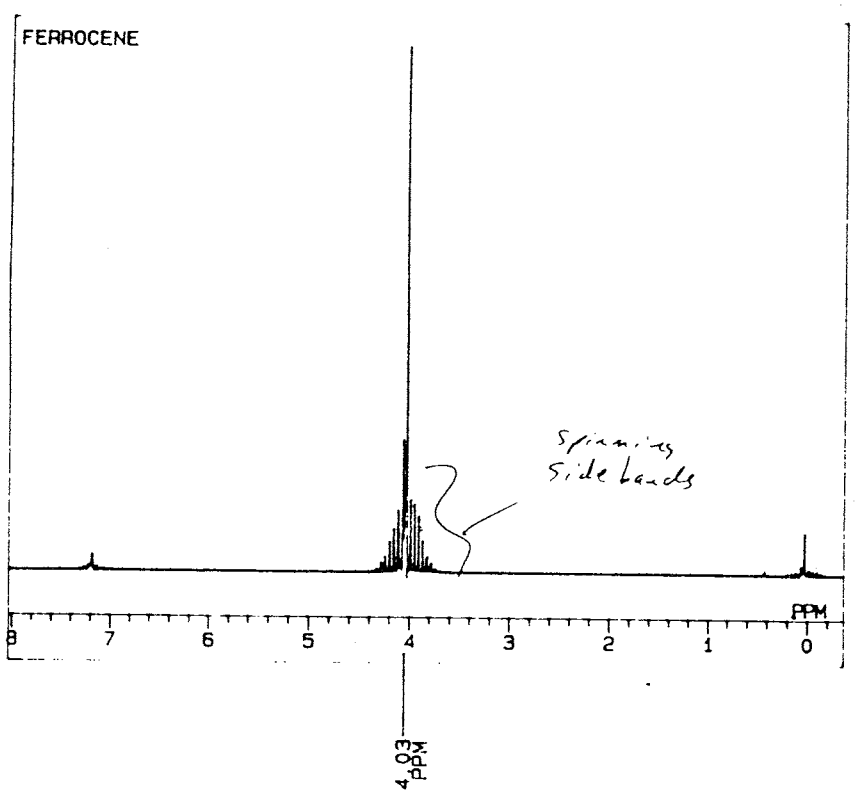

08-FEB-95	15: 33: 37	
MENUF	1H	
OBNUC	1H	
OBFRQ	399.65	MHz
OBSET	124.00	kHz
OBFIN	6301.0	Hz
PW1	14.0	us
DEADT	68.0	us
PREDL	0.2000	ms
INIWT	1.0	sec
POINT	16384	
SAMPO	16384	
TIMES	16	
DUMMY	0	
FREQU	8000.0	Hz
FILTR	4000	Hz
DELAY	50.0	us
ACQTM	1.024	sec
PD	1.500	sec
ADBIT	12	
RGAIN	16	
BF	0.00	Hz
T1	0.0	%
T2	0.0	%
T3	90.0	%
T4	100.0	%
EXMOD	SGNON	
EXPCM	SGNON: Single.Cou	
IRNUC	1H	
IRFRQ	399.65	MHz
IRSET	124.00	kHz
IRFIN	9841.0	Hz
IRRPW	77	us

Figure I.1. Tert-butyl ammonium chloride (TBAC) NMR spectrum for purity analysis. The single large peak is attributable to TBAC while the smaller peaks are due to resonance.

Surface Area Std
12/2/94

UNIVERSITY OF GEORGIA SREL
ASAP 2000 V2.03

Batch #8571

PAGE 5

SAMPLE DIRECTORY/NUMBER: DATA1 /43
SAMPLE ID: ALUMINA STD 158m^2/g
SUBMITTER: JCS
OPERATOR: JCS
UNIT NUMBER: 1
ANALYSIS GAS: Nitrogen

Bureau of Stds
US Dept of Comm
Nat Inst of Stds
& Tech
Gaithersburg MD
20899

START 10:18:22 12/02/94
COMPL 14:01:39 12/02/94
REPRT 14:01:39 12/02/94
SAMPLE WT: 1.1972 g
FREE SPACE: 52.4858 cc
EQUIL INTRVL: 10 sec

SUMMARY REPORT

AREA

158 = std

BET SURFACE AREA:	154.0765	sq. m/g
SINGLE POINT SURFACE AREA AT P/Po 0.3047:	151.0616	sq. m/g

VOLUME

SINGLE POINT TOTAL PORE VOLUME OF PORES LESS THAN 2402.9255 A DIAMETER AT P/Po 0.9919:	0.413393	cc/g

PORE SIZE

AVERAGE PORE DIAMETER (4V/A BY BET):	107.3214	A

Table I. 2.1 Surface area analysis results for alumina standard.

UNIVERSITY OF GEORGIA SREL

ASAP 2000 V2.03 PAGE 5

SAMPLE DIRECTORY/NUMBER: DATA1 /48
SAMPLE ID: cow chow no heat treat (25C)
SUBMITTER: js
OPERATOR: js
UNIT NUMBER: 1
ANALYSIS GAS: Nitrogen

START 10:38:31 12/07/94
COMPL 12:19:13 12/07/94
REPRT 12:19:13 12/07/94
SAMPLE WT: 1.0667 g
FREE SPACE: 51.4433 cc
EQUIL INTRVL: 10 sec

SUMMARY REPORT

AREA

BET SURFACE AREA:	13.1188	sq. m/g
SINGLE POINT SURFACE AREA AT P/Po 0.3172:	12.8282	sq. m/g

VOLUME

SINGLE POINT TOTAL PORE VOLUME OF PORES LESS THAN 1849.3560 A DIAMETER AT P/Po 0.9894:	0.055521	cc/g

PORE SIZE

AVERAGE PORE DIAMETER (4V/A BY BET):	169.2868	A

Conchon #48
no heat.

Table I. 2.2 Surface area analysis results for clinoptilolite with no pre-drying.

UNIVERSITY OF GEORGIA SREL

ASAP 2000 V2.03 PAGE 5

SAMPLE DIRECTORY/NUMBER: DATA1 /45
SAMPLE ID: cow chow 100c dried
SUBMITTER: js
OPERATOR: js
UNIT NUMBER: 1
ANALYSIS GAS: Nitrogen

START 12:43:54 12/03/94
COMPL 14:26:19 12/03/94
REPRT 14:26:20 12/03/94
SAMPLE WT: 1.2713 g
FREE SPACE: 52.0177 cc
EQUIL INTRVL: 10 sec

SUMMARY REPORT

AREA

BET SURFACE AREA:	15.2862	sq. m/g
SINGLE POINT SURFACE AREA AT P/Po 0.3165:	15.0359	sq. m/g

VOLUME

SINGLE POINT TOTAL PORE VOLUME OF PORES LESS THAN 1730.9580 A DIAMETER AT P/Po 0.9887:	0.057267	cc/g

PORE SIZE

AVERAGE PORE DIAMETER (4V/A BY BET):	149.8540	A

Table I. 2.3 Surface area analysis results for clinoptilolite dried at 100°C.

UNIVERSITY OF GEORGIA SREL

ASAP 2000 V2.03 PAGE 6

SAMPLE DIRECTORY/NUMBER: DATA1 /47
SAMPLE ID: cow chow 200C
SUBMITTER: js
OPERATOR: js
UNIT NUMBER: 1
ANALYSIS GAS: Nitrogen

START 12:23:37 12/04/94
COMPL 14:10:40 12/04/94
REPRT 14:10:40 12/04/94
SAMPLE WT: 1.2294 g
FREE SPACE: 53.4100 cc
EQUIL INTRVL: 10 sec

SUMMARY REPORT

AREA

BET SURFACE AREA:	15.7263	sq. m/g
LANGMUIR SURFACE AREA:	24.7980	sq. m/g
SINGLE POINT SURFACE AREA AT P/Po 0.3170:	15.5822	sq. m/g

VOLUME

SINGLE POINT TOTAL PORE VOLUME OF PORES LESS THAN 1945.2847 A DIAMETER AT P/Po 0.9900:	0.057941	cc/g

PORE SIZE

AVERAGE PORE DIAMETER (4V/A BY LANGMUIR):	93.4615	A

Table I. 2.4 Surface area analysis results for clinoptilolite dried at 200°C.

External and Internal Cation Exchange Capacity Experiments
HDTMA used for External CEC
Cs used for internal CEC
Experiment 6A 4/27/95 J. Sullivan

Phase 1, NaOAC treatment to remove Ca2+ from original samples.

Samples	*Sample No.*	*Solution Ca2+ Concentration* **mg/L**	*Solution Ca2+ Quantity* **mmoles**	*Ca2+ Quantity* **meq**	*Ca2+ Removed* **meq/100g zeo**	*Mean Values* **meq/100g zeo**
J. Sullivan 24 hr	**1A**	44.6	0.134	0.267	26.7	**26.9**
	1B	44.8	0.134	0.268	26.8	
J. Sullivan Blank 24 hr	**1C**	45.2	0.135	0.271	27.1	
G. Haggerty 24 hr	**2A**	92.5	0.277	0.554	55.4	**53.4**
	2B	94.2	0.282	0.564	56.4	
G. Haggerty Blank 24 hr	**2C**	81	0.243	0.485	48.5	
J. Sullivan 48 hr	**3A**	43.6	0.131	0.261	26.1	**25.9**
	3B	42.9	0.128	0.257	25.7	
J. Sullivan Blank 48 hr	**3C**	43.4	0.130	0.260	26.0	
G. Haggerty 48 hr	**4A**	90	0.269	0.539	53.9	**48.9**
	4B	80	0.240	0.479	47.9	
G. Haggerty Blank 48 hr	**4C**	74.9	0.224	0.449	44.9	

Table I.3.1. Resurlts of external and interanl cation exchange capacity measurements on G. Haggerty and J. Sullivan clinoptilolite.

External and Internal Cation Exchange Capacity Experiments
HDTMA used for External CEC
Cs used for internal CEC
Experiment 6A 4/27/95 J. Sullivan

Phase 2a, HDTMA Sorption, This was measured to compare with desorbed Na+ and Ca2+ in Phase 2b. This step was not used to directly determine the ECEC.

Samples	*Sample No.*	*HDTMA Concentration* **cpm/ml**	*HDTMA Quantity minus backgrnd.* **cpm**	*HDTMA Quantity* **meq**	*HDTMA Sorbed* **meq**	*HDTMA Sorbed* **meq/100g zeo**
J. Sullivan 24 hr	**1A**	1592.6	156680	1.55	0.25	**24.67**
	1B	1534.5	150870	1.50	0.30	**30.43**
J. Sullivan Blank 24 hr	**1C**	25.8				
G. Haggerty 24 hr	**2A**	1572.1	155250	1.54	0.26	**26.09**
	2B	1602.4	158280	1.57	0.23	**23.09**
G. Haggerty Blank 24 hr	**2C**	19.6				
J. Sullivan 48 hr	**3A**	1509.1	148640	1.47	0.33	**32.64**
	3B	1514.5	149180	1.48	0.32	**32.11**
J. Sullivan Blank 48 hr	**3C**	22.7				
G. Haggerty 48 hr	**4A**	1578.9	155720	1.54	0.26	**25.62**
	4B	1569.6	154790	1.53	0.27	**26.55**
G. Haggerty Blank 48 hr	**4C**	21.7				
Mean Sullivan 24h						**27.55**
Mean Haggerty 24h						**24.59**
Mean Sullivan 48h						**32.37**
Mean Haggerty 48h						**26.08**

Table I.3.2. Results of external and interanl cation exchange capacity measurements on G. Haggerty and J. Sullivan clinoptilolite.

External and Internal Cation Exchange Capacity Experiments
HDTMA used for External CEC
Cs used for internal CEC
Experiment 6A 4/27/95 J. Sullivan

Na+/Ca2+ Desorption using HDTMA. This measures the ECEC.

Samples	*Sample No.*	*Na+ Conc.* **mg/L**	*Ca2+ Conc.* **mg/L**	*Na+ Quantity* **mmoles**	*Ca2+ Quantity* **mmoles**	*Na+ Quantity minus backg.* **meq**	*Ca2+ Quantity minus backg.* **meq**	Total *Na+ and Ca2+ Removed* **meq/100g zeo**
J. Sullivan 24 hr	**1A**	23.11	0.56	0.10	1.39E-03	0.09	2.38E-03	9.17
	1B	23.29	0.51	0.10	1.28E-03	0.09	2.16E-03	9.23
J. Sullivan Blank 24 hr	**1C**	2.57	0.08	0.01	2.00E-04			
G. Haggerty 24 hr	**2A**	23.66	0.10	0.10	2.50E-04	0.07	4.17E-04	7.40
	2B	23.05	0.07	0.10	1.66E-04	0.07	2.49E-04	7.12
G. Haggerty Blank 24 hr	**2C**	6.74	0.02	0.03	4.17E-05			
J. Sullivan 48 hr	**3A**	23.54	0.50	0.10	1.26E-03	0.09	2.02E-03	9.21
	3B	23.78	0.56	0.10	1.41E-03	0.09	2.32E-03	9.35
J. Sullivan Blank 48 hr	**3C**	2.82	0.10	0.01	2.50E-04			
G. Haggerty 48 hr	**4A**	24.63	0.06	0.11	1.46E-04	0.08	1.55E-04	7.61
	4B	22.21	0.07	0.10	1.63E-04	0.07	1.88E-04	6.56
G. Haggerty Blank 48 hr	**4C**	7.17	0.03	0.03	6.86E-05			
Mean Sullivan 24h								**9.20**
Mean Haggerty 24h								**7.26**
Mean Sullivan 48h								**9.28**
Mean Haggerty 48h								**7.09**

Table I.3.3. Results of external and interanl cation exchange capacity measurements on G. Haggerty and J. Sullivan clinoptilolite.

External and Internal Cation Exchange Capacity Experiments
HDTMA used for External CEC
Cs used for internal CEC
Experiment 6A 4/27/95 J. Sullivan

Phase 3a, Total HDTMA Desorption, ETOH Wash Only.
This step was used only to track the HDTMA in the system.

Samples	*Sample No.*	*HDTMA Conc.* **cpm/ml**	*HDTMA Quantity minus backg.* **cpm**	*HDTMA Quantity Desorbed* **meq**	*HDTMA Sorbed* **meq**	*Remaining HDTMA Sorbed* **meq/100g zeo**
J. Sullivan 24 hr	**1A**	267.9	12105	0.12	0.13	**12.67**
	1B	296.4	13530	0.13	0.17	**17.02**
J. Sullivan Blank 24 hr	**1C**	25.8				
G. Haggerty 24 hr	**2A**	241.9	11115	0.11	0.15	**15.07**
	2B	257.9	11915	0.12	0.11	**11.27**
G. Haggerty Blank 24 hr	**2C**	19.6				
J. Sullivan 48 hr	**3A**	307.9	14260	0.14	0.19	**18.51**
	3B	285.3	13130	0.13	0.19	**19.09**
J. Sullivan Blank 48 hr	**3C**	22.7				
G. Haggerty 48 hr	**4A**	261.2	11975	0.12	0.14	**13.75**
	4B	249.7	11400	0.11	0.15	**15.24**
G. Haggerty Blank 48 hr	**4C**	21.7				
Mean Sullivan 24h						**14.84**
Mean Haggerty 24h						**13.17**
Mean Sullivan 48h						**18.80**
Mean Haggerty 48h						**14.50**

Table I.3.4. Results of external and interanl cation exchange capacity measurements on G. Haggerty and J. Sullivan clinoptilolite.

External and Internal Cation Exchange Capacity Experiments
HDTMA used for External CEC
Cs used for internal CEC
Experiment 6A 4/27/95 J. Sullivan

Phase 3b, Na+/Ca2+ Desorption, ETOH Wash Only. Used to check completeness of the wash process for removing residual cations

Samples	*Sample No.*	*Na+ Conc.* **mg/L**	*Ca2+ Conc.* **mg/L**	*Na+ Quantity* **mmoles**	*Ca2+ Quantity* **mmoles**	*Na+ Quantity* **meq**	*Ca2+ Quantity* **meq**	*Na+ and Ca2+ Removed* **meq/100g zeo**	*Total Na+ and Ca2+ Removed* **meq/100g zeo**
J. Sullivan 24 hr	**1A**	0.045	0.02	1.96E-04	5.18E-05	1.96E-04	1.04E-04	0.03	9.20
	1B	0.034	0.00	1.48E-04	0.00E+00	1.48E-04	0.00E+00	0.01	9.24
J. Sullivan Blank 24 hr	**1C**								
G. Haggerty 24 hr	**2A**	0.022	0.00	9.57E-05	0.00E+00	9.57E-05	0.00E+00	0.01	7.41
	2B	0.045	0.00	1.96E-04	0.00E+00	1.96E-04	0.00E+00	0.02	7.14
G. Haggerty Blank 24 hr	**2C**								
J. Sullivan 48 hr	**3A**	0.019	0.00	8.26E-05	0.00E+00	8.26E-05	0.00E+00	0.01	9.22
	3B	0.019	0.00	8.26E-05	0.00E+00	8.26E-05	0.00E+00	0.01	9.36
J. Sullivan Blank 48 hr	**3C**								
G. Haggerty 48 hr	**4A**	0.014	0.00	6.09E-05	0.00E+00	6.09E-05	0.00E+00	0.01	7.62
	4B	0.016	0.00	6.96E-05	0.00E+00	6.96E-05	0.00E+00	0.01	6.57
G. Haggerty Blank 48 hr	**4C**								
Mean Sullivan 24h								**0.02**	**9.22**
Mean Haggerty 24h								**0.01**	**7.27**
Mean Sullivan 48h								**0.01**	**9.29**
Mean Haggerty 48h								**0.01**	**7.09**

Table I.3.5. Results of external and interanl cation exchange capacity measurements on G. Haggerty and J. Sullivan clinoptilolite.

External and Internal Cation Exchange Capacity Experiments
HDTMA used for External CEC
Cs used for internal CEC
Experiment 6A 4/27/95 J. Sullivan

Na+/Ca2+ desorption, CsCl wash only. This measures the ICEC

Samples	*Sample No.*	*Na+ Conc.* **mg/L**	*Ca2+ Conc.* **mg/L**	*Na+ Quantity* **mmoles**	*Ca2+ Quantity* **mmoles**	*Na+ Quantity minus backg.* **meq**	*Ca2+ Quantity minus backg* **meq**	*Na+ and Ca2+ Removed* **meq/100g zeo**
J. Sullivan 24 hr	**1A**	71.8	68.70	0.31	1.71E-01	0.31	3.42E-01	64.87
	1B	70.8	71.90	0.31	1.79E-01	0.30	3.58E-01	66.03
J. Sullivan Blank 24 hr	**1C**	1.39	0.08	0.01	1.99E-04			
G. Haggerty 24 hr	**2A**	189.1	27.30	0.82	6.81E-02	0.82	1.36E-01	95.42
	2B	183.4	31.30	0.80	7.81E-02	0.79	1.56E-01	94.94
G. Haggerty Blank 24 hr	**2C**	1.03	0.02	0.00	4.52E-05			
J. Sullivan 48 hr	**3A**	69.5	69.00	0.30	1.72E-01	0.30	3.44E-01	64.31
	3B	68.9	66.20	0.30	1.65E-01	0.30	3.30E-01	62.65
J. Sullivan Blank 48 hr	**3C**	0.69	0.10	0.00	2.48E-04			
G. Haggerty 48 hr	**4A**	188.6	28.10	0.82	7.01E-02	0.82	1.40E-01	95.87
	4B	182.4	25.80	0.79	6.44E-02	0.79	1.29E-01	92.02
G. Haggerty Blank 48 hr	**4C**	0.41	0.03	0.00	7.13E-05			
Mean Sullivan 24h								**65.45**
Mean Haggerty 24h								**95.18**
Mean Sullivan 48h								**63.48**
Mean Haggerty 48h								**93.94**

Table I.3.6. Results of external and interanl cation exchange capacity measurements on G. Haggerty and J. Sullivan clinoptilolite.

External and Internal Cation Exchange Capacity Experiments
HDTMA used for External CEC
Cs used for internal CEC
Experiment 6A 4/27/95 J. Sullivan

Phase 2c, Bromide Sorption. Bromide was tracked for completeness.

Samples	Sample No.	*Br- Diluted Conc.* **mg/L**	*Br- Conc.* **mg/L**	*Br- Quantity* **mg**	*Br- Quantity* **meq**	*Br- Sorbed* **meq**	*Br- Sorbed* **meq/100g zeo**	*HDTMA Sorbed* **meq/100g zeo**
J. Sullivan 24 hr	**1A**	11.4238	1142.4	113.496	1.42	0.19	18.80	24.67
	1B	14.5798	1458	145.056	1.82	-0.21	-20.69	30.43
J. Sullivan Blank 24 hr	**1C**	0.0742	7.42	0.742				
G. Haggerty 24 hr	**2A**	13.4568	1345.7	133.801	1.67	-0.07	-6.61	26.09
	2B	13.0042	1300.4	129.275	1.62	-0.01	-0.94	23.09
G. Haggerty Blank 24 hr	**2C**	0.0767	7.67	0.767				
J. Sullivan 48 hr	**3A**	14.5484	1454.8	145.114	1.82	-0.21	-20.76	32.64
	3B	13.2624	1326.2	132.254	1.66	-0.05	-4.67	32.11
J. Sullivan Blank 48 hr	**3C**	0.037	3.7	0.37				
G. Haggerty 48 hr	**4A**	11.9433	1194.3	118.798	1.49	0.12	12.17	25.62
	4B	12.7413	1274.1	126.778	1.59	0.02	2.18	26.55
G. Haggerty Blank 48 hr	**4C**	0.0635	6.35	0.635				
Mean Sullivan 24h							-0.94	27.55
Mean Haggerty 24h							-3.77	24.59
Mean Sullivan 48h							-12.72	32.37
Mean Haggerty 48h							7.18	26.08

Table I.3.7. Results of external and internal cation exchange capacity measurements on G. Haggerty and J. Sullivan clinoptilolite.

External and Internal Cation Exchange Capacity Experiments
TBAC used for External CEC
Cs used for internal CEC
1/16/95 J. Sullivan/J. Verploegh
The two blanks were contaminated before the TBAC and CsCl washings.
All TBAC Exchanges Run for 24 hours only.

TBAC Sorption, Na+/Ca2+ Desorption. This measures the ECEC.

Samples	*Sample No.*	*Na+ Conc.* **mg/L**	*Ca2+ Conc.* **mg/L**	*Na+ Quantity* **meq/L**	*Ca2+ Quantity* **meq/L**	*Na+ Quantity Removed* **meq/100g zeo**	*Ca2+ Quantity Removed* **meq/100g zeo**	*Na+ and Ca2+ Removed* **meq/100g zeo**
J. Sullivan	**CC-A**	18.9	2.93	0.82	0.15	8.22	1.46	**9.68**
	CC-B	18.8	2.7	0.82	0.13	8.18	1.35	**9.53**
	CC-C	18.8	2.87	0.82	0.14	8.18	1.43	**9.61**
G. Haggerty	**G-A**	21.5	0.02	0.94	0.00	9.35	0.01	**9.36**
	G-B	22.3	0.01	0.97	0.00	9.70	0.00	**9.71**
	G-C	20	0	0.87	0.00	8.70	0.00	**8.70**
No Blanks Available.								
Mean J. Sullivan								**9.61**
Mean G. Haggerty								**9.26**

Table I.3.8. Results of external and internal cation exchange capacity measurements on G. Haggerty and J. Sullivan clinoptilolite.

External and Internal Cation Exchange Capacity Experiments
TBAC used for External CEC
Cs used for internal CEC
1/16/95 J. Sullivan/J. Verploegh
The two blanks were contaminated before the TBAC and CsCl washings.
All TBAC Exchanges Run for 24 hours only.

Na+/Ca2+ desorption, CsCl wash only. This measures the ICEC

Samples	*Sample No.*	*Na+ Conc.* **mg/L***	*Ca2+ Conc.* **mg/L**	*Na+ Quantity* **meq/L**	*Ca2+ Quantity* **meq/L**	*Na+ Quantity Removed** **meq/100g zeo**	*Ca2+ Quantity Removed* **meq/100g zeo**	*Na+ and Ca2+ Removed* **meq/100g zeo**
J. Sullivan	**CC-A**	20.2	18.3	0.88	0.91	8.79	9.13	**17.92**
	CC-B	20.7	18	0.9	0.9	9	8.98	**17.98**
	CC-C	19.3	17.9	0.84	0.89	8.4	8.93	**17.33**
G. Haggerty	**G-A**	199	3.4	8.66	0.17	86.57	1.7	**88.27**
	G-B	199	3.3	8.66	0.16	86.57	1.63	**88.20**
	G-C	215	3.2	9.35	0.16	93.53	1.61	**95.14**
No Blanks Available.								
Mean J. Sullivan*								**17.74**
Mean G. Haggerty								**90.54**

*Analytical error suspected.

Table I.3.9. Results of external and internal cation exchange capacity measurements on G. Haggerty and J. Sullivan clinoptilolite.

Surface Tension Data for HDTMA-bromide Solutions at 25C.
J. Sullivan 3/25/96, PRRC Instrument

Solution Concentration mmol/L	P	Square Root of equation	F correction factor	P*F corrected value dyne/cm^2
0	74.5	0.210	0.935	69.661
0	74.4	0.210	0.935	69.561
0.25	50.9	0.186	0.911	46.373
0.25	50.8	0.186	0.911	46.276
0.5	41.3	0.175	0.900	37.184
0.5	41.2	0.175	0.900	37.090
0.75	41.2	0.175	0.900	37.090
0.75	41.2	0.175	0.900	37.090
1	37	0.170	0.895	33.128
1	37.1	0.170	0.895	33.221
1.5	39	0.173	0.898	35.010
1.5	38.9	0.173	0.898	34.916
2	39	0.173	0.898	35.010
2	39.1	0.173	0.898	35.104

C	5.995	
C^2	35.94003	
r/R	0.0186	
D	0.99708	lower phase density, water/solution at 25C
	0.99823	density of water at 20C
	0.997655	mean density
d	0.001122	upper phase density of air at 25 C
D-d	0.997108	
F	0.725	

Table I. 4 Surface tension results for varying concentrations of HDTMA-bromide at 25°C in Type I water.

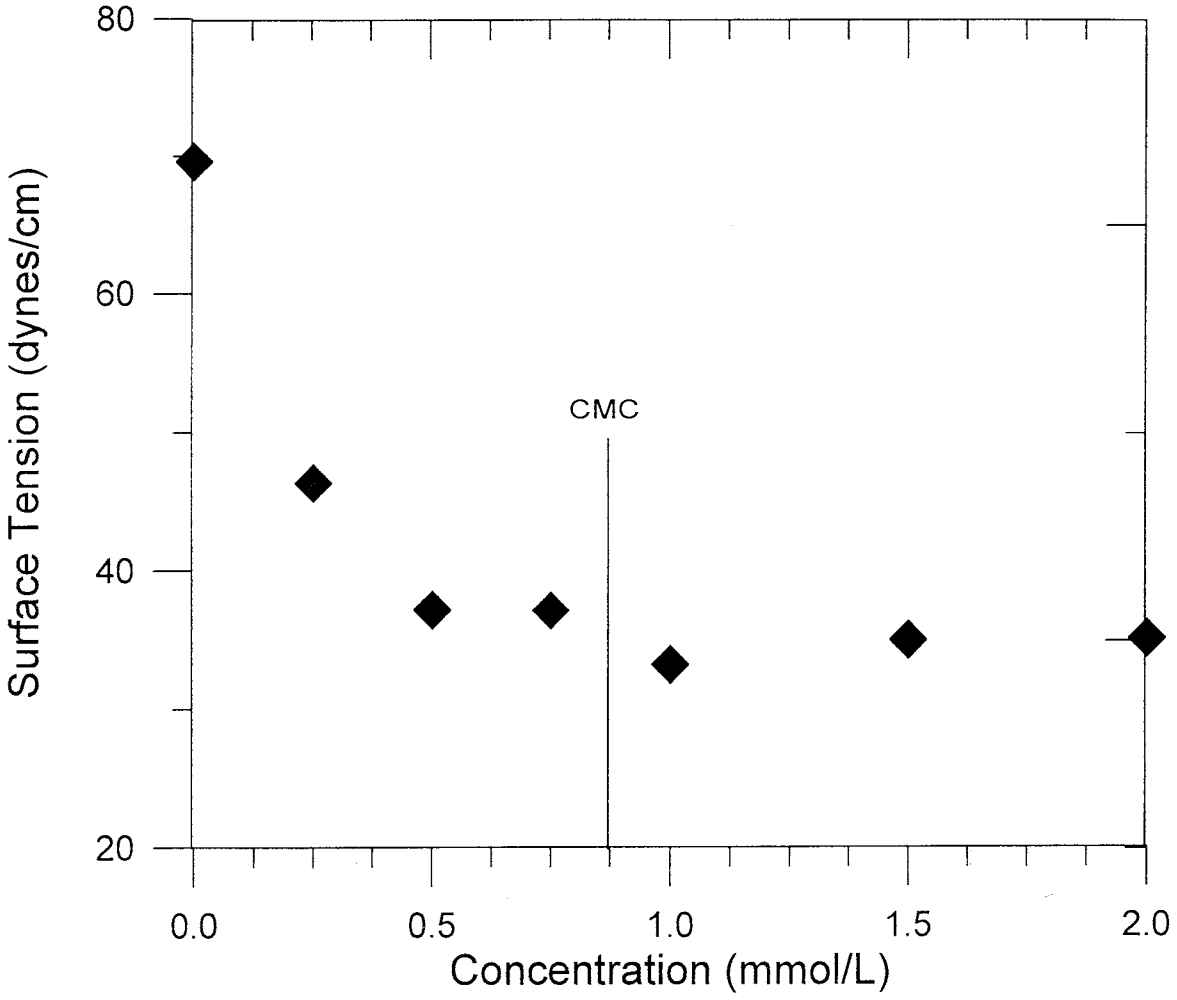

Figure I. 2. Graph of surface tension versus concentration, HDTMA, 25°C.

APPENDIX II

This appendix shows the background data for the adsorption isotherms in Chapter 3. This experiment was run in three stages, one each for adsorption of HDTMA micelles (>CMC), monomers (<CMC) and TEA. For the HDTMA sorption tables, the sample number is indicative of the amount of surfactant applied, in percent of ECEC (here, 90 meq/kg). Counts per minute per ml are the results from the scintillation counter, with background counts subtracted in the next column. This amount was then converted to mmol/ml by multiplying by a conversion factor determined from the original spiked solution, which has a known concentration and a cpm/ml value determined in the same scintillation counter run. These values are then multiplied by the equilibrated volume, and subtracted from the original quantity available to determine mmol sorbed.

For bromide, the measured amount is multiplied by the dilution factor to get the concentration in solution. This is converted to mmol/L of bromide, multiplied by the volume to produce mmol, and subtracted from the original quantity of mmol present to get the amount sorbed. Because the bromide values in this experiment were found to be greater in some of the final solutions than in the original solution, it was concluded that anion exclusion was occurring. This is because the amount of surface area of the zeolite is high compared to the solution volume and concentration. The negatively-charged surface of the zeolite excludes the bromide ions from some volume near the surface, increasing the apparent concentration in the bulk solution. This excluded volume must be calculated and subtracted from the "known" volume to accurately convert the mg/L

values to mg of bromide. This was done on page II-3 and II-10 of the tables. No excluded volume was calculated for TEA because the solution concentrations of bromide changed very little during the sorption process; i.e., essentially no bromide was sorbed.

Sodium, calcium, and magnesium desorbed from the surface were all measured and the values converted to meq/l. The values are added together on pages II-7 and II-14 of the tables.

APPENDIX II
Experiment 10B by J. Sullivan/E. Keene 2/15/96
7-day equilibration of >CMC (micelle) 1.8 mmol/L solution
Results for HDTMA sorption , bromide sorption, and cation desorption

HDTMA Sorption Results, 14C-HDTMA used, scintillation counting results

Sample Number	Percent ECEC Treatment	cpm/ml	cpm/ml minus backg.	cpm/ml Converted to mmol/ml	mmol in solution	mmol sorbed	grams of Clinop.	Equil Soln Conc mmol/l	Equil Sorbed Conc mmol/kg
25A	25	59.1	17.3	2.05E-06	8.18E-05	7.19E-02	3.2002	2.05E-03	22.47
25B	25	59.4	17.6	2.08E-06	8.33E-05	7.19E-02	3.2005	2.08E-03	22.47
50A	50	70.4	28.6	3.38E-06	1.35E-04	7.19E-02	1.5999	3.38E-03	44.92
50B	50	65	23.2	2.74E-06	1.10E-04	7.19E-02	1.6003	2.74E-03	44.92
75A	75	127.7	85.9	1.02E-05	4.06E-04	7.16E-02	1.0701	1.02E-02	66.90
75B	75	117.3	75.5	8.93E-06	3.57E-04	7.16E-02	1.0706	8.93E-03	66.92
100A	100	335.5	293.7	3.47E-05	1.39E-03	7.06E-02	0.8005	3.47E-02	88.21
100B	100	375.6	333.8	3.95E-05	1.58E-03	7.04E-02	0.8003	3.95E-02	87.99
150A	150	834.2	792.4	9.37E-05	3.75E-03	6.83E-02	0.5332	9.37E-02	128.00
150B	150	902.5	860.7	1.02E-04	4.07E-03	6.79E-02	0.5335	1.02E-01	127.33
200A	200	1957.6	1915.8	2.27E-04	9.06E-03	6.29E-02	0.4004	2.27E-01	157.18
200B	200	1795.2	1753.4	2.07E-04	8.30E-03	6.37E-02	0.4005	2.07E-01	159.06
250A	250	3006.1	2964.3	3.51E-04	1.40E-02	5.80E-02	0.3206	3.51E-01	180.84
250B	250	3031	2989.2	3.54E-04	1.41E-02	5.79E-02	0.3201	3.54E-01	180.75
300A	300	4206.4	4164.6	4.93E-04	1.97E-02	5.23E-02	0.2675	4.93E-01	195.51
300B	300	4222.8	4181	4.94E-04	1.98E-02	5.22E-02	0.267	4.94E-01	195.58
400A	400	5939.6	5897.8	6.98E-04	2.79E-02	4.41E-02	0.2006	6.98E-01	219.83
400B	400	6049.3	6007.5	7.11E-04	2.84E-02	4.36E-02	0.2001	7.11E-01	217.79
500A	500	7740.7	7698.9	9.11E-04	3.64E-02	3.56E-02	0.1601	9.11E-01	222.22
500B	500	7714.7	7672.9	9.07E-04	3.63E-02	3.57E-02	0.1604	9.07E-01	222.57
600A	600	8788.3	8746.5	1.03E-03	4.14E-02	3.06E-02	0.1334	1.03E+00	229.55
600B	600	8897.2	8855.4	1.05E-03	4.19E-02	3.01E-02	0.1335	1.05E+00	225.52

APPENDIX II
Experiment 10B by J. Sullivan/E. Keene 2/15/96
7-day equilibration of >CMC (micelle) 1.8 mmol/L solution
Results for HDTMA sorption , bromide sorption, and cation desorption

Bromide Sorbed--HPLC Results

Sample	Conc. Br mg/L	dilution factor	Actual Conc. mg/L	Amount mmol/L	Amount mmol	Amt. Sorbed mmol	grams of Clinop.	Equil Soln Conc mmol/l	Equil Sorbed Conc mmol/kg
Known mmol/L				1.8	0.072				
mean of solns A&B				1.7	0.068	6.73E-02			
Original soln. A	28.1	5	140.5	1.8	7.03E-02	-2.99E-03	0	1.8	not applic.
Original soln. B	25.7	5	128.6	1.6	6.43E-02	2.99E-03	0	1.6	not applic.
25A	28.4	5	142.2	1.8	7.12E-02	-3.85E-03	3.2002	1.8	-1.2
25B	36.8	5	184.2	2.3	9.22E-02	-2.49E-02	3.2005	2.3	-7.8
50A	28.6	5	142.9	1.8	7.15E-02	-4.19E-03	1.5999	1.8	-2.6
50B	31.2	5	156.1	2.0	7.81E-02	-1.08E-02	1.6003	2.0	-6.7
75A	34.2	4	136.9	1.7	6.85E-02	-1.19E-03	1.0701	1.7	-1.1
75B	34.8	4	139.3	1.7	6.97E-02	-2.37E-03	1.0706	1.7	-2.2
100A	34.4	4	137.5	1.7	6.88E-02	-1.51E-03	0.8005	1.7	-1.9
100B	34.4	4	137.6	1.7	6.89E-02	-1.53E-03	0.8003	1.7	-1.9
150A	28.8	4	115.1	1.4	5.76E-02	9.75E-03	0.5332	1.4	18.3
150B	29.5	4	117.9	1.5	5.90E-02	8.34E-03	0.5335	1.5	15.6
200A	24.4	4	97.4	1.2	4.88E-02	1.86E-02	0.4004	1.2	46.4
200B	25.0	4	99.8	1.2	5.00E-02	1.74E-02	0.4005	1.2	43.3
250A	23.1	4	92.6	1.2	4.63E-02	2.10E-02	0.3206	1.2	65.5
250B	23.4	4	93.5	1.2	4.68E-02	2.05E-02	0.3201	1.2	64.2
300A	23.9	4	95.7	1.2	4.79E-02	1.94E-02	0.2675	1.2	72.6
300B	23.1	4	92.5	1.2	4.63E-02	2.10E-02	0.267	1.2	78.7
400A	23.9	4	95.7	1.2	4.79E-02	1.94E-02	0.2006	1.2	96.9
400B	24.0	4	95.9	1.2	4.80E-02	1.93E-02	0.2001	1.2	96.7
500A	25.2	4	101.0	1.3	5.06E-02	1.68E-02	0.1601	1.3	104.9
500B	26.3	4	105.4	1.3	5.27E-02	1.46E-02	0.1604	1.3	91.0
600A	27.1	4	108.4	1.4	5.43E-02	1.31E-02	0.1334	1.4	98.1
600B	27.5	4	110.0	1.4	5.51E-02	1.23E-02	0.1335	1.4	91.9

APPENDIX II

Experiment 10B by J. Sullivan/E. Keene 2/15/96

7-day equilibration of >CMC (micelle) 1.8 mmol/L solution

Results for HDTMA sorption , bromide sorption, and cation desorption

Bromide Sorbed--Anion Exclusion Adjustment Calculations

Anion Exclusion was noted when the final solution concentrations were found to be higher than the original solution concentration of HDTMA-Br

A formula from Israelachvili, 1991, was used to adjust the final solution concentrations based upon the surface area and excluded volume of the clinoptilolite in each sample.

Conc.	6.73402E-05	M
sqrt of conc.	0.008206109	
Debye length	37.04557189	nm
	3.70456E-05	cm

Sample No.	Excluded Debye Volume cm^3 (ml)	adjusted volume ml	"normalized" mg**	amount in soln mmol	Amount sorbed mmol	Actual Equil Soln Conc mmol/l	Actual Equil Sorbed Conc mmol/kg
Original soln. A	n/a						
Original soln. B	n/a						
25A	18.6	21.4	3.0	3.81E-02	2.93E-02	1.8	9.1
25B	18.6	21.4	3.9	4.93E-02	1.80E-02	2.3	5.6
50A	9.3	30.7	4.4	5.49E-02	1.25E-02	1.8	7.8
50B	9.3	30.7	4.8	5.99E-02	7.39E-03	2.0	4.6
75A	6.2	33.8	4.6	5.79E-02	9.47E-03	1.7	8.9
75B	6.2	33.8	4.7	5.89E-02	8.48E-03	1.7	7.9
100A	4.7	35.3	4.9	6.08E-02	6.51E-03	1.7	8.1
100B	4.7	35.3	4.9	6.09E-02	6.49E-03	1.7	8.1
150A	3.1	36.9	4.2	5.31E-02	1.42E-02	1.4	26.7
150B	3.1	36.9	4.3	5.44E-02	1.29E-02	1.5	24.2
200A	2.3	37.7	3.7	4.59E-02	2.14E-02	1.2	53.5
200B	2.3	37.7	3.8	4.71E-02	2.03E-02	1.2	50.6
250A	1.9	38.1	3.5	4.42E-02	2.32E-02	1.2	72.2
250B	1.9	38.1	3.6	4.46E-02	2.27E-02	1.2	71.0
300A	1.6	38.4	3.7	4.60E-02	2.13E-02	1.2	79.6
300B	1.6	38.4	3.6	4.45E-02	2.28E-02	1.2	85.4
400A	1.2	38.8	3.7	4.65E-02	2.08E-02	1.2	103.9
400B	1.2	38.8	3.7	4.66E-02	2.07E-02	1.2	103.6
500A	0.9	39.1	3.9	4.94E-02	1.80E-02	1.3	112.2
500B	0.9	39.1	4.1	5.15E-02	1.58E-02	1.3	98.7
600A	0.8	39.2	4.3	5.32E-02	1.41E-02	1.4	106.0
600B	0.8	39.2	4.3	5.40E-02	1.33E-02	1.4	99.9

APPENDIX II
Experiment 10B by J. Sullivan/E. Keene 2/15/96
7-day equilibration of >CMC (micelle) 1.8 mmol/L solution
Results for HDTMA sorption , bromide sorption, and cation desorption

Sodium Cations Desorbed--Atomic Absorption Spectrophotometry Analyses

Sample No.	Na Analysis Conc mg/L	Grams Sample g	Amount in Sample mg	Amount in Sample meq	Equil.Soln Conc. meq/L	Desorbed Conc. meq/kg
25A	11.37	3.2002	0.45	0.02	0.49	6.18
25B	11.33	3.2005	0.45	0.02	0.49	6.16
50A	8.83	1.5999	0.35	0.02	0.38	9.60
50B	8.89	1.6003	0.36	0.02	0.39	9.67
75A	7.82	1.0701	0.31	0.01	0.34	12.71
75B	7.64	1.0706	0.31	0.01	0.33	12.42
100A	6.39	0.8005	0.26	0.01	0.28	13.89
100B	6.32	0.8003	0.25	0.01	0.27	13.74
150A	4.89	0.5332	0.20	0.01	0.21	15.96
150B	4.89	0.5335	0.20	0.01	0.21	15.95
200A	3.76	0.4004	0.15	0.01	0.16	16.34
200B	3.88	0.4005	0.16	0.01	0.17	16.86
250A	3.015	0.3206	0.12	0.01	0.13	16.36
250B	2.988	0.3201	0.12	0.01	0.13	16.24
300A	2.553	0.2675	0.10	0.00	0.11	16.61
300B	2.52	0.267	0.10	0.00	0.11	16.42
400A	2.018	0.2006	0.08	0.00	0.09	17.50
400B	1.981	0.2001	0.08	0.00	0.09	17.23
500A	1.696	0.1601	0.07	0.00	0.07	18.43
500B	1.704	0.1604	0.07	0.00	0.07	18.48
600A	1.489	0.1334	0.06	0.00	0.06	19.42
600B	1.512	0.1335	0.06	0.00	0.07	19.71

APPENDIX II
Experiment 10B by J. Sullivan/E. Keene 2/15/96
7-day equilibration of >CMC (micelle) 1.8 mmol/L solution
Results for HDTMA sorption , bromide sorption, and cation desorption

Calcium Cations Desorbed--Atomic Absorption Spectrophotometry Analyses

Sample No.	Ca Analysis Conc mg/L	Grams of Sample g	Amount in Sample mg	Amount in Sample meq	Equil.Soln Conc. meq/L	Desorbed Conc. meq/kg
25A	16.67	3.2002	0.67	0.03	0.83	10.40
25B	16.22	3.2005	0.65	0.03	0.81	10.12
50A	15.63	1.5999	0.63	0.03	0.78	19.50
50B	15.74	1.6003	0.63	0.03	0.79	19.63
75A	18.64	1.0701	0.75	0.04	0.93	34.77
75B	16.3	1.0706	0.65	0.03	0.81	30.39
100A	14.33	0.8005	0.57	0.03	0.72	35.73
100B	14.13	0.8003	0.57	0.03	0.71	35.24
150A	10.75	0.5332	0.43	0.02	0.54	40.24
150B	11.78	0.5335	0.47	0.02	0.59	44.07
200A	7.28	0.4004	0.29	0.01	0.36	36.29
200B	9.33	0.4005	0.37	0.02	0.47	46.50
250A	6.1	0.3206	0.24	0.01	0.30	37.98
250B	5.68	0.3201	0.23	0.01	0.28	35.42
300A	4.59	0.2675	0.18	0.01	0.23	34.25
300B	4.77	0.267	0.19	0.01	0.24	35.66
400A	3.87	0.2006	0.15	0.01	0.19	38.51
400B	3.94	0.2001	0.16	0.01	0.20	39.30
500A	2.97	0.1601	0.12	0.01	0.15	37.03
500B	4.51	0.1604	0.18	0.01	0.23	56.12
600A	2.35	0.1334	0.09	0.00	0.12	35.16
600B	2.44	0.1335	0.10	0.00	0.12	36.48

APPENDIX II
Experiment 10B by J. Sullivan/E. Keene 2/15/96
7-day equilibration of >CMC (micelle) 1.8 mmol/L solution
Results for HDTMA sorption , bromide sorption, and cation desorption

Magnesium Cations Desorbed--Atomic Absorption Spectrophotometry Analyses

Sample No.	Mg Analysis Conc mg/L	Grams of Sample g	Amount in Sample mg	Amount in Sample meq	Equil.Soln Conc. meq/L	Desorbed Conc. meq/kg
25A	8.744	3.2002	0.35	0.03	0.72	8.99
25B	8.896	3.2005	0.36	0.03	0.73	9.15
50A	7.708	1.5999	0.31	0.03	0.63	15.86
50B	7.872	1.6003	0.31	0.03	0.65	16.19
75A	7.688	1.0701	0.31	0.03	0.63	23.65
75B	7.728	1.0706	0.31	0.03	0.64	23.76
100A	6.86	0.8005	0.27	0.02	0.56	28.21
100B	6.888	0.8003	0.28	0.02	0.57	28.33
150A	5.304	0.5332	0.21	0.02	0.44	32.74
150B	5.392	0.5335	0.22	0.02	0.44	33.27
200A	3.12	0.4004	0.12	0.01	0.26	25.65
200B	3.344	0.4005	0.13	0.01	0.28	27.48
250A	2.62	0.3206	0.10	0.01	0.22	26.90
250B	2.692	0.3201	0.11	0.01	0.22	27.68
300A	2.316	0.2675	0.09	0.01	0.19	28.50
300B	2.324	0.267	0.09	0.01	0.19	28.65
400A	1.836	0.2006	0.07	0.01	0.15	30.13
400B	1.82	0.2001	0.07	0.01	0.15	29.94
500A	1.584	0.1601	0.06	0.01	0.13	32.57
500B	1.644	0.1604	0.07	0.01	0.14	33.74
600A	1.464	0.1334	0.06	0.00	0.12	36.12
600B	1.5	0.1335	0.06	0.00	0.12	36.98

APPENDIX II
Experiment 10B by J. Sullivan/E. Keene 2/15/96
7-day equilibration of >CMC (micelle) 1.8 mmol/L solution
Results for HDTMA sorption , bromide sorption, and cation desorption

Total Cations Desorbed--Na + Ca + Mg--Atomic Absorption Spectrophotometry Analyses

Sample No.	Solution Total meq	Total Equil Soln meq/L	Total Equil Sorbed meq/kg	Total Sorbed Normalized to ECEC unitless
25A	0.08	2.05	25.57	0.28
25B	0.08	2.03	25.42	0.28
50A	0.07	1.80	44.96	0.50
50B	0.07	1.82	45.49	0.51
75A	0.08	1.90	71.13	0.79
75B	0.07	1.78	66.57	0.74
100A	0.06	1.56	77.83	0.86
100B	0.06	1.55	77.31	0.86
150A	0.05	1.19	88.94	0.99
150B	0.05	1.24	93.29	1.04
200A	0.03	0.78	78.28	0.87
200B	0.04	0.91	90.84	1.01
250A	0.03	0.65	81.24	0.90
250B	0.03	0.63	79.34	0.88
300A	0.02	0.53	79.35	0.88
300B	0.02	0.54	80.73	0.90
400A	0.02	0.43	86.14	0.96
400B	0.02	0.43	86.46	0.96
500A	0.01	0.35	88.02	0.98
500B	0.02	0.43	108.34	1.20
600A	0.01	0.30	90.71	1.01
600B	0.01	0.31	93.17	1.04

Appendix II

Experiment 10 C by J. Sullivan/Emily Keene 2/15/96

7 day equilibration of <CMC (monomer) 0.45 mmol/L solution

HDTMA sorption results, 14C-HDTMA used, scintillation counting results

Sample Number	cpm/ml	cpm/ml minus backg.	cpm/ml Converted to mmol/ml	mmol in solution	mmol sorbed	grams of Clinop.	Equil Soln Conc mmol/l	Equil Sorbed Conc mmol/kg
25A	135.5	91	3.9E-06	1.5E-04	1.8E-02	0.8003	3.9E-03	22.3
25B	172.6	128.1	5.4E-06	2.2E-04	1.8E-02	0.8001	5.4E-03	22.2
50A	387.7	343.2	1.5E-05	5.8E-04	1.7E-02	0.4004	1.5E-02	43.5
50B	293	248.5	1.1E-05	4.2E-04	1.8E-02	0.4009	1.1E-02	43.8
75A	869.3	824.8	3.5E-05	1.4E-03	1.7E-02	0.2671	3.5E-02	62.1
75B	914	869.5	3.7E-05	1.5E-03	1.7E-02	0.2673	3.7E-02	61.8
100A	2194.6	2150.1	9.1E-05	3.7E-03	1.4E-02	0.2	9.1E-02	71.7
100B	1810.2	1765.7	7.5E-05	3.0E-03	1.5E-02	0.2002	7.5E-02	74.9
150A	3439.4	3394.9	1.4E-04	5.8E-03	1.2E-02	0.1335	1.4E-01	91.6
150B	3380.8	3336.3	1.4E-04	5.7E-03	1.2E-02	0.1331	1.4E-01	92.6
200A	4965.1	4920.6	2.1E-04	8.4E-03	9.6E-03	0.1007	2.1E-01	95.7
200B	4776.3	4731.8	2.0E-04	8.0E-03	1.0E-02	0.1006	2.0E-01	99.0
300A	5988	5943.5	2.5E-04	1.0E-02	7.9E-03	0.0678	2.5E-01	116.5
300B	5726.5	5682	2.4E-04	9.7E-03	8.3E-03	0.0677	2.4E-01	123.2
400A	6835.6	6791.1	2.9E-04	1.2E-02	6.5E-03	0.0502	2.9E-01	128.7
400B	6957.3	6912.8	2.9E-04	1.2E-02	6.3E-03	0.0501	2.9E-01	124.8
500A	7427.7	7383.2	3.1E-04	1.3E-02	5.5E-03	0.0407	3.1E-01	134.0
500B	7204.5	7160	3.0E-04	1.2E-02	5.8E-03	0.0406	3.0E-01	143.6
600A	7948.7	7904.2	3.4E-04	1.3E-02	4.6E-03	0.0339	3.4E-01	134.7
600B	7311.3	7266.8	3.1E-04	1.2E-02	5.7E-03	0.0336	3.1E-01	168.2

APPENDIX II
Experiment 10C by J. Sullivan/E. Keene 2/15/96
7-day equilibration of <CMC (monomer) 0.45 mmol/L solution
Results for HDTMA sorption, bromide sorption, and cation desorption

Bromide Sorbed--HPLC Results

Sample	Conc. Br mg/L	dilution factor	Actual Conc. mg/L	Amount mmol/L	Amount mmol	Amt. Sorbed mmol	grams of Clinop.	Equil soln Conc mmolL	Equil Sorbed mmol/kg
Known mmol/L				0.45	0.018				
ean of solns A&B						1.83E-02			
Original Soln A	9.12	4	36.46	0.46	1.83E-02	8.31E-06	0	0.46	not applic.
Original Soln B	9.12	4	36.50	0.46	1.83E-02	-8.31E-06	0	0.46	not applic.
25A	9.53	4	38.12	0.48	1.91E-02	-8.19E-04	0.8003	0.48	-1.02
25B	9.76	4	39.03	0.49	1.95E-02	-1.27E-03	0.8001	0.49	-1.59
50A	9.57	4	38.26	0.48	1.92E-02	-8.92E-04	0.4004	0.48	-2.23
50B	9.13	4	36.53	0.46	1.83E-02	-2.47E-05	0.4009	0.46	-0.06
75A	9.35	4	37.40	0.47	1.87E-02	-4.62E-04	0.2671	0.47	-1.73
75B	9.21	4	36.85	0.46	1.84E-02	-1.86E-04	0.2673	0.46	-0.70
100A	8.89	4	35.56	0.44	1.78E-02	4.62E-04	0.2	0.44	2.31
100B	8.05	4	32.21	0.40	1.61E-02	2.14E-03	0.2002	0.40	10.68
150A	8.83	4	35.30	0.44	1.77E-02	5.90E-04	0.1335	0.44	4.42
150B	8.87	4	35.48	0.44	1.78E-02	5.00E-04	0.1331	0.44	3.76
200A	8.56	4	34.22	0.43	1.71E-02	1.13E-03	0.1007	0.43	11.22
200B	8.62	4	34.49	0.43	1.73E-02	9.97E-04	0.1006	0.43	9.91
300A	8.46	4	33.82	0.42	1.69E-02	1.33E-03	0.0678	0.42	19.62
300B	8.77	4	35.09	0.44	1.76E-02	6.96E-04	0.0677	0.44	10.29
400A	8.38	4	33.54	0.42	1.68E-02	1.47E-03	0.0502	0.42	29.35
400B	8.46	4	33.85	0.42	1.69E-02	1.32E-03	0.0501	0.42	26.30
500A	8.62	4	34.50	0.43	1.73E-02	9.91E-04	0.0407	0.43	24.35
500B	8.43	4	33.70	0.42	1.69E-02	1.39E-03	0.0406	0.42	34.24
600A	8.34	4	33.38	0.42	1.67E-02	1.55E-03	0.0339	0.42	45.79
600B	8.48	4	33.93	0.42	1.70E-02	1.28E-03	0.0336	0.42	37.96

APPENDIX II

Experiment 10C by J. Sullivan/E. Keene 2/15/96

7-day equilibration of <CMC (monomer) 0.45 mmol/L solution

Results for HDTMA sorption, bromide sorption, and cation desorption

Bromide Sorbed--Anion Exclusion Adjustment Calculations

Anion Exclusion was noted when the final solution concentrations were found to be higher than the original solution concentration of HDTMA-Br

A formula from Israelachvili, 1991, was used to adjust the final solution concentrations based upon the surface area and excluded volume of the clinoptilolite in each sample.

Conc.	0.00045 M						
sqrt of conc.	0.021213203						
Debye length	14.33069743 nm						
	1.43307E-05 cm						
Sample No.	Excluded Debye Volume cm^3 (ml)	adjusted volume ml	"normalized" mg**	amount in soln mmol	Amount sorbed mmol	Actual Equil Soln Conc mmol/l	Actual Equil Sorbed Conc mmol/kg
25A	1.8	38.2	1.4	1.7E-02	8.3E-04	4.6E-01	1.0
25B	1.8	38.2	1.4	1.7E-02	8.1E-04	4.6E-01	1.0
50A	0.9	39.1	1.5	1.9E-02	-3.9E-04	4.8E-01	-1.0
50B	0.9	39.1	1.5	1.9E-02	-8.3E-04	4.9E-01	-2.1
75A	0.6	39.4	1.5	1.9E-02	-6.0E-04	4.8E-01	-2.3
75B	0.6	39.4	1.4	1.8E-02	2.5E-04	4.6E-01	0.9
100A	0.4	39.6	1.5	1.9E-02	-2.5E-04	4.7E-01	-1.3
100B	0.5	39.5	1.5	1.8E-02	2.1E-05	4.6E-01	0.1
150A	0.3	39.7	1.4	1.8E-02	6.0E-04	4.4E-01	4.5
150B	0.3	39.7	1.3	1.6E-02	2.3E-03	4.0E-01	17.0
200A	0.2	39.8	1.4	1.8E-02	6.9E-04	4.4E-01	6.9
200B	0.2	39.8	1.4	1.8E-02	6.0E-04	4.4E-01	6.0
300A	0.2	39.8	1.4	1.7E-02	1.2E-03	4.3E-01	17.6
300B	0.2	39.8	1.4	1.7E-02	1.1E-03	4.3E-01	15.7
400A	0.1	39.9	1.3	1.7E-02	1.4E-03	4.2E-01	27.4
400B	0.1	39.9	1.4	1.8E-02	7.5E-04	4.4E-01	14.9
500A	0.1	39.9	1.3	1.7E-02	1.5E-03	4.2E-01	37.1
500B	0.1	39.9	1.4	1.7E-02	1.4E-03	4.2E-01	33.4
600A	0.1	39.9	1.4	1.7E-02	1.0E-03	4.3E-01	30.2
600B	0.1	39.9	1.3	1.7E-02	1.4E-03	4.2E-01	42.3

APPENDIX II
Experiment 10C by J. Sullivan/E. Keene 2/15/96
7-day equilibration of <CMC (monomer) 0.45 mmol/L solution
Results for HDTMA sorption, bromide sorption, and cation desorption

Sodium Cations Desorbed--Atomic Absorption Spectrophotometry Analyses

Sample No.	Na Analysis Conc mg/L	Grams Sample g	Amount in Sample mg	Amount in Sample meq	Equil.Soln Conc. meq/L	Desorbed Conc. meq/kg
25A	4.443	0.8003	0.18	0.01	0.19	9.66
25B	4.659	0.8001	0.19	0.01	0.20	10.13
50A	3.275	0.4004	0.13	0.01	0.14	14.23
50B	3.457	0.4009	0.14	0.01	0.15	15.00
75A	2.325	0.2671	0.09	0.00	0.10	15.15
75B	2.295	0.2673	0.09	0.00	0.10	14.94
100A	1.705	0.2	0.07	0.00	0.07	14.83
100B	1.758	0.2002	0.07	0.00	0.08	15.28
150A	1.217	0.1335	0.05	0.00	0.05	15.86
150B	1.31	0.1331	0.05	0.00	0.06	17.12
200A	0.965	0.1007	0.04	0.00	0.04	16.67
200B	0.996	0.1006	0.04	0.00	0.04	17.23
300A	0.627	0.0678	0.03	0.00	0.03	16.09
300B	0.798	0.0677	0.03	0.00	0.03	20.51
400A	0.417	0.0502	0.02	0.00	0.02	14.45
400B	0.41	0.0501	0.02	0.00	0.02	14.24
500A	0.39	0.0407	0.02	0.00	0.02	16.67
500B	0.398	0.0406	0.02	0.00	0.02	17.06
600A	0.34	0.0339	0.01	0.00	0.01	17.45
600B	0.38	0.0336	0.02	0.00	0.02	19.68

APPENDIX II
Experiment 10C by J. Sullivan/E. Keene 2/15/96
7-day equilibration of <CMC (monomer) 0.45 mmol/L solution
Results for HDTMA sorption, bromide sorption, and cation desorption

Calcium Cations Desorbed--Atomic Absorption Spectrophotometry Analyses

Sample No.	Ca Analysis Conc mg/L	Grams of Sample g	Amount in Sample mg	Amount in Sample meq	Equil.Soln Conc. meq/L	Desorbed Conc. meq/kg
25A	2.89	0.8003	0.1156	5.77E-03	1.44E-01	7.21
25B	3.37	0.8001	0.1348	6.73E-03	1.68E-01	8.41
50A	2.92	0.4004	0.1168	5.83E-03	1.46E-01	14.56
50B	3.31	0.4009	0.1324	6.61E-03	1.65E-01	16.48
75A	2.32	0.2671	0.0928	4.63E-03	1.16E-01	17.34
75B	2.4	0.2673	0.096	4.79E-03	1.20E-01	17.92
100A	1.74	0.2	0.0696	3.47E-03	8.68E-02	17.37
100B	1.98	0.2002	0.0792	3.95E-03	9.88E-02	19.74
150A	1.33	0.1335	0.0532	2.65E-03	6.64E-02	19.89
150B	1.37	0.1331	0.0548	2.73E-03	6.84E-02	20.54
200A	1.04	0.1007	0.0416	2.08E-03	5.19E-02	20.61
200B	1.05	0.1006	0.042	2.10E-03	5.24E-02	20.83
300A	0.79	0.0678	0.0316	1.58E-03	3.94E-02	23.26
300B	HIGH	0.0677	no data	no data	no data	no data
400A	0.56	0.0502	0.0224	1.12E-03	2.79E-02	22.27
400B	0.55	0.0501	0.022	1.10E-03	2.74E-02	21.91
500A	0.58	0.0407	0.0232	1.16E-03	2.89E-02	28.44
500B	0.5	0.0406	0.02	9.98E-04	2.50E-02	24.58
600A	0.45	0.0339	0.018	8.98E-04	2.25E-02	26.50
600B	0.31	0.0336	0.0124	6.19E-04	1.55E-02	18.42

APPENDIX II
Experiment 10C by J. Sullivan/E. Keene 2/15/96
7-day equilibration of <CMC (monomer) 0.45 mmol/L solution
Results for HDTMA sorption , bromide sorption, and cation desorption

Magnesium Cations Desorbed--Atomic Absorption Spectrophotometry Analyses

Sample No.	Mg Analysis Conc mg/L	Grams of Sample g	Amount in Sample mg	Amount in Sample meq	Equil.Soln Conc. meq/L	Desorbed Conc. meq/kg
25A	0.92	0.8003	0.0368	3.03E-03	7.57E-02	3.78
25B	1.11	0.8001	0.0444	3.65E-03	9.13E-02	4.57
50A	0.89	0.4004	0.0356	2.93E-03	7.32E-02	7.32
50B	0.97	0.4009	0.0388	3.19E-03	7.98E-02	7.96
75A	0.72	0.2671	0.0288	2.37E-03	5.92E-02	8.87
75B	0.74	0.2673	0.0296	2.44E-03	6.09E-02	9.11
100A	0.55	0.2	0.022	1.81E-03	4.53E-02	9.05
100B	0.6	0.2002	0.024	1.97E-03	4.94E-02	9.86
150A	0.45	0.1335	0.018	1.48E-03	3.70E-02	11.09
150B	0.47	0.1331	0.0188	1.55E-03	3.87E-02	11.62
200A	0.33	0.1007	0.0132	1.09E-03	2.72E-02	10.79
200B	0.33	0.1006	0.0132	1.09E-03	2.72E-02	10.80
300A	0.24	0.0678	0.0096	7.90E-04	1.97E-02	11.65
300B	0.32	0.0677	0.0128	1.05E-03	2.63E-02	15.56
400A	0.19	0.0502	0.0076	6.25E-04	1.56E-02	12.46
400B	0.18	0.0501	0.0072	5.92E-04	1.48E-02	11.83
500A	0.16	0.0407	0.0064	5.27E-04	1.32E-02	12.94
500B	0.17	0.0406	0.0068	5.60E-04	1.40E-02	13.78
600A	0.13	0.0339	0.0052	4.28E-04	1.07E-02	12.62
600B	0.13	0.0336	0.0052	4.28E-04	1.07E-02	12.73

APPENDIX II
Experiment 10C by J. Sullivan/E. Keene 2/15/96
7-day equilibration of <CMC (monomer) 0.45 mmol/L solution
Results for HDTMA sorption , bromide sorption, and cation desorption

Total Cations Desorbed--Na + Ca + Mg--Atomic Absorption Spectrophotometry Analyses

Sample No.	Solution Total meq	Total Equil Soln meq/L	Total Equil Desorbed meq/kg	Total Desorbed Normalized to ECEC unitless
25A	0.0165	0.4132	20.65	0.23
25B	0.0185	0.4622	23.11	0.26
50A	0.0145	0.3614	36.10	0.40
50B	0.0158	0.3954	39.45	0.44
75A	0.0110	0.2761	41.35	0.46
75B	0.0112	0.2805	41.97	0.47
100A	0.0082	0.2062	41.25	0.46
100B	0.0090	0.2246	44.88	0.50
150A	0.0063	0.1563	46.84	0.52
150B	0.0066	0.1640	49.29	0.55
200A	0.0048	0.1210	48.07	0.53
200B	0.0049	0.1229	48.86	0.54
300A	0.0035	0.0864	51.00	0.57
300B	no data	no data	no data	no data
400A	0.0025	0.0617	49.18	0.55
400B	0.0024	0.0601	47.98	0.53
500A	0.0024	0.0591	58.06	0.65
500B	0.0023	0.0563	55.42	0.62
600A	0.0019	0.0479	56.57	0.63
600B	0.0017	0.0427	50.83	0.56

APPENDIX II

Experiment 12 by J. Sullivan/E. Keene 2/15/96

24 hour equilibration of TEA (1.8 mmol/L) solution

Results for TEA sorption, bromide sorption, and cation desorption

TEA Sorption Results, 14C-TEA used, scintillation counting results

Sample Number	Percent ECEC Treatment	cpm/ml	cpm/ml minus backg.	cpm/ml Converted to mmol/ml	mmol in solution	mmol sorbed	grams of Clinop.	Equil Soln Conc mmol/l	Equil Sorbed Conc mmol/kg
2A	100	6964.7	6922.1	1.2E-03	4.7E-02	2.5E-02	0.8003	1.17	31.19
2B	100	6838.7	6796.1	1.1E-03	4.6E-02	2.6E-02	0.8001	1.14	32.26
2C	100	6907.1	6864.5	1.2E-03	4.6E-02	2.5E-02	0.8004	1.16	31.67
3A	200	8551.2	8508.6	1.4E-03	5.7E-02	1.4E-02	0.4007	1.43	35.62
3B	200	8648.9	8606.3	1.4E-03	5.8E-02	1.4E-02	0.4007	1.45	33.97
3C	200	8563.9	8521.3	1.4E-03	5.7E-02	1.4E-02	0.401	1.44	35.38
4A	300	9188.3	9145.7	1.5E-03	6.2E-02	1.0E-02	0.2678	1.54	37.26
4B	300	9255.5	9212.9	1.6E-03	6.2E-02	9.5E-03	0.2677	1.55	35.59
4C	300	9261.5	9218.9	1.6E-03	6.2E-02	9.5E-03	0.2677	1.55	35.43
5A	400	9451.7	9409.1	1.6E-03	6.3E-02	8.2E-03	0.2007	1.58	40.88
5B	400	9472.9	9430.3	1.6E-03	6.4E-02	8.1E-03	0.2006	1.59	40.19
5C	400	9493.8	9451.2	1.6E-03	6.4E-02	7.9E-03	0.2004	1.59	39.52
6A	600	9882.6	9840	1.7E-03	6.6E-02	5.3E-03	0.1337	1.66	39.65
6B	600	9931.8	9889.2	1.7E-03	6.7E-02	5.0E-03	0.1331	1.67	37.34
6C	600	9926.7	9884.1	1.7E-03	6.7E-02	5.0E-03	0.1335	1.66	37.48
7A	800	9685.4	9642.8	1.6E-03	6.5E-02	6.6E-03	0.1009		
7B	800	10059.8	10017.2	1.7E-03	6.7E-02	4.1E-03	0.1008	1.69	40.74
7C	800	10092.2	10049.6	1.7E-03	6.8E-02	3.9E-03	0.1008	1.69	38.58
8A	1200	10261.9	10219.3	1.7E-03	6.9E-02	2.7E-03	0.0674	1.72	40.73
8B	1200	10334.1	10291.5	1.7E-03	6.9E-02	2.3E-03	0.067	1.73	33.71
8C	1200	10336.8	10294.2	1.7E-03	6.9E-02	2.2E-03	0.0678	1.73	33.05
9A	1600	10398.8	10356.2	1.7E-03	7.0E-02	1.8E-03	0.0507	1.74	35.95
9B	1600	10458.2	10415.6	1.8E-03	7.0E-02	1.4E-03	0.05	1.75	28.45
9C	1600	6131.9	6089.3	1.0E-03	4.1E-02	3.1E-02	0.0503	1.03	607.79

APPENDIX II

Experiment 12 by J. Sullivan/E. Keene 2/15/96

24 hour equilibration of TEA (1.8 mmol/L) solution

Results for TEA sorption, bromide sorption, and cation desorption

TEA Sorption Results, 14C-TEA used, scintillation counting results

Sample Number	Percent ECEC Treatment	cpm/ml	cpm/ml minus backg.	cpm/ml Converted to mmol/ml	mmol in solution	mmol sorbed	grams of Clinop.	Equil Soln Conc mmol/l	Equil Sorbed Conc mmol/kg
11A1	25	2626.7	2587.5	4.3E-04	1.7E-02	5.4E-02	3.2003	0.43	17.01
11B1	25	2704.3	2665.1	4.4E-04	1.8E-02	5.4E-02	3.2008	0.44	16.85
11C1	25	2613.2	2574	4.3E-04	1.7E-02	5.5E-02	3.2011	0.43	17.04
12A1	50	4738.6	4699.4	7.8E-04	3.1E-02	4.0E-02	1.5999	0.78	25.27
12B1	50	4737.3	4698.1	7.8E-04	3.1E-02	4.0E-02	1.6	0.78	25.28
12C1	50	4776	4736.8	7.9E-04	3.1E-02	4.0E-02	1.6001	0.79	25.12
13A1	75	6180	6140.8	1.0E-03	4.1E-02	3.1E-02	1.0707	1.02	28.84
13B1	75	6082	6042.8	1.0E-03	4.0E-02	3.2E-02	1.0708	1.00	29.44
13C1	75	6125.8	6086.6	1.0E-03	4.0E-02	3.1E-02	1.0705	1.01	29.18

APPENDIX II

Experiment 12 by J. Sullivan/E. Keene 2/15/96

24 hour equilibration of TEA (1.8 mmol/L) solution

Results for TEA sorption, bromide sorption, and cation desorption

Bromide Sorbed--HPLC Results

Sample	Conc. Br mg/L	Amount mmol/L	Amount mmol	Amt. Sorbed mmol **	grams of Clinop.	Equil Soln Conc mmol/l	Equil Sorbed Conc mmol/kg
a1	45.72	0.57	0.02288711	0	0	0.57	0
b1	45.57	0.57	0.02281269	0	0	0.57	0
2a1	45.21	0.57	2.26E-02	2.20E-04	0.8003	0.57	0.28
2b1	45.40	0.57	2.27E-02	1.26E-04	0.8001	0.57	0.16
2c1	45.03	0.56	2.25E-02	3.07E-04	0.8004	0.56	0.38
3a1	45.67	0.57	2.29E-02	-9.55E-06	0.4007	0.57	-0.02
3b1	45.04	0.56	2.25E-02	3.06E-04	0.4007	0.56	0.76
3c1	45.43	0.57	2.27E-02	1.08E-04	0.401	0.57	0.27
4a1	43.03	0.54	2.15E-02	1.31E-03	0.2678	0.54	4.89
4b1	44.50	0.56	2.23E-02	5.77E-04	0.2677	0.56	2.15
4c1	45.05	0.56	2.26E-02	2.98E-04	0.2677	0.56	1.11
5a1	46.12	0.58	2.31E-02	-2.37E-04	0.2007	0.58	-1.18
5b1	45.89	0.57	2.30E-02	-1.19E-04	0.2006	0.57	-0.59
5c1	45.32	0.57	2.27E-02	1.65E-04	0.2004	0.57	0.82
6a1	45.69	0.57	2.29E-02	-2.27E-05	0.1337	0.57	-0.17
6b1	46.00	0.58	2.30E-02	-1.76E-04	0.1331	0.58	-1.33
6c1	45.75	0.57	2.29E-02	-5.33E-05	0.1335	0.57	-0.40
7a1	46.41	0.58	2.32E-02	-3.83E-04	0.1009	0.58	-3.80
7b1	44.53	0.56	2.23E-02	5.59E-04	0.1008	0.56	5.55
7c1	46.43	0.58	2.32E-02	-3.93E-04	0.1008	0.58	-3.90

**Amount sorbed not adjusted for anion exclusion, because essentially none was sorbed.

APPENDIX II

Experiment 12 by J. Sullivan/E. Keene 2/15/96

24 hour equilibration of TEA (1.8 mmol/L) solution

Results for TEA sorption, bromide sorption, and cation desorption

Bromide Sorbed--HPLC Results

Sample	Conc. Br mg/L	Amount mmol/L	Amount mmol	Amt. Sorbed mmol **	grams of Clinop.	Equil Soln Conc mmol/l	Equil Sorbed Conc mmol/kg
8a1	46.52	0.58	2.33E-02	-4.37E-04	0.0674	0.58	-6.49
8b1	45.65	0.57	2.28E-02	9.57E-07	0.067	0.57	0.01
8c1	46.27	0.58	2.32E-02	-3.13E-04	0.0678	0.58	-4.61
9a1	46.76	0.59	2.34E-02	-5.56E-04	0.0507	0.59	-10.96
9b1	46.70	0.58	2.34E-02	-5.26E-04	0.05	0.58	-10.51
9c1	48.51	0.61	2.43E-02	-1.43E-03	0.0503	0.61	-28.49
10a1	46.01	0.58	2.30E-02	-1.80E-04	no data	0.58	no data
11a1	42.31	0.53	2.12E-02	1.67E-03	3.2003	0.53	0.52
11b1	42.40	0.53	2.12E-02	1.63E-03	3.2008	0.53	0.51
11c1	43.00	0.54	2.15E-02	1.32E-03	3.2011	0.54	0.41
12a1	42.66	0.53	2.14E-02	1.50E-03	1.5999	0.53	0.94
12b1	46.14	0.58	2.31E-02	-2.49E-04	1.6	0.58	-0.16
12c1	41.83	0.52	2.09E-02	1.91E-03	1.6001	0.52	1.19
13a1	47.13	0.59	2.36E-02	-7.44E-04	1.0707	0.59	-0.69
13b1	46.59	0.58	2.33E-02	-4.73E-04	1.0708	0.58	-0.44
13c1	46.28	0.58	2.32E-02	-3.18E-04	1.0705	0.58	-0.30

**Amount sorbed not adjusted for anion exclusion, because essentially none was sorbed.

APPENDIX II
Experiment 12 by J. Sullivan/E. Keene 2/15/96
24 hour equilibration of TEA (1.8 mmol/L) solution
Results for TEA sorption, bromide sorption, and cation desorption

Sodium Cations Desorbed--Atomic Absorption Spectrophotometry Analyses

Sample No.	Na Analysis Conc mg/L	Grams Sample g	Amount in Sample mg	Amount in Sample meq	Equil.Soln Conc. meq/L	Desorbed Conc. meq/kg
2A	4.9	0.8003	2.0E-01	8.6E-03	0.2	10.7
2B	4.9	0.8001	2.0E-01	8.6E-03	0.2	10.7
2C	4.8	0.8004	1.9E-01	8.4E-03	0.2	10.5
3A	2.7	0.4007	1.1E-01	4.7E-03	0.1	11.8
3B	2.6	0.4007	1.0E-01	4.5E-03	0.1	11.4
3C	2.6	0.401	1.0E-01	4.5E-03	0.1	11.3
4A	1.8	0.2678	7.3E-02	3.2E-03	0.1	11.8
4B	1.8	0.2677	7.3E-02	3.2E-03	0.1	11.8
4C	1.9	0.2677	7.7E-02	3.3E-03	0.1	12.4
5A	1.4	0.2007	5.7E-02	2.5E-03	0.1	12.3
5B	1.3	0.2006	5.3E-02	2.3E-03	0.1	11.4
5C	1.3	0.2004	5.3E-02	2.3E-03	0.1	11.4
6A	0.8	0.1337	3.3E-02	1.4E-03	0.0	10.6
6B	0.8	0.1331	3.3E-02	1.4E-03	0.0	10.7
6C	0.8	0.1335	3.3E-02	1.4E-03	0.0	10.6
7A	0.6	0.1009	2.5E-02	1.1E-03	0.0	10.6
7B	0.5	0.1008	2.1E-02	9.0E-04	0.0	8.9
7C	0.6	0.1008	2.5E-02	1.1E-03	0.0	10.6
8A	0.2	0.0674	8.6E-03	3.7E-04	0.0	5.6
8B	0.2	0.067	8.6E-03	3.7E-04	0.0	5.6
8C	0.2	0.0678	8.6E-03	3.7E-04	0.0	5.5

APPENDIX II
Experiment 12 by J. Sullivan/E. Keene 2/15/96
24 hour equilibration of TEA (1.8 mmol/L) solution
Results for TEA sorption, bromide sorption, and cation desorption

Sodium Cations Desorbed--Atomic Absorption Spectrophotometry Analyses

Sample No.	Na Analysis Conc mg/L	Grams Sample g	Amount in Sample mg	Amount in Sample meq	Equil.Soln Conc. meq/L	Desorbed Conc. meq/kg
9A	0.2	0.0507	8.6E-03	3.7E-04	0.0	7.4
9B	0.1	0.05	4.6E-03	2.0E-04	0.0	4.0
9C	0.2	0.0503	8.6E-03	3.7E-04	0.0	7.4
10A	-0.2	0	-6.2E-03	-2.7E-04	0.0	0.0
11A	12.1	3.2003	4.8E-01	2.1E-02	0.5	6.6
11B	12.2	3.2008	4.9E-01	2.1E-02	0.5	6.6
11C	12.2	3.2011	4.9E-01	2.1E-02	0.5	6.6
12A	8.0	1.5999	3.2E-01	1.4E-02	0.3	8.7
12B	7.8	1.6	3.1E-01	1.4E-02	0.3	8.5
12C	7.7	1.6001	3.1E-01	1.3E-02	0.3	8.4
13A	5.6	1.0707	2.2E-01	9.8E-03	0.2	9.1
13B	5.8	1.0708	2.3E-01	1.0E-02	0.3	9.4
13C	5.5	1.0705	2.2E-01	9.6E-03	0.2	9.0

APPENDIX II

Experiment 12 by J. Sullivan/E. Keene 2/15/96

24 hour equilibration of TEA (1.8 mmol/L) solution

Results for TEA sorption, bromide sorption, and cation desorption

Calcium Cations Desorbed--Atomic Absorption Spectrophotometry Analyses

Sample No.	Ca Analysis Conc mg/L	Grams Sample g	Amount in Sample mg	Amount in Sample meq	Equil.Soln Conc. meq/L	Desorbed Conc. meq/kg
2A	6.415	0.8003	2.57E-01	1.28E-02	3.20E-01	16.00
2B	6.635	0.8001	2.65E-01	1.32E-02	3.31E-01	16.55
2C	6.505	0.8004	2.60E-01	1.30E-02	3.25E-01	16.22
3A	3.825	0.4007	1.53E-01	7.63E-03	1.91E-01	19.05
3B	3.825	0.4007	1.53E-01	7.63E-03	1.91E-01	19.05
3C	3.825	0.401	1.53E-01	7.63E-03	1.91E-01	19.04
4A	2.715	0.2678	1.09E-01	5.42E-03	1.35E-01	20.24
4B	2.715	0.2677	1.09E-01	5.42E-03	1.35E-01	20.24
4C	2.665	0.2677	1.07E-01	5.32E-03	1.33E-01	19.87
5A	1.885	0.2007	7.54E-02	3.76E-03	9.41E-02	18.75
5B	2.055	0.2006	8.22E-02	4.10E-03	1.03E-01	20.45
5C	2.035	0.2004	8.14E-02	4.06E-03	1.02E-01	20.27
6A	1.455	0.1337	5.82E-02	2.90E-03	7.26E-02	21.72
6B	1.425	0.1331	5.70E-02	2.84E-03	7.11E-02	21.37
6C	1.465	0.1335	5.86E-02	2.92E-03	7.31E-02	21.90
7A	1.165	0.1009	4.66E-02	2.33E-03	5.81E-02	23.05
7B	1.145	0.1008	4.58E-02	2.29E-03	5.71E-02	22.67
7C	1.195	0.1008	4.78E-02	2.39E-03	5.96E-02	23.66
8A	0.825	0.0674	3.30E-02	1.65E-03	4.12E-02	24.43
8B	0.725	0.067	2.90E-02	1.45E-03	3.62E-02	21.60
8C	0.795	0.0678	3.18E-02	1.59E-03	3.97E-02	23.40

APPENDIX II

Experiment 12 by J. Sullivan/E. Keene 2/15/96

24 hour equilibration of TEA (1.8 mmol/L) solution

Results for TEA sorption, bromide sorption, and cation desorption

Calcium Cations Desorbed--Atomic Absorption Spectrophotometry Analyses

Sample No.	Ca Analysis Conc mg/L	Grams Sample g	Amount in Sample mg	Amount in Sample meq	Equil.Soln Conc. meq/L	Desorbed Conc. meq/kg
9A	0.555	0.0507	2.22E-02	1.11E-03	2.77E-02	21.85
9B	0.655	0.05	2.62E-02	1.31E-03	3.27E-02	26.15
9C	0.765	0.0503	3.06E-02	1.53E-03	3.82E-02	30.36
10A	0	0	0.00E+00	0.00E+00	0.00E+00	0.00
11A	15.305	3.2003	6.12E-01	3.05E-02	7.64E-01	9.55
11B	15.745	3.2008	6.30E-01	3.14E-02	7.86E-01	9.82
11C	15.715	3.2011	6.29E-01	3.14E-02	7.84E-01	9.80
12A	11.255	1.5999	4.50E-01	2.25E-02	5.62E-01	14.04
12B	11.065	1.6	4.43E-01	2.21E-02	5.52E-01	13.80
12C	11.085	1.6001	4.43E-01	2.21E-02	5.53E-01	13.83
13A	7.935	1.0707	3.17E-01	1.58E-02	3.96E-01	14.79
13B	7.895	1.0708	3.16E-01	1.58E-02	3.94E-01	14.72
13C	7.985	1.0705	3.19E-01	1.59E-02	3.98E-01	14.89

Appendix II

Experiment 12 by J. Sullivan/Emily Keene 2/15/96

24 hour equilibration of TEA (1.8 mmol/L) solution

Results for TEA sorption, bromide sorption, and cation desorption

Magnesium Cations Desorbed--Atomic Absorption Spectrophotometry Analyses

Sample No.	Mg Analysis Conc mg/L	Grams Sample g	Amount in Sample mg	Amount in Sample meq	Equil.Soln Conc. meq/L	Desorbed Conc. meq/kg
2A	1.335	0.8003	5.34E-02	4.39E-03	1.10E-01	5.49
2B	1.345	0.8001	5.38E-02	4.43E-03	1.11E-01	5.53
2C	1.325	0.8004	5.30E-02	4.36E-03	1.09E-01	5.45
3A	0.765	0.4007	3.06E-02	2.52E-03	6.30E-02	6.28
3B	0.765	0.4007	3.06E-02	2.52E-03	6.30E-02	6.28
3C	0.765	0.401	3.06E-02	2.52E-03	6.30E-02	6.28
4A	0.535	0.2678	2.14E-02	1.76E-03	4.40E-02	6.58
4B	0.545	0.2677	2.18E-02	1.79E-03	4.48E-02	6.70
4C	0.545	0.2677	2.18E-02	1.79E-03	4.48E-02	6.70
5A	0.425	0.2007	1.70E-02	1.40E-03	3.50E-02	6.97
5B	0.425	0.2006	1.70E-02	1.40E-03	3.50E-02	6.97
5C	0.415	0.2004	1.66E-02	1.37E-03	3.41E-02	6.82
6A	0.305	0.1337	1.22E-02	1.00E-03	2.51E-02	7.51
6B	0.285	0.1331	1.14E-02	9.38E-04	2.35E-02	7.05
6C	0.295	0.1335	1.18E-02	9.71E-04	2.43E-02	7.27
7A	0.235	0.1009	9.40E-03	7.74E-04	1.93E-02	7.67
7B	0.225	0.1008	9.00E-03	7.41E-04	1.85E-02	7.35
7C	0.245	0.1008	9.80E-03	8.06E-04	2.02E-02	8.00
8A	0.165	0.0674	6.60E-03	5.43E-04	1.36E-02	8.06
8B	0.145	0.067	5.80E-03	4.77E-04	1.19E-02	7.12
8C	0.155	0.0678	6.20E-03	5.10E-04	1.28E-02	7.52

Appendix II

Experiment 12 by J. Sullivan/Emily Keene 2/15/96

24 hour equilibration of TEA (1.8 mmol/L) solution

Results for TEA sorption, bromide sorption, and cation desorption

Magnesium Cations Desorbed--Atomic Absorption Spectrophotometry Analyses

Sample No.	Mg Analysis Conc mg/L	Grams Sample g	Amount in Sample mg	Amount in Sample meq	Equil.Soln Conc. meq/L	Desorbed Conc. meq/kg
9A	0.165	0.0507	6.60E-03	5.43E-04	1.36E-02	10.71
9B	0.105	0.05	4.20E-03	3.46E-04	8.64E-03	6.91
9C	0.135	0.0503	5.40E-03	4.44E-04	1.11E-02	8.83
10A	0	0	0.00E+00	0.00E+00	0.00E+00	0.00
11A	3.185	3.2003	1.27E-01	1.05E-02	2.62E-01	3.28
11B	3.165	3.2008	1.27E-01	1.04E-02	2.60E-01	3.25
11C	3.185	3.2011	1.27E-01	1.05E-02	2.62E-01	3.27
12A	2.275	1.5999	9.10E-02	7.49E-03	1.87E-01	4.68
12B	2.225	1.6	8.90E-02	7.32E-03	1.83E-01	4.58
12C	2.235	1.6001	8.94E-02	7.36E-03	1.84E-01	4.60
13A	1.655	1.0707	6.62E-02	5.45E-03	1.36E-01	5.09
13B	1.605	1.0708	6.42E-02	5.28E-03	1.32E-01	4.93
13C	1.655	1.0705	6.62E-02	5.45E-03	1.36E-01	5.09

Appendix II

Experiment 12 by J. Sullivan/Emily Keene 2/15/96

24 hour equilibration of TEA (1.8 mmol/L) solution

Results for TEA sorption, bromide sorption, and cation desorption

Total Cations Desorbed--Na + Ca + Mg--Atomic Absorption Spectrophotometry Analyses

Sample No.	Solution Total meq	Total Equil Soln meq/L	Total Equil desorbe meq/kg	Total Sorbed Normalized to ECEC unitless
2A	2.58E-02	0.64	32.18	0.36
2B	2.62E-02	0.66	32.77	0.36
2C	2.57E-02	0.64	32.14	0.36
3A	1.49E-02	0.37	37.13	0.41
3B	1.47E-02	0.37	36.69	0.41
3C	1.47E-02	0.37	36.66	0.41
4A	1.03E-02	0.26	38.60	0.43
4B	1.04E-02	0.26	38.74	0.43
4C	1.04E-02	0.26	39.02	0.43
5A	7.62E-03	0.19	37.98	0.42
5B	7.79E-03	0.19	38.83	0.43
5C	7.72E-03	0.19	38.50	0.43
6A	5.33E-03	0.13	39.84	0.44
6B	5.20E-03	0.13	39.07	0.43
6C	5.31E-03	0.13	39.80	0.44
7A	4.17E-03	0.10	41.32	0.46
7B	3.92E-03	0.10	38.91	0.43
7C	4.26E-03	0.11	42.28	0.47
8A	2.56E-03	0.06	38.04	0.42
8B	2.30E-03	0.06	34.31	0.38

Appendix II

Experiment 12 by J. Sullivan/Emily Keene 2/15/96

24 hour equilibration of TEA (1.8 mmol/L) solution

Results for TEA sorption, bromide sorption, and cation desorption

Total Cations Desorbed--Na + Ca + Mg--Atomic Absorption Spectrophotometry Analyses

Sample No.	Solution Total meq	Total Equil Soln meq/L	Total Equil desorbe meq/kg	Total Sorbed Normalized to ECEC unitless
8C	2.47E-03	0.06	36.45	0.40
9A	2.02E-03	0.05	39.94	0.44
9B	1.85E-03	0.05	37.06	0.41
9C	2.35E-03	0.06	46.63	0.52
10A	-2.70E-04	-0.01	0.00	0.00
11A	6.21E-02	1.55	19.41	0.22
11B	6.31E-02	1.58	19.71	0.22
11C	6.31E-02	1.58	19.71	0.22
12A	4.39E-02	1.10	27.44	0.30
12B	4.30E-02	1.08	26.88	0.30
12C	4.29E-02	1.07	26.81	0.30
13A	3.11E-02	0.78	29.00	0.32
13B	3.12E-02	0.78	29.10	0.32
13C	3.10E-02	0.77	28.94	0.32

APPENDIX III

This appendix gives the adsorption data for HDTMA, bromide, and chromate which is plotted in Chapter 4, Fig. 1. This experiment was performed in three stages. First, the HDTMA-bromide and zeolite were equilibrated, for HDTMA below the CMC (0.45 mmol/L) and above the CMC (1.8 mmol/L). Then, HDTMA and bromide sorbed were measured. Finally, chromate was added to the same reaction vessels and equilibrated with the SMZ created in the first step. The bromide and chromate sorbed were then measured. Fewer samples were used in this study, where only the 50%, 100%, and 400% of ECEC levels were examined, both below and above the CMC. Page III-1 of the tables shows the initial HDTMA sorption data. Concentration of HDTMA is first measured in terms of cpm/ml, then converted using data from the original spiked solution concentration and cpm/ml data. Background is subtracted, then the amount sorbed is determined by subtraction from the original available quantity of HDTMA. Bromide was measured by HPLC methods and is shown on tables III-2 and III-3. No anion exclusion calculation was required here because the solution volumes were much larger than in the previous study (Appendix II). Results shown include the amount sorbed to the zeolite in mmol/kg zeolite, and that sorbed value normalized to the ECEC (Table III-2). Table III-3 shows the amount of bromide remaining on the SMZ after equilibration with chromate. Chromate was measured by HPLC and is shown on tables III-4. Again, the normalized amounts were calculated by dividing the amount sorbed in meq/kg by the ECEC of 90 meq/kg.

Appendix III

Experiment 13, Sorption of HDTMA <CMC, >CMC, and subsequent Cr04 sorption 4/12/96

All Samples Cow Chow, 25C

14C HDTMA data

Sample No.	Weight Zeolite g	HDTMA Concentration cpm/ml	HDTMA Conc. minus backgr. cpm/ml	HDTMA Quantity minus backgrnd. cpm	Equilibrium HDTMA Quantity in Soln. meq	HDTMA Sorbed meq	HDTMA in soln meq/L	HDTMA Sorbed meq/kg zeo
H2O 1	0	46.1	mean backgrnd:		0.045			
H2O 2	0	41.4	43.8					
					ratio: mmol/cpm			
0.45 mmol/L	0	9645.6	9601.9	960185	4.6866E-08			
13A 50A	1.0006	86.6	42.9	4285	2.01E-04	4.48E-02	2.01E-03	44.8
13A 50B	1.0004	78	34.3	3425	1.61E-04	4.48E-02	1.61E-03	44.8
13A 100A	0.5001	307.7	264.0	26395	1.24E-03	4.38E-02	1.24E-02	87.5
13A 100B	0.5006	350.9	307.2	30715	1.44E-03	4.36E-02	1.44E-02	87.0
13A 400A	0.1254	5542.5	5498.8	549875	2.58E-02	1.92E-02	2.58E-01	153.3
13A 400B	0.1255	5995.4	5951.7	595165	2.79E-02	1.71E-02	2.79E-01	136.3
BKA	0.5009	44.5	0.8					
BKB	0.5009	42.5	-1.3					
					0.18			
					ratio: mmol/cpm			
1.8 mmol/L	0	10254.3	10210.55	1021055	1.76288E-07			
13B 50A	4.0012	78	34.25	3425	6.04E-04	1.79E-01	6.04E-03	44.8
13B 50B	4	73.5	29.75	2975	5.24E-04	1.79E-01	5.24E-03	44.9
13B 100A	2.0003	172.4	128.65	12865	2.27E-03	1.78E-01	2.27E-02	88.9
13B 100B	2.0009	165.1	121.35	12135	2.14E-03	1.78E-01	2.14E-02	88.9
13B 400A	0.5009	4159.9	4116.15	411615	7.26E-02	1.07E-01	7.26E-01	214.5
13B 400B	0.5004	3771.8	3728.05	372805	6.57E-02	1.14E-01	6.57E-01	228.4
BKA	2.0005	43.3	-0.45					
BKB	2.0002	43	-0.75					

Appendix III

Initial Bromide Sorbed <CMC (Step 2)

Sample No.	Conc. Br mg/L	Actual Conc. mmol/L	Amount mmol	Weight Zeo g	Amt. Sorbed mmol	Amt. Sorbed mmol/kg zeo	accounting amount removed for analysis mmol	Normalized to ECEC no units
13a 50A	33.8924566	0.42413816	0.04241382	1.0006	0.00125502	1.25426596	0.002120691	0.01393629
13a 50B	34.2251736	0.42830186	0.04283019	1.0004	0.00083865	0.83831326	0.002141509	0.00931459
13a 100A	35.3407188	0.44226206	0.04422621	0.5001	-0.00055737	-1.1145188	0.00221131	-0.01238354
13a 100B	35.2619099	0.44127582	0.04412758	0.5006	-0.00045875	-0.91639523	0.002206379	-0.01018217
13a 400A	30.7972277	0.38540374	0.03854037	0.1254	0.00512846	40.8968153	0.001927019	0.45440906
13a 400B	31.3829616	0.39273375	0.03927338	0.1255	0.00439546	35.0235823	0.001963669	0.38915091
0.45 mmol Br	34.8953293	0.43668835	0.04366883	0				

Initial Bromide sorbed, >CMC (step 2)

13b 50A	152.729908	1.91129795	0.1911298	4.0012	-0.02045392	-5.11194682	0.00955649	-0.05679941
13b 50B	154.318872	1.93118262	0.19311826	4	-0.02244239	-5.61059707	0.009655913	-0.06233997
13b 100A	136.829496	1.71231646	0.17123165	2.0003	-0.00055577	-0.27784466	0.008561582	-0.00308716
13b 100B	136.792977	1.71185945	0.17118595	2.0009	-0.00051007	-0.2549212	0.008559297	-0.00283246
13b 400A	93.9473351	1.17567902	0.1175679	0.5009	0.05310797	106.025097	0.005878395	1.17805663
13b 400B	92.4070634	1.1564037	0.11564037	0.5004	0.0550355	109.98302	0.005782019	1.22203356
1.8 mmol Br	136.385384	1.70675874	0.17067587					

Appendix III

Bromide Potentially Desorbed by Chromate Sorption (Step 3)
<CMC

Sample	Actual Conc. mg/L	Actual Conc. mmol/L	Amount mmol	Weight Zeo g	Amt. Sorbed this step only mmol	Amt Sorbed, adj. from step 2 mmol	Amt. Sorbed mmol/kg zeo	Normalized Amount no units
13a CR 50C	35.559	0.445	0.044	1.0003	-4.21E-03	-2.95E-03	-2.95	-0.03
13a CR 50D	35.060	0.439	0.044	1.0007	-3.19E-03	-2.35E-03	-2.35	-0.03
13a CR 100A	32.843	0.411	0.041	0.5001	9.14E-04	3.57E-04	0.71	0.01
13a CR 100B	33.290	0.417	0.042	0.5006	2.61E-04	-1.97E-04	-0.39	0.00
13a CR 400A	28.233	0.353	0.035	0.1254	1.28E-03	6.41E-03	51.12	0.57
13a CR 400B	29.130	0.365	0.036	0.1255	8.56E-04	5.25E-03	41.84	0.46
Blank A	0.078							
Blank B	0.002							

Bromide Desorbed by Chromate, >CMC (Step 3)

Sample	Actual Conc. mg/L	Actual Conc. mmol/L	Amount mmol	Weight Zeo g	Amt. Sorbed mmol	Amt Sorbed, adj. from step 2 mmol	Amt. Sorbed mmol/kg zeo	Normalized Amount no units
13b CR 50A	146.419	1.832	0.183	4.0012	-1.66E-03	-2.21E-02	-5.53	-0.06
13b CR 50B	147.946	1.851	0.185	4	-1.68E-03	-2.41E-02	-6.03	-0.07
13b CR 100A	135.208	1.692	0.169	2.0003	-6.53E-03	-7.09E-03	-3.54	-0.04
13b CR 100B	137.247	1.718	0.172	2.0009	-9.13E-03	-9.64E-03	-4.82	-0.05
13b CR 400A	105.009	1.314	0.131	0.5009	-1.97E-02	3.34E-02	66.65	0.74
13b CR 400B	104.073	1.302	0.130	0.5004	-2.04E-02	3.47E-02	69.25	0.77
Blank A	6.528	0.082	0.008					
Blank B	6.694	0.084	0.008					
1.8 mmol Br	136.385	1.707	0.171					

Appendix III

Chromate Sorbed <CMC 7 day (Step 3)

Sample	Conc mg/L	Conc mmol/L	Amount mmol	amount meq	amount in soln meq/L	Amt. Sorbed meq	Weight Zeo g	Amt. Sorbed meq/kg zeo	Normalized Amount no units
13a CR 50C	1.44	1.24E-02	1.24E-03	2.48E-03	2.48E-02	6.82E-04	1.0006	0.68	0.01
13a CR 50 D	1.48	1.28E-02	1.28E-03	2.56E-03	2.56E-02	6.09E-04	1.0004	0.61	0.01
13a CR 100C	1.20	1.04E-02	1.04E-03	2.08E-03	2.08E-02	1.09E-03	0.5001	2.18	0.02
13a CR 100D	1.51	1.31E-02	1.31E-03	2.61E-03	2.61E-02	5.53E-04	0.5006	1.11	0.01
13a CR 400C	0.53	4.57E-03	4.57E-04	9.14E-04	9.14E-03	2.25E-03	0.1254	17.94	0.20
13a CR 400D	0.39	3.37E-03	3.37E-04	6.74E-04	6.74E-03	2.49E-03	0.1255	19.84	0.22

Chromate Sorbed >CMC 7 day (Step 3)

Sample	Conc. mg/L	Conc. mmol/L	Amount mmol	Amount meq	Amount in soln meq/L	Amt. Sorbed meq	Weight Zeo g	Amt. Sorbed meq/kg zeo	Normalized Amount no units
13b CR 50C	9.27	7.99E-02	7.99E-03	1.60E-02	1.60E-01	1.39E-02	4.0012	3.48	0.04
13b CR 50 D	2.31	1.99E-02	1.99E-03	3.98E-03	3.98E-02	2.59E-02	4	6.48	0.07
13b CR 100C	7.67	6.61E-02	6.61E-03	1.32E-02	1.32E-01	1.67E-02	2.0003	8.33	0.09
13b CR 100D	7.94	6.85E-02	6.85E-03	1.37E-02	1.37E-01	1.62E-02	2.0009	8.09	0.09
13b CR 400C	3.81	3.28E-02	3.28E-03	6.56E-03	6.56E-02	2.33E-02	0.5009	46.58	0.52
13b CR 400D	3.86	3.33E-02	3.33E-03	6.66E-03	6.66E-02	2.32E-02	0.5004	46.43	0.52